LYAPUNOV STABILITY ANALYSIS OF A CLASS OF BASE-EXCITED INVERTED PENDULUMS WITH APPLICATION TO BIPEDAL LOCOMOTION SYSTEMS

DISSERTATION

Presented in Partial Fulfillment of the Requirement for the Degree of Doctor of Philosophy in the Graduate School of The University of Manitoba

by

Qiong (Christine) Wu, B.Sc., M.Sc.

*****

Department of Mechanical & Industrial Engineering
The University of Manitoba
Winnipeg, Manitoba

1996

National Library
of Canada

Acquisitions and
Bibliographic Services Branch

395 Wellington Street
Ottawa, Ontario
K1A 0N4

Bibliothèque nationale
du Canada

Direction des acquisitions et
des services bibliographiques

395, rue Wellington
Ottawa (Ontario)
K1A 0N4

Your file *Votre référence*

Our file *Notre référence*

ISBN 0-612-13580-2

Canada

Name _____

Dissertation Abstracts International and *Masters Abstracts International* are arranged by broad, general subject categories. Please select the one subject which most nearly describes the content of your dissertation or thesis. Enter the corresponding four-digit code in the spaces provided.

_____ SUBJECT TERM

☐☐☐☐ SUBJECT CODE

UMI

Subject Categories

THE HUMANITIES AND SOCIAL SCIENCES

COMMUNICATIONS AND THE ARTS
Architecture 0729
Art History 0377
Cinema 0900
Dance 0378
Fine Arts 0357
Information Science 0723
Journalism 0391
Library Science 0399
Mass Communications 0708
Music 0413
Speech Communication 0459
Theater 0465

EDUCATION
General 0515
Administration 0514
Adult and Continuing 0516
Agricultural 0517
Art 0273
Bilingual and Multicultural 0282
Business 0688
Community College 0275
Curriculum and Instruction 0727
Early Childhood 0518
Elementary 0524
Finance 0277
Guidance and Counseling 0519
Health 0680
Higher 0745
History of 0520
Home Economics 0278
Industrial 0521
Language and Literature 0279
Mathematics 0280
Music 0522
Philosophy of 0998
Physical 0523
Psychology 0525
Reading 0535
Religious 0527
Sciences 0714
Secondary 0533
Social Sciences 0534
Sociology of 0340
Special 0529
Teacher Training 0530
Technology 0710
Tests and Measurements 0288
Vocational 0747

LANGUAGE, LITERATURE AND LINGUISTICS
Language
- General 0679
- Ancient 0289
- Linguistics 0290
- Modern 0291

Literature
- General 0401
- Classical 0294
- Comparative 0295
- Medieval 0297
- Modern 0298
- African 0316
- American 0591
- Asian 0305
- Canadian (English) 0352
- Canadian (French) 0355
- English 0593
- Germanic 0311
- Latin American 0312
- Middle Eastern 0315
- Romance 0313
- Slavic and East European 0314

PHILOSOPHY, RELIGION AND THEOLOGY
Philosophy 0422
Religion
- General 0318
- Biblical Studies 0321
- Clergy 0319
- History of 0320
- Philosophy of 0322

Theology 0469

SOCIAL SCIENCES
American Studies 0323
Anthropology
- Archaeology 0324
- Cultural 0326
- Physical 0327

Business Administration
- General 0310
- Accounting 0272
- Banking 0770
- Management 0454
- Marketing 0338

Canadian Studies 0385
Economics
- General 0501
- Agricultural 0503
- Commerce-Business 0505
- Finance 0508
- History 0509
- Labor 0510
- Theory 0511

Folklore 0358
Geography 0366
Gerontology 0351
History
- General 0578
- Ancient 0579
- Medieval 0581
- Modern 0582
- Black 0328
- African 0331
- Asia, Australia and Oceania 0332
- Canadian 0334
- European 0335
- Latin American 0336
- Middle Eastern 0333
- United States 0337

History of Science 0585
Law 0398
Political Science
- General 0615
- International Law and Relations 0616
- Public Administration 0617

Recreation 0814
Social Work 0452
Sociology
- General 0626
- Criminology and Penology ... 0627
- Demography 0938
- Ethnic and Racial Studies 0631
- Individual and Family Studies 0628
- Industrial and Labor Relations 0629
- Public and Social Welfare 0630
- Social Structure and Development 0700
- Theory and Methods 0344

Transportation 0709
Urban and Regional Planning 0999
Women's Studies 0453

THE SCIENCES AND ENGINEERING

BIOLOGICAL SCIENCES
Agriculture
- General 0473
- Agronomy 0285
- Animal Culture and Nutrition 0475
- Animal Pathology 0476
- Food Science and Technology 0359
- Forestry and Wildlife 0478
- Plant Culture 0479
- Plant Pathology 0480
- Plant Physiology 0817
- Range Management 0777
- Wood Technology 0746

Biology
- General 0306
- Anatomy 0287
- Biostatistics 0308
- Botany 0309
- Cell 0379
- Ecology 0329
- Entomology 0353
- Genetics 0369
- Limnology 0793
- Microbiology 0410
- Molecular 0307
- Neuroscience 0317
- Oceanography 0416
- Physiology 0433
- Radiation 0821
- Veterinary Science 0778
- Zoology 0472

Biophysics
- General 0786
- Medical 0760

EARTH SCIENCES
Biogeochemistry 0425
Geochemistry 0996
Geodesy 0370
Geology 0372
Geophysics 0373
Hydrology 0388
Mineralogy 0411
Paleobotany 0345
Paleoecology 0426
Paleontology 0418
Paleozoology 0985
Palynology 0427
Physical Geography 0368
Physical Oceanography 0415

HEALTH AND ENVIRONMENTAL SCIENCES
Environmental Sciences 0768
Health Sciences
- General 0566
- Audiology 0300
- Chemotherapy 0992
- Dentistry 0567
- Education 0350
- Hospital Management 0769
- Human Development 0758
- Immunology 0982
- Medicine and Surgery 0564
- Mental Health 0347
- Nursing 0569
- Nutrition 0570
- Obstetrics and Gynecology .. 0380
- Occupational Health and Therapy 0354
- Ophthalmology 0381
- Pathology 0571
- Pharmacology 0419
- Pharmacy 0572
- Physical Therapy 0382
- Public Health 0573
- Radiology 0574
- Recreation 0575
- Speech Pathology 0460
- Toxicology 0383

Home Economics 0386

PHYSICAL SCIENCES
Pure Sciences
Chemistry
- General 0485
- Agricultural 0749
- Analytical 0486
- Biochemistry 0487
- Inorganic 0488
- Nuclear 0738
- Organic 0490
- Pharmaceutical 0491
- Physical 0494
- Polymer 0495
- Radiation 0754

Mathematics 0405
Physics
- General 0605
- Acoustics 0986
- Astronomy and Astrophysics 0606
- Atmospheric Science 0608
- Atomic 0748
- Electronics and Electricity 0607
- Elementary Particles and High Energy 0798
- Fluid and Plasma 0759
- Molecular 0609
- Nuclear 0610
- Optics 0752
- Radiation 0756
- Solid State 0611

Statistics 0463

Applied Sciences
Applied Mechanics 0346
Computer Science 0984
Engineering
- General 0537
- Aerospace 0538
- Agricultural 0539
- Automotive 0540
- Biomedical 0541
- Chemical 0542
- Civil 0543
- Electronics and Electrical 0544
- Heat and Thermodynamics ... 0348
- Hydraulic 0545
- Industrial 0546
- Marine 0547
- Materials Science 0794
- Mechanical 0548
- Metallurgy 0743
- Mining 0551
- Nuclear 0552
- Packaging 0549
- Petroleum 0765
- Sanitary and Municipal 0554
- System Science 0790

Geotechnology 0428
Operations Research 0796
Plastics Technology 0795
Textile Technology 0994

PSYCHOLOGY
General 0621
Behavioral 0384
Clinical 0622
Developmental 0620
Experimental 0623
Industrial 0624
Personality 0625
Physiological 0989
Psychobiology 0349
Psychometrics 0632
Social 0451

THE UNIVERSITY OF MANITOBA

FACUTY OF GRADUATE STUDIES

COPYRIGHT PERMISSION

LYAPUNOV STABILITY ANALYSIS OF A CLASS OF BASE-EXCITED INVERTED PENDULUMS WITH APPLICATION TO BIPEDAL LOCOMOTION SYSTEMS

BY

QIONG (CHRISTINE) WU

A Thesis/Practicum submitted to the Faculty of Graduate Studies of the University of Manitoba in partial fulfillment of the requirements for the degree of

DOCTOR OF PHILOSOPHY

ABSTRACT

A methodology is presented to study the control and stability of base-excited inverted pendulums. The pendulum has two degrees of rotational freedom and the base point can move in the three dimensional space with the only restriction of continuous acceleration. The study is motivated by the modeling of the control mechanisms of upright posture of a human upper body during walking. The dynamic system of such an inverted pendulum is non-autonomous and under constantly acting disturbance, that is, the system does not have a unique equilibrium point which makes the control task highly challenging. Non-smooth analysis is first performed since piecewise continuous controllers are inevitable for the stability analysis using Lyapunov's stability theory. Lyapunov's second method is then extended for non-smooth dynamics systems. An extended integral method is developed to construct Lyapunov functions. Two piecewise continuous control strategies are designed, one is based on the total stability theory which guarantees that the solution trajectory can be arbitrarily close to the upright position under the condition of small disturbances. The second strategy guarantees that the system trajectory can be bounded in a controlled region about the upright position without any restrictions on the magnitude of the disturbance. Next, the discontinuous terms in the controller are replaced by continuous functions to reflect the actual implementation scenario. It is proven, by the generalized Lyapunov analysis, that the pendulum under investigation can be stabilized in a controlled region around the upright position. The sensitivity of the system stability with respect to the uncertainties of physical parameters and of the measurement of the base point acceleration is also analyzed. It is found that the stability is largely insensitive to such

uncertainties. The pendulum model is then applied in the simulation of the human upper body movement for walking. It is found that the simulation results follow the measurement reasonably well. Such a comparison establishes the promise of the model for the application of modeling the upright postural control of the human upper body. The methodology developed here can not only benefit the biomechanics community, but can also make an important contribution to the analysis of non-smooth systems, such as the mechanical systems with friction and sliding mode control systems.

ACKNOWLEDGMENTS

First, I wish to thank my advisor, Dr. A. B. Thornton-Trump, for creating an environment which, at all time, felt comfortable. Throughout the course of my project, he provided the freedom and the encouragement which cultivates both originality and imagination. I am also indebted to him for sharing the frustrations of defining the problem.

Second, I would like to express my appreciation to Dr. Steve Onyshko, for giving me the fundamental knowledge of Lyapunov's stability theory, for the first time, and for his continuing support whenever called upon.

My sincere appreciation is also due to Dr. Marion Alexander and her graduate student Bob Nikel for their help during gait measurements and data processing and for providing a pleasant working atmosphere.

Finally, and most important of all, I thank my family for their support, love and devotion throughout the course of the work. My deepest thanks to my parents for the numerous sacrifices made on my behalf; to my husband for all his help.

TABLE OF CONTENTS

LIST OF FIGURES

LIST OF TABLES

CHAPTER ONE

INTRODUCTION

1.1 General background

1.1.1 Motivations

The essence of human walking is to move the upper body from one place to another with reliable stability. A human upper body contains the head, arms, the thorax and the pelvis; and represents about 60% of the total body weight. The motor control mechanism to keep the upper body stable is subtle and most complex (Rahmani, 1979 and Pandy, 1987). Furthermore, understanding and modeling of such control systems are important in the development of bipedal walking machines.

There are not many publications about control and stability analysis of a human upper body during walking using the modeling approach. As lucidly described by Cappozzo *et al.* (1978), the movement of the upper body contributes to the reduction of the energy exchange between body segments and has considerable influence on the whole body stability during walking. In pathological gait, altered upper body motion is a common occurrence. Such alteration is caused by the variation of two factors; motion of the pelvis and the torques and forces applied to the upper body. The pelvic motion plays a crucial role in the stabilization of the human upper body and is no longer as smooth and as simple in pathological gait as that of normal walking. Cappozzo (1981,1983) and Stokes and Forssberg (1989) have shown that the stability of the upper body is highly dependent upon the motion of the pelvis. Also, the movements of the pelvis (pelvic list, rotation and lateral displacement) are contained in three of the six major determinants of gait (Saunders *et al.*,

1953). (The remaining three determinants are stance knee flexion-extension, foot and knee interactions.) Therefore, the investigation of upper body stability with complex pelvis motion is of great significance to understanding human locomotion.

1.1.2 Inverted pendulum models

In nearly all previous studies of dynamics for both human beings and bipedal robots, models were often chosen as either an inverted pendulum whose gravity center is above the suspending point (referred to here as the base point) or a chain of inverted pendulums. To specify a few such studies, it is noted that Vukobratovic *et al.* (1970, 1972, 1973 and 1975), Onyshko and Winter (1980), Hemami (1977a, 1977b, 1979, 1980, 1984 and 1986), Scheiner *et al.* (1993) and Yang (1994) used multiple-rigid-link models to simulate the body movement during normal walking. Chow and Jacobson (1971), Pandy and Berme (1988a, 1988b and 1989) used the model of a chain of inverted pendulums to simulate lower limb motion for both normal and pathological gait. Chow and Jacobson (1972) used a single base-excited inverted pendulum to model the human trunk, and the stability of the pendulum system was studied when the base point imitates the pelvic motion during walking.

An inverted pendulum or a chain of inverted pendulums is an inherently unstable system and the studies of control and stabilization of such a system is one of the challenging problems in the field of automatic control (Mori, 1972). Studies of control and stabilization of single pendulums can be grouped into two classes. The first class, which has been investigated extensively, deals with the benchmark problem of an inverted pendulum in which the base point is rocked to maintain the upright position of the

pendulum. To cite a few cases, Schaefer and Cannon (1966), Koenigsberg and Frederick (1970), Mori *et al.* (1976) and Henders and Soudack (1992) used linearized feedback control algorithms to achieve stability by base point movement. Barto *et al.* (1983), Widrow (1987), Guez and Selinsky (1988) and Anderson (1989) applied neural network approaches to the same problem. Levi (1988) presented a topological explanation and a proof of stability for an inverted pendulum with a specific vertical base motion.

Unlike the benchmark problem of an inverted pendulum with only one degree of rotational freedom where the base point is 'rocked' in a way to stabilize the pendulum, the stabilization of an inverted pendulum in the second group is achieved by applying control torques at the base point and the motion of the base point is one of the causes of the instability of the pendulum. As far as the previous study is concerned, Chow and Jacobson (1972) developed a control strategy to stabilize an inverted pendulum with two degrees of rotational freedom about the base point. The control strategy contained on-off perturbations and the base point was allowed to move in the vertical direction in a prescribed way. Hemami and Katbab (1982) studied stabilization of a pendulum with three degrees of rotational freedom. In their stability analysis, the base point was fixed at the origin. Also, in order to construct a Lyapunov function, the derivative gains in their control algorithm had to be a set of specific values which caused their state trajectories to be oscillatory. Geromel and Cruz (1987) used an inverted pendulum example to study the robustness of closed loop systems with respect to two different classes of perturbations in the control laws. Anderson and Grantham (1989) developed an optimal Lyapunov feedback control for a single degree of freedom inverted pendulum and with a fixed base

point. Their contribution was that the control torque was constrained to be within a certain range, yet the stability was guaranteed.

Though many advanced control theories have been developed to control the inverted pendulum by applying appropriate control torques, the base point in most of the previous work was fixed, except in the study of Chow and Jacobson (1972) in which the base point was allowed to move in the vertical direction and in a prescribed way. The challenge in controlling the proposed inverted pendulum model is that the inclusion of the base point motion in the model leads to the dynamic equations of the inverted pendulum system consisting of second order differential equations with time variable parametric excitation (Mendica, 1987) which makes the control task even more challenging. Furthermore, horizontal accelerations have significant effects on the system stability and the inclusion of horizontal movements leads to the control system not having an equilibrium point, which makes the stability analysis extremely difficult. The control and stabilization of a base-excited inverted pendulum have not been studied rigorously.

1.2 Problem formulation and scope

In human locomotion, the upper body is simply modeled in this study as one inverted pendulum with two degrees of rotational freedom. The base point of the pendulum (the bony landmarks at the sacrum in this study) must be free to move in three-dimensional space with no restrictions on the motion except that base point accelerations must be continuous. Thus, the inverted pendulum model has five degrees of freedom; two for rotations and three for translations. The objective of the work, presented in this thesis, is to develop a methodology to study systematically the control and to predict the stability of

the above inverted pendulum. The work is motivated by two concerns. From the biomechanical point of view, the current studies of the stability of human locomotion using a modeling approach are sparse. From the viewpoint of automatic control, the control and stabilization of base-excited pendulums have not been studied rigorously.

The methodology developed here is composed of two aspects. The first aspect is the stability analysis of the control system and the second aspect is the design of control strategies. These two aspects are implicitly linked. The design of the control strategies is based on the stability analysis. The stability mentioned above is related to the stability in the sense of Lyapunov (1992). The objective of the stability analysis is to draw conclusions about the behavior of a system without actually computing its solution trajectories. The challenge in using Lyapunov's method is the construction of a Lyapunov function, for there are no constructive rules or suggestions available.

The challenge in controlling the proposed inverted pendulum model is that the inclusion of the base point accelerations causes the mathematical model of the control system to be non-autonomous. Furthermore, the inclusion of the horizontal movements of the base point leads to the control system not having an equilibrium point, which violates the fundamental assumption of Lyapunov's stability theory. Such systems are regarded as systems under disturbance (Slotine and Li, 1991). The stability of such a system, referred to in Russian literature as stability under constantly-acting perturbation, has to be treated by total stability theory (Hahn, 1960 and Slotine and Li, 1991). The methodology of studying the control and stability of a base-excited inverted pendulum is developed from the following five steps.

1.2.1 Development of the extended integral method for construction of Lyapunov functions

Lyapunov's stability theory allows one to analyze nonlinear dynamic systems directly. Lyapunov not only introduced the basic definition of stability that is used today, but also proved many of the fundamental theorems. Since Lyapunov published his theory (Lyapunov, 1892), a great deal of work has been done on stability of nonlinear systems based on Lyapunov's stability theory.

The key to prove the system stability based on Lyapunov's stability theory is to construct a Lyapunov function. Since no constructive rules or suggestions were given in his theory, the construction of a Lyapunov function for a nonlinear system remains a great challenge which restricts the application of this otherwise powerful theory. In the past thirty years, numerous techniques have been proposed to construct Lyapunov functions for some special nonlinear systems, as attested to by the existence of many papers on the subject. Amongst these techniques are the method of analogy with linear systems by Barbasin (1960), the method of integration by parts by Ponzo (1965) and Huaux (1967), the method of system energy by Marino and Nicosia (1983), the integral methods, the scalar-Lyapunov-function method and the intrinsic method by Chin (1986, 1987, 1988 and 1989). These methods, though valuable, are developed for specific classes of nonlinear differential equations which may not apply to many physical systems. Among them, Chin's generalized integral method (Chin, 1987) provides a systematic approach to the construction of Lyapunov functions for general nonlinear systems represented by state space models in the form of n first-order differential equations. It has been successfully

applied to derive Lyapunov functions for a number of autonomous systems. However, during the initial stage of this research, it was noticed that, using Chin's integral method, the success in construction of a Lyapunov function depends not only on the proper choice of weighting functions but also on the existence or development of suitable state space models. Such state space models are referred to here as compatible models. The requirement for the compatibility between the state space model and a Lyapunov function has often restricted the application of the integral method. Based on the above consideration, an extended integral method is developed in this work to allow construction of a Lyapunov function for nonlinear control systems; achieving the main objective of reducing the sensitivity of the integral method to the form of the state space model.

1.2.2 Non-smooth analysis

In the course of stability analysis of the inverted pendulum system under study, it is found that the use of discontinuous controllers are inevitable to validate a Lyapunov function. Discontinuous controllers make the dynamic systems non-smooth; that is, the dynamic equations contain discontinuous terms with respect to the states or time. Two fundamental mathematical issues must be considered when studying non-smooth dynamic systems. One is the solution concept for non-smooth systems. This is because all conventional solution theories for differential equations, which require each term of the equations to be at least continuous, are no longer valid. Thus, the existence and the uniqueness of the solution cannot be guaranteed. Furthermore, with respect to the conventional solution theories, one cannot even define solutions for non-smooth dynamic

systems. The second issue is that Lyapunov's stability theory must be extended to non-smooth systems since it was developed based on smooth systems.

What is first needed for non-smooth systems is a solution theory which allows the study of differential equations with discontinuous right-hand sides. One of the pioneers in this field is Filippov (1960, 1979 and 1988) who developed a solution theory (Filippov's solution theory) for non-smooth differential equations. Although the solution problem for non-smooth control systems has been considered to be important (Slotine and Sastry, 1983; Southward *et al.*, 1991; Utkin, 1977 and 1991 and Corless, 1993), it has not been studied rigorously for many discontinuous control systems because "it requires much heavier mathematical machinery" (Corless, 1993). In this dissertation, Filippov's solution concept is used to define solutions for the proposed piecewise continuous control systems and the existence and uniqueness of such solutions are proven rigorously using Filippov's solution theory (1960, 1979 and 1988). Once the existence and uniqueness of the solutions for control systems presented in this work is established, it is then possible to analyze the stability of the control system.

It is important to point out that Lyapunov's stability theory is based on conventional solution theory, that is the dynamic systems must be smooth. For the stability analysis of non-smooth systems, Lyapunov's second method needs to be extended. Paden and Sastry (1987) first generalized Lyapunov's second method by imposing a non-zero upper bound of the derivative of the Lyapunov function with respect to time. They proved, in a somewhat descriptive manner, that the states of the system (solution in the sense of Filippov) converge to the equilibrium point in a finite time. Another extension of

Lyapunov's stability theory based on Filippov's solution theory was done by Southwood *et al.* (1991) where the derivative of Lyapunov functions on the discontinuity surfaces were replaced with Dini-derivate defined by Rouch *et al.* (1977). The most recent and systematic extension of Lyapunov's second method for non-smooth dynamic systems was developed by Shevitz and Paden (1994) in which a non-smooth Lyapunov function is constructed. Such an extension was based on Filippov's solution concept and Clarke's generalized gradient (Clark, 1983). Their result is a theory applicable to systems with switches, for which Lyapunov functions are only piecewise smooth. The above extensions of Lyapunov's stability theory to non-smooth systems were based on the belief that non-smooth Lyapunov functions are natural for non-smooth dynamic systems. The belief is true because the derivative of a Lyapunov function with respect to time is the inner product of the gradient of the Lyapunov function itself and the rate of the state vector. Since the rate of the state vector is discontinuous, the derivative of the Lyapunov function with respect to time may be discontinuous, i.e., the Lyapunov function is non-smooth. However, the main challenge in construction of non-smooth Lyapunov functions is the evaluation of the derivatives of Lyapunov functions when the solution trajectories approach the discontinuity surfaces where Dini-derivate or Clarke's generalized gradients were introduced. Such an evaluation is related to the determination of the intersection of infinite convex sets and is extremely difficult especially when the discontinuity surface is the intersection of several discontinuity surfaces.

In this work, we prove, rigorously, that if the existence and uniqueness of Filippov's solution are guaranteed, Lyapunov's second method can be applied directly to non-smooth

dynamic systems. Furthermore, a method is developed to construct smooth Lyapunov functions for non-smooth systems and it is shown that the construction of smooth Lyapunov functions is much easier for some engineering systems as compared to its non-smooth counterpart. With the above preparation, the stability of the inverted pendulum system with piecewise continuous control strategies can be proven rigorously.

1.2.3 Development of discontinuous controllers and non-smooth analysis

It was found in the course of this research that discontinuous controllers are inevitable to validate Lyapunov functions for the base-excited inverted pendulum systems. Discontinuous controllers are first designed to stabilize the base-excited inverted pendulum and non-smooth analysis is performed which includes the solution analysis and stability analysis.

Lyapunov's stability theory is developed for the stability of nonlinear systems about an isolated equilibrium point with respect to initial conditions. For the systems that do not have isolated equilibrium points, total stability theory must be used. Total stability theory was first proposed by Russian scientists (Dubosin, 1940; Vorovich, 1956 and Vrkoc, 1959) and is based on Lyapunov's stability theory. A nonlinear system without an isolated equilibrium point is referred to as the system under constantly acting perturbations. In the total stability analysis, such a system is divided into two parts; the undisturbed system with an isolated equilibrium point and the disturbed system in which the disturbance is included. With certain conditions on the undisturbed system, the stability of the disturbed system can be determined.

In the development of piecewise continuous control strategies, two piecewise continuous control strategies are developed to determine the required control torques for stabilization. One control strategy guarantees the total stability of the control system under the condition of small perturbations, that is, the solution trajectories are arbitrarily close to the upright position. Such a small perturbation condition requires accurate measurement of horizontal accelerations and some physical parameters. To remove such a requirement, an improved control strategy is developed which keeps the system trajectory around the upright position within a controlled bound.

1.2.4 Development of continuous controllers and stability analysis

The use of a discontinuous control strategy is not without a price. If one attempts to implement a discontinuous control strategy, the effects of discontinuous forces on actuators and gear trains can be destructive. Besides, the control exhibits chattering as the state trajectories reach the discontinuous region (Corless, 1993). Chattering is not desirable both in itself and in the fact that it may represent a high-frequency signal component in the state trajectories or in the controller (Slotine and Sastry, 1983). Thus, in real systems, the control discontinuity is smoothed by replacing the discontinuous terms with some continuous functions so that the system trajectory moves to the neighborhood of the approximate discontinuity. However, the effect of smoothing the control discontinuity on the system stability becomes a crucial issue. In this part, the discontinuous terms in the control algorithm are approximated by a class of continuous functions to better reflect the actual implementation scenario. It is then found that given such a continuous control law, stability in the sense of Lyapunov may not be established.

However, the inverted pendulum can still be stabilized in a controlled region around the upright position. Such stability is referred to here as practical stability, and is proven using the generalized Lyapunov analysis. The concept of generalized Lyapunov analysis was discussed by Reissig (1959 and 1960) and Hahn (1963) and was later employed to design a robust control strategy for a general class of non-linear or linear systems with bounded uncertainties (Qu and Dorsey, 1992).

It is important to point out that though discontinuous control strategies are not desirable from a practical point of view, the study of the idealized discontinuous controller gives a clear picture of the salient properties of the system dynamics and the descriptions of the ideal behavior can serve as a limit of the non-ideal motions (Utkin, 1977 and 1991; Paden and Sastry, 1987).

1.2.5 Simulations of human upper body movements during walking

The mathematical model developed in this work is applied to study the dynamics of the human upper body during walking. The movement of the upper body is measured in the gait laboratory for the corresponding gait patterns. The simulated displacements of the gravity center of the upper body are compared with those measured and the control torques are compared with the trunk torques calculated from the kinematics of walking. The purpose of such a comparison is to establish the promise of the model for further studies.

With the above theoretical extensions and the design of the control strategies, the stabilization of a base-excited inverted pendulum can be studied systematically. Such a methodology is to be applied to the modeling and simulation of the upright postural

control of human upper body during walking. The methodology developed here can not only benefit the biomechanics community, but also has important contribution to the analysis of non-smooth systems, such as the mechanical systems with friction and sliding mode control systems.

1.3 Organization of the thesis

Chapter Two contains the theoretical preliminaries which include the review of the main results of Filippov's solution theory, Lyapunov's stability theory, total stability theory and the idea of the generalized Lyapunov analysis. In Chapter Three, the extension of Lyapunov's second method to non-smooth dynamic systems is verified and an extended integral method is developed to construct Lyapunov functions for nonlinear systems. The method of construction of smooth Lyapunov functions is also developed in the same chapter.

In Chapter Four, control strategies are developed to stabilize a single-degree-of-rotational-freedom inverted pendulum about its upright position. The base point of the pendulum can move in the vertical plane. The reason a single degree of rotational freedom inverted pendulum is analyzed is to establish the methodology for a relatively simple case since the multiple degrees of freedom inverted pendulum is very complicated. In Chapter Five, two types of control strategies are designed to stabilize a two-degree-of-rotational-freedom inverted pendulum about the upright position with general base point motion. One type of control algorithm is piecewise continuous and the other is continuous.

In Chapter Six, the inverted pendulum model developed in this work is applied to simulate human upper body movements during walking. The simulated movement of the

inverted pendulum and the control torques predicted from the proposed control strategy are compared to the measured motion and the resultant trunk torques obtained through analysis of laboratory gait measurements. The purpose of such a comparison is to establish the potential for further extensions of the model to include more segments to simulate bipedal locomotion. In the same chapter, the protocol of gait measurement of the human upper body movement during walking is detailed and the sensitivity of the measurement is also discussed. The conclusions and recommended future work are outlined in Chapter Seven.

CHAPTER TWO

THEORETICAL PRELIMINARY

As stated previously, at the heart of the approach developed in this dissertation lie two theoretical bases. One is Filippov's solution theory and another one is Lyapunov's stability theory. Filippov's solution theory and Lyapunov's stability theory are first reviewed in this chapter.

2.1 Review of Filippov's solution theory

2.1.1 Nature of non-smooth dynamic systems

Just as "non-linear" is understood in mathematics to mean "not necessarily linear", "non-smooth" refers to certain situations in which smoothness (differentiability) of the data is not necessarily ensured. A non-smooth dynamic system means that the differential equations describing the system contain discontinuous terms. Non-smooth dynamic systems appear naturally and frequently in control fields. Examples of these systems include systems with Coulomb friction, contact interactions, variable structure systems and optimal control systems. It is essential to rigorously analyze these systems and address such issues as the existence and uniqueness of the solutions, their stability and qualitative dynamics. As important as non-smooth systems are in practice, techniques are still lacking for their analysis. All classical solution theories require vector fields to be at least Lipschitz continuous. The aforementioned systems, and many others, fail this Lipschitz-continuous requirement. With respect to these classical solution theories, one cannot even define a solution, much less discuss existence and uniqueness of the solutions and their stability.

What is needed is a set of tools for non-smooth systems which allows the analysis of differential equations with discontinuous terms. Several solution theories were developed for non-smooth systems by Russian scientists due to their contributions on rigorous research on variable structure control and optimal control after 1960. One of the earliest and conceptually straightforward approaches is the method of Filippov (1960, 1979 and 1988) which has been often used in the solution analysis of non-smooth systems (Slotine and Sastry, 1983; Paden and Sastry, 1987; DeCarlo *et al.*, 1988; Southwood *et al.*, 1991 and Shevitz and Paden, 1994). Filippov's solution theory represents a significant contribution to the theory and is of particular practical interest (Andre, 1960). In his work, a new definition of solution to differential equations with discontinuous terms was given which is referred to here as Filippov's solution, and theorems were proven for existence, uniqueness and continuity dependence on the initial conditions. Filippov's work was later extended to include more general situations (Wagner, 1977; Clarke, 1983 and Aubin and Cellina, 1987) which is known as the field of *differential inclusions* (Aubin and Cellina, 1987). *Differential inclusions* is the study of dynamic systems having state derivatives not uniquely determined by the states of the system, but depending loosely upon them.

As non-smooth dynamic systems become popular in control engineering, the solution concept, as well as the existence and uniqueness of the solutions has attracted some attention from control scientists. However, due to the fact that '...much heavier mathematical machinery is required...' (Corless, 1993) to analyze the solutions to the non-smooth dynamic systems, the analysis of the solutions to many non-smooth control systems have not been performed, though the importance of such an analysis has been

addressed in the literature (Slotine and Sastry, 1983; Southward, *et al.*, 1991 and Corless, 1993). Before the existence and uniqueness of the solution to the proposed non-smooth dynamic system is analyzed, the solution concept developed by Filippov (1960, 1979 and 1987) and those theorems of existence and uniqueness used in this work are summarized here.

2.1.2 Main results of Filippov's solution theory

Definition of Filippov's solution

Consider the vector differential equation

$$\dot{\mathbf{x}} = \mathbf{f}(\mathbf{x}, \mathbf{t}) \tag{2.1}$$

where $\mathbf{f}: \mathbf{R}^n \times \mathbf{R} \rightarrow \mathbf{R}^n$ is measurable and essentially locally bounded. The solution to equation (2.1) was given by Filippov (1960) as follows:

Definition 2.1: A vector function $\mathbf{x(t)}$, defined on the interval $(\mathbf{t_1}, \mathbf{t_2})$, is called a solution of equation (2.1) if it is absolutely continuous and if for almost all $\mathbf{t} \in (\mathbf{t_1}, \mathbf{t_2})$ and for arbitrary $\delta > 0$ the vector $\mathbf{dx(t)/dt}$ belongs to the smallest convex closed set (of n-dimensional space) containing all the values of the vector function $\mathbf{f(t,x')}$, when $\mathbf{x'}$ ranges over almost all of the δ-neighborhood of the point $\mathbf{x(t)}$ in the space of $\mathbf{x}$ (with $\mathbf{t}$ fixed), i.e., the entire neighborhood except for a set of measure zero. In the notation adopted above,

$$\frac{\mathbf{dx(t)}}{\mathbf{dt}} \in \mathbf{F\{f(t,x(t))\}} \tag{2.2}$$

where

$$\mathbf{F\{f(t,x(t))\}} \equiv \cap_{\delta>0} \cap_{\mu N=0} \overline{\mathbf{co}}\, \mathbf{f(t,B(x(t),\ \delta) - N)}$$

and $\overline{\text{co}}$ refers to the convex hull of a set. **N** are the sets of Lebesgue measure zero.

To illustrate the limiting procedure used to define $\mathbf{F\{f(t, x(t))\}}$, Figure 2.1 shows the vector images of a small neighborhood around the point **x**. The interface is a neglected set of measure zero where the vector field is not defined. The set $\mathbf{F\{f(t, x(t))\}}$ reduces to the convex hull of two limit vectors as the neighborhood becomes vanishingly small.

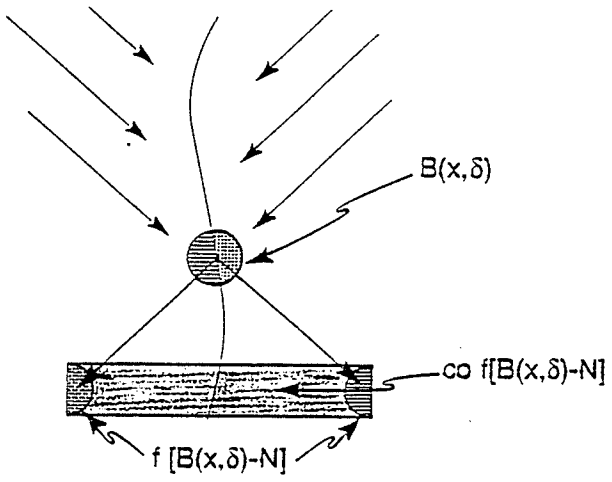

Figure 2.1 Illustrative explanation of $\mathbf{F\{f(t, x(t))\}}$ (reproduced from Shevitz and Paden, 1994)

Remarks

(1) The content of Filippov's solution is that the tangent vector to a solution, where it exists, must lie in the convex closure of the limiting values of the vector field in progressively smaller neighborhoods around the solution point. The above definition allows us to exclude sets of zero measure. This technical detail allows solutions to be defined at points even where the vector field itself is not defined, such as at the interface of two regions in a piecewise defined vector field.

(2) Definition (2.1) is quite general, that is, it includes more general classes of discontinuous differential equations than those with a piecewise continuous controller. Definition (2.1) is referred to as a Filippov's solution in this report and the solutions satisfying the classical solution theories are referred to as conventional solutions.

(3) Filippov's solution theory is useful in engineering problems because Filippov's solutions are limits of solutions with the right-hand side averaged over smaller and smaller neighborhoods. Thus, it is expected that the Filippov's trajectories of non-smooth systems will be close to the true trajectories (Paden and Sastry, 1987).

Comparison with conventional solutions

Suppose that for $\mathbf{t_1 < t < t_2}$ the graph of the vector function $\mathbf{x(t)}$ extends inside the region in which the right-hand side of equation (2.1) is continuous with respect to (t, x). In order that $\mathbf{x(t)}$ be a solution to equation (2.1) in the sense of definition (2.1) for these values of t, it is necessary and sufficient that it be a solution to this equation in the usual sense, i.e., that over the entire interval $(\mathbf{t_1}, \mathbf{t_2})$ it have a derivative equal to $\mathbf{f(t, x(t))}$.

Theorem on the existence and continuation of a solution

Let the right-hand side of equation (2.1) be measurable and bounded in a region Ω. Then for an arbitrary initial condition $\mathbf{x(t_0) = a}$, where $(\mathbf{t_0}, \mathbf{a}) \in \Omega$, a solution of equation (2.1) exists satisfying the above initial conditions which is also continuable on the interval.

Theorems on the uniqueness of the solutions

The theorems of the uniqueness of the solution were developed separately for the cases where the discontinuity surface is a single surface and the case where the discontinuity surface is the intersection of several discontinuity surfaces.

For the case of single discontinuity surfaces $S:=\{x: s(x)=0\}$, the region Ω is divided into domains Ω^- and Ω^+ which are defined as $\Omega^- =\{x: s(x)<0\}$ and $\Omega^+ =\{x: s(x)>0\}$. Functions f^- and f^+ are defined as the right-hand sides of the dynamic equations in the regions Ω^- and Ω^+ which are measurable and bounded. Let the functions f_i be continuous with respect to $x_1,\ldots,x_n$ in Ω^- and Ω^+, and let there exist limiting values of the functions f_i under approach to an arbitrary point of the surface S from domain Ω^- to Ω^+. Vector h is defined as $h = f^+ - f^-$ at all points of the discontinuity surface S. In addition, h_N is defined as the projection of h on the normal to the discontinuity surface S. If it is found that $h_N \le 0$, then in the domain Ω for the system (2.1) we have the uniqueness and continuous dependence of the solution on the initial conditions. Furthermore, if we have $f_N^+ > 0$ and $f_N^- > 0$ (or $f_N^+ < 0$ and $f_N^- < 0$) at all points of S, the solution goes through S and has only one point in common with S.

For the case where the discontinuity surface is the intersection of several surfaces, consistent with Filippov's theory, the regions Ω_j are projected on the n-dimensional state space into regions S_j^n, j=1,2,...,r. The smooth surfaces bounding the S_j^n will be denoted by S_i^m, where m is the dimension and i is the number of the surfaces. For each $x \in S_i^l$, the intersection of discontinuity surfaces, set $K_i^l(t,x)$ is defined as

$$\mathbf{K}_i^l(t,x) = \mathbf{F}_i^l(t,x) \cap \mathbf{P}_i^l(x) \tag{2.3}$$

where $\mathbf{F}_i^l(t,x) = \mathbf{F}(t,x)$ and $\mathbf{P}_i^l(x)$ is the set of all vectors paralleled to the l-dimensional surface $\mathbf{S}_i^l$ at the point on the discontinuity surface including the null vector. $\mathbf{H}_i^l(t,x)$ is the set of vectors of $\mathbf{K}_i^l(t,x)$ tangent to $\mathbf{S}_i^l$ at the point on the edge (boundary) of $\mathbf{S}_i^l$.

For the case of intersecting discontinuity surface $\mathbf{S}_i^l$, Theorem 1 of Filippov (1979) stated that for $t_1 \le t \le t_2$ in Ω, 1) each solution of (2.1) goes from one set $\mathbf{S}_i^l$ into another only a finite number of times; 2) there is uniqueness of the solution up to the boundary in each $\mathbf{S}_i^l$ and 3) each $\mathbf{S}_i^l$ possesses one of the following two properties: a) for all $\mathbf{S}_i^p$ abutting $\mathbf{S}_i^l$ the sets $\mathbf{H}_i^p(t,x)$ are empty for all $x \in \mathbf{S}_i^l$, b) only one of these sets is non-empty and $\mathbf{K}_i^l(t,x)$ is empty. Then, equation (2.1) has the property of unique solution.

2.2 Review of Lyapunov's stability theory and related stability theories

2.2.1 Lyapunov's stability theory

The theory of stability is primarily concerned with motions determined by ordinary differential equations where the initial values serve as parameters. When speaking of stability of these motions, the appendage "with respect to the initial values" will be omitted. Let us consider equation (2.1) where $\mathbf{f(t, x)}$ is continuous and it is further assumed that the equation has a unique solution corresponding to each initial condition, that is, $\mathbf{f(t, x)}$, satisfies a global Lipschitz condition. Vidyasagar (1993) showed that roughly speaking, almost all continuous functions satisfy Lipschitz condition. Let $\mathbf{v}$ be a particular solution determining the unperturbed motion. Assuming

$$y = x - v$$

The differential equation becomes

$$\dot{y} = f(y + v, t) - f(v, t)$$

which is called the differential equation of the perturbed motion. This equation has the trivial solution $y=0$ as an equilibrium. Thus, it is always possible for a system trajectory to correspond to only a single point. Such a point is called an equilibrium point which is defined below

Definition 2.2: A state x^* is an equilibrium state (or equilibrium point) of the system if once $x(t)$ is equal to x^*, it remains equal to x^* for all future time.

Mathematically, it means that the vector x^* satisfies

$$f(t, x^*) = 0$$

Furthermore, we shall make the assumption that the differential equations shall have the trivial solution as an isolated equilibrium.

Definition 2.3: stability in the sense of Lyapunov (i.s.l.)

The equilibrium of equation (2.1) is stable in the sense of Lyapunov (i.s.l.) if and only if for an arbitrary $\varepsilon > 0$, a $\delta > 0$ (δ depends on ε) can be found such that

$$\|x_0\| < \delta$$

implies that

$$\|x(t, x_0)\| < \varepsilon$$

for all $t > t_0$.

Definition 2.4: Lyapunov function

A function $\mathbf{V(x)}$: $\mathbf{R^n \times R \rightarrow R}$ is called a Lyapunov function if the following three conditions are satisfied:

(1) $\mathbf{V(x)}$ is continuous and has continuous first order partial derivatives with respect to $x_1, x_2, \ldots, x_n$ and time t (if t shows in function $\mathbf{V(t, x)}$) in the solution region Ω.

(2) $\mathbf{V(x)}$ is a positive and definite function in the same solution region.

(3) The derivative of $\mathbf{V(x)}$ with respect to time t, $\dot{\mathbf{V}}(\mathbf{x})$, is negative and semi-definite in Ω. For the case that a Lyapunov function is time-varying, $\mathbf{V(t,x)}$ is positive definite if $\mathbf{V(t, 0)=0}$ and there exists a time-invariant positive definite function $\mathbf{V_0(x)}$ such that

$$\forall t \geq 0, \qquad \mathbf{V(t,x) \geq V_0(x)} \tag{2.4}$$

Lyapunov's second method

If equation (2.1) is such that it is possible to find a positive and definite Lyapunov function $\mathbf{V}$, of which the derivative of $\mathbf{V}$ with respect to time, $\dot{\mathbf{V}}$, is negative or reduces identically to zero, the solution of equation (2.1) is stable in the sense of Lyapunov (i.s.l.)

2.2.2 Advanced Lyapunov's stability theory

Consider the situation that the function, $\mathbf{V}$, is positive-definite, and that its derivative, $\dot{\mathbf{V}}$, represents a negative and semi-definite function or is identically zero. For autonomous systems, LaSalle's invariant principle (LaSalle, 1960) can be used to prove the asymptotic stability when the derivative of a Lyapunov function, $\dot{\mathbf{V}}$, is negative and semi-definite. For non-autonomous systems, La Salle's principle is not applicable. Generally, asymptotic stability analysis of non-autonomous systems is much harder than that of autonomous systems. An important and simple result which partially remedies this situation is

Barbalat's lemma, which is purely a mathematical result concerning the asymptotic properties of functions and their derivatives (Slotine and Li, 1993). When properly used for dynamic systems, particularly non-autonomous systems, it may lead to the satisfactory solution of many asymptotic stability problems.

Lyapunov-like lemma (based on Barbalat's lemma): If a Lyapunov function $\mathbf{V(x,t)}$ satisfies the following conditions; (1) $\mathbf{V(x,t)}$ is lower bounded; (2) $\dot{\mathbf{V}}(\mathbf{t},\mathbf{x})$ is negative semi-definite and, (3) $\dot{\mathbf{V}}(\mathbf{t},\mathbf{x})$ is uniformly continuous in time. Then $\dot{\mathbf{V}}(\mathbf{t},\mathbf{x}) \rightarrow \mathbf{0}$ as $\mathbf{t} \rightarrow \mathbf{0}$.

2.2.3 Total stability

Lyapunov theory is mainly developed for stability analysis of nonlinear systems about the equilibrium state with respect to initial conditions. Consider the following equations

$$\dot{\mathbf{x}} = \mathbf{f}(\mathbf{t},\mathbf{x}) + \mathbf{g}(\mathbf{t},\mathbf{x}) \tag{2.5}$$

where $\mathbf{g(x, t)}$ is a perturbation term. We assumed that $\mathbf{x^*=0}$ is an equilibrium point for a unperturbed dynamic system, that is, $\mathbf{f(t,x^*)=0}$. But $\mathbf{x^*=0}$ is not necessarily an equilibrium point for the perturbed system (2.5). If the assumption of an isolated equilibrium point is dropped, the stability in the sense of Lyapunov cannot be formulated. An extension of Lyapunov's stability concept is needed. This extension is the main question addressed by the total stability theory (or stability under persistent disturbances).

Definition 2.5: The equilibrium point $\mathbf{x^*=0}$ for the unperturbed system (2.1) is said to be totally stable if for every $\varepsilon \geq \mathbf{0}$, two numbers δ_1 and δ_2 exist such that $\|\mathbf{x}(\mathbf{t}_0)\| < \delta_1$ and $\|\mathbf{g}(\mathbf{t},\mathbf{x})\| < \delta_2$ imply that every solution $\mathbf{x(t)}$ of the perturbed system (2.5) satisfies the condition $\|\mathbf{x}(\mathbf{t})\| < \varepsilon$.

Definition 2.5 means that an equilibrium point is totally stable if the state of the perturbed system can be kept arbitrarily close to zero by restricting the initial state and the perturbation to sufficiently small values. Note that total stability is a local version (with small input) of bounded input bounded output stability. In Russian literature, this type of stability is called stability under constantly acting perturbations (Dubosin, 1940). Vorovich (1956) extended the definition to the case where the perturbation forces are statistically given random functions.

Theorem of total stability: If the equilibrium point of the undisturbed system is uniformly asymptotically stable, then it is totally stable for a system defined by equation (2.5).

Total stability guarantees boundness to only small disturbance, and requires only local asymptotic stability of the equilibrium point. A natural question is whether the global uniform asymptotic stability can guarantee the boundness of the state in the presence of large (though still bounded) perturbations. The general condition for the total stability with large, but bounded perturbations is not yet known. Krasovskii (1954) derived the sufficient conditions of total stability with large perturbations for some specific autonomous systems. Vrkoc (1959) closely investigated the above case in which the perturbation function satisfies certain integral conditions.

2.2.4 Generalized Lyapunov analysis

The major challenge in using Lyapunov's second method is that there is no constructive rule available on how to construct a Lyapunov function. The requirement of non-negative $\dot{\mathbf{V}}$ implies that $\mathbf{V}$ must decrease monotonically or remain constant. In some work, Lyapunov's second method was generalized to relax the condition on monotonical

decrease in V (referred to here as a quasi Lyapunov function). Such an approach was initially developed by Reissig (1959 and 1960) and summarized by Hahn (1963). The idea of such a generalized Lyapunov analysis is explained using the following example:

The phase plane is divided into three regions (A, B and C) as shown in Fig. 2.2. In Region A and B, the quasi Lyapunov function V is the same as the standard Lyapunov function, that is, the function itself and its derivative with respect to time are continuous and furthermore, the function V is positive and its time derivative, $\dot{V}$, is negative. In

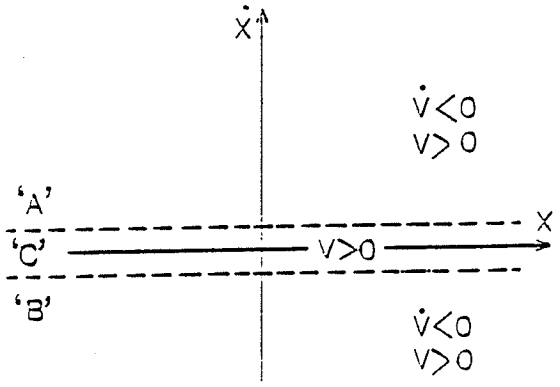

Figure 2.2 Generalized Lyapunov analysis

Region C, all the above conditions are satisfied except that the time derivative of function V can not be guaranteed to be negative. The fact of a non-negative time derivative of $\dot{V}$ might lead to an increase in the quasi Lyapunov function in Region C. However, if we know that the amount of the increase in the quasi Lyapunov function in Region C is lower than the amount of the decrease in the Region A or B, respectively, the system stability is still guaranteed (Hahn, 1963). The stability is believed weaker than the stability in the sense of Lyapunov. Therefore, it is referred to in this dissertation as practical stability, that is, the solution to equation (2.1) is stable in a controlled region around the zero states.

CHAPTER THREE

ON LYAPUNOV STABILITY ANALYSIS OF NONLINEAR/NON-SMOOTH DYNAMIC SYSTEMS

3.1 Introduction

As discussed before, Lyapunov's second method is valid only for smooth dynamic systems. It is to be proven in this chapter that Lyapunov's second method can be extended to non-smooth dynamic systems given the condition of the existence and uniqueness of Filippov's solutions.

It was believed that non-smooth Lyapunov functions are natural for non-smooth systems. However, using non-smooth Lyapunov functions, the evaluation of its derivative with respect to time can be extremely difficult which makes the stability analysis of non-smooth systems almost impossible. In this chapter, it is shown that smooth Lyapunov functions can be constructed for some non-smooth systems in a simpler way as compared with the non-smooth ones.

As was also discussed in the previous chapter, the construction of a Lyapunov function is highly challenging since there are no rules or methodology mentioned in Lyapunov's theory. Though much work has been done on development of techniques to construct Lyapunov functions, those techniques are for specific classes of nonlinear systems. Chin's generalized integral method (Chin, 1987) provides a systematic approach to the construction of Lyapunov functions for general nonlinear systems. However, the success in construction of a Lyapunov function using Chin's integral method depends not only on the proper choice of weighting functions but also on the existence or development of compatible state-space models. This need for a compatible dynamic state-space model may

restrict the range of systems suitable for application of the integral method. Therefore, an extended integral method is also developed in this chapter to reduce the sensitivity of Chin's integral method to the form of the state-space model.

3.2 Extension of Lyapunov's second method to non-smooth dynamic systems

To prove that Lyapunov's second method can be extended to non-smooth dynamic system directly, the following lemmas (Vidyasagar, 1993) are to be used.

Definition: A function $\phi: \mathbf{R}_+ \rightarrow \mathbf{R}_+$ is of class **K** if it is continuous, strictly increasing, and $\phi(0) = 0$.

Lemma: Suppose $\phi: \mathbf{R}_+ \rightarrow \mathbf{R}_+$ is continuous, that $\phi(0) = 0$, ϕ is non-decreasing, and that $\phi(r) > 0$, $\forall r > 0$. Then there exists a function α of class **K** such that $\alpha(r) \leq \phi(r)$ for $\forall r$. Moreover, if $\phi(r) \rightarrow \infty$ as $r \rightarrow \infty$, then α can be chosen to have the same property.

Proof of the validity of Lyapunov's second method to non-smooth dynamic systems

If a Lyapunov function can be constructed for a nonlinear system, two constants **H** and **T** can be found such that, for all values of the state variables $x_1, \ldots, x_n, t$ which satisfy the condition that if $t \geq T$,

$$\|x\| \leq H \tag{3.1}$$

the following inequalities exist:

$$\dot{V}(t,x) \leq 0 \tag{3.2}$$

According to the above lemma, we have

$$V(t,x) \geq W(\|x\|) \tag{3.3}$$

where **W** is a function of class **K**.

Let us consider $\mathbf{x}$ (the vector function of time $\mathbf{t}$) as a solution to the differential equations in the sense of Filippov which is uniquely dependent on the initial conditions. It is also assumed that the vector function $\mathbf{x_0}$ for $\mathbf{t = T}$ satisfying (3.1) with an inequality sign. Then, by virtue of the continuity of these functions, (3.1) is satisfied for all values of $\mathbf{t}$ sufficiently near $\mathbf{T}$. Let us only consider values of $\mathbf{t}$ not less than $\mathbf{T}$.

Function $\mathbf{V}$ for time $\mathbf{t = T}$ is designated by $\mathbf{V_0}$ and consider relation (3.2) and (3.3) to be satisfied. It can be concluded that function $\mathbf{x}$ will satisfy the condition

$$\mathbf{W(\|x\|) \leq V_0} \tag{3.4}$$

of which the right-hand side can be made arbitrarily small by making $\|\mathbf{x_0}\|$ sufficiently small.

To prove that $\mathbf{0^*}$ is a stable equilibrium point, it must be shown that given any $\varepsilon > \mathbf{0}$ and any $\mathbf{t \geq T}$, we can find a $\delta = \delta(\varepsilon, \mathbf{T})$ such that if $\|\mathbf{x_0}\| < \delta(\varepsilon, \mathbf{T})$, then, $\|\mathbf{x(t, x_0)}\| < \varepsilon$, for any $\mathbf{t \geq T}$. Accordingly, given any ε, $\mathbf{W}(\varepsilon)$ can be determined. Based on the definition of the functions of class $\mathbf{K}$, $\mathbf{W}(\varepsilon)$ is a positive, non-zero function. Consequently, it is always possible to make $\mathbf{V_0}$ less than $\mathbf{W}(\varepsilon)$. This is because $\mathbf{W}(\varepsilon)$ is a positive and non-zero function and $\mathbf{V_0}$ can tend to zero as $\mathbf{x_0}$ tends to zero. Thus, it is always possible to find a number $\delta(\varepsilon, \mathbf{T})$ such that whenever $\mathbf{x_0}$ satisfies the condition

$$\|\mathbf{x_0}\| \leq \delta(\varepsilon, \mathbf{T}) \tag{3.5}$$

the following inequality

$$\mathbf{V_0 < W}(\varepsilon) \tag{3.6}$$

is satisfied.

According to equations (3.2) and (3.6), the following form results

$$V(t, x(t, x_0)) \leq V_0 < W(\varepsilon) \tag{3.7}$$

Based on (3.3),

$$V(t, x(t, x_0)) \geq W(\|x\|) \tag{3.8}$$

and the following inequality exists

$$W(\|x\|) < W(\varepsilon) \tag{3.9}$$

Since $W(\|x\|)$ is a strictly increasing and positive function, it can be concluded that

$$\|x\| < \varepsilon \tag{3.10}$$

From this analysis and logical development, it is seen that the theorem is proven.

3.3 Construction of smooth Lyapunov functions for non-smooth dynamic systems

In the previous work of extension of Lyapunov's second method (Paden and Sastry, 1987, Southwood *et al.*, 1993 and Shevitz and Paden, 1994), Lyapunov functions are non-smooth because it was believed that non-smooth Lyapunov functions are natural for non-smooth systems. The main difficulty in using those methods, however, is the determination of the sign of the total derivative of non-smooth Lyapunov functions as the solution trajectories approach the discontinuity surfaces. Such a determination of the sign is related to the intersection of infinite convex sets which becomes more difficult when the discontinuity surface is the intersection of several discontinuity surfaces.

It is demonstrated in this section that smooth Lyapunov functions can be constructed for some non-smooth systems in a simpler way. The reason is that the discontinuous derivative of the vector of states does not necessarily lead to a discontinuous derivative of a Lyapunov function. The key step to construct smooth Lyapunov functions for non-

smooth dynamic systems is to construct Lyapunov functions such that its derivative with respect to time can be divided into two parts — one part relates to the discontinuous derivative of the vector of states which is bounded due to the existence of Filippov's solution, and the other part is continuous and tends to zero when the first part is discontinuous. Although such a requirement of keeping the derivative of the Lyapunov function as zero on the discontinuity surfaces appears to impose restrictions to the form of Lyapunov functions, it can be easily satisfied for many systems as shown in the following examples.

Example 1: Stability of a non-smooth system (Shevitz and Paden, 1994)

Consider the construction of Lyapunov functions for the following non-smooth system

$$\dot{\mathbf{x}} = -\mathbf{R}(\mathbf{x}(t), t)\nabla\|\mathbf{x}\|_1 \tag{3.11}$$

where $\mathbf{R}$ is an $\mathbf{n}\times\mathbf{n}$ matrix such that $\mathbf{R}_{ii} \geq \sum_{\substack{j=1 \\ j\neq i}}^{n} |\mathbf{R}_{ij}|$. The above example is generalized from the one given in the work of Shevitz and Paden (1994) where $\mathbf{R}$ is a special case of the one shown above. $\|\mathbf{x}\|_1 = \sum_{i=1}^{n} |\mathbf{x}_i|$ and $\nabla\|\mathbf{x}\|_1$ is not defined on the $\mathbf{x}_i$ axis, sets of measure zero. On the $\mathbf{x}_i$ axis, $\nabla\|\mathbf{x}\|_1$ is the convex hull, for example of $\mathbf{n=2}$, when the solution trajectory approaches the origin $(\mathbf{0}, \mathbf{0})$ (the intersection of the discontinuity surfaces), we have

$$\mathbf{K[f](x)} = \overline{\mathbf{co}}\{(-1, 1), (1, 1), (1, -1), (-1, -1)\}$$

The right-hand side of (3.11) is a discontinuous vector function. The existence and uniqueness of Filippov's solution for (3.11) can be proven, but not detailed here. Choosing

$V = \frac{1}{2}\sum_{i=1}^{n} x_i^2 = \frac{1}{2}\|x\|_2$ as a Lyapunov function for (3.11), V is continuous, positive and definite. The derivative of V can be calculated as follows:

For $x_i \neq 0$ $(i = 1,\ldots,n)$

$$\dot{V} = x^T\dot{x} = -x^T R\nabla\|x\|_1 = -x^T R(\mathrm{sgn}(x_1),\ \mathrm{sgn}(x_2),\ldots,\mathrm{sgn}(x_n))^T$$

$$= -[|x_1|R_{11} + \sum_{i=2}^{n} x_1 R_{1j}\,\mathrm{sgn}(x_j) + |x_2|R_{22} + \sum_{\substack{i=1 \\ j\neq 2}}^{n} x_2 R_{2j}\,\mathrm{sgn}(x_j) + \ldots, +$$

$$|x_n|R_{nn} + \sum_{i=1}^{n-1} x_n R_{nj}\,\mathrm{sgn}(x_j)]$$

Since $R_{ii} \geq \sum_{\substack{j=1 \\ j\neq i}}^{n} |R_{ij}|$, we have $\dot{V} \leq 0$.

For $x_i = 0$ $(i = 1,2,\ldots,n)$ where the discontinuity surface is the intersection of all the single discontinuity surfaces.

$$\lim_{x_i\to 0^+}\dot{V} = \lim_{x_i\to 0^+}\lim_{\Delta t\to 0^+}\frac{\|x(t+\Delta t)\|_2 - \|x(t)\|_2}{\Delta t} = \frac{1}{2}\lim_{x_i\to 0^+}\lim_{\Delta t\to 0^+}\frac{1}{\Delta t}\sum_{i=1}^{n}[x_i^2(t+\Delta t) - x_i^2(t)]$$

$$= \lim_{x_i\to 0^+}\lim_{\Delta t\to 0^+}\sum_{i=1}^{n} x_i\frac{x_i(t+\Delta t) - x_i(t)}{\Delta t} = 0$$

Note that from the condition of the existence of Filippov's solution, we have that $\frac{x_i(t+\Delta t) - x_i(t)}{\Delta t}$ is bounded. Following the same procedure shown above, it can be shown that $\lim_{x_i\to 0^-}\dot{V} = 0$ and $\dot{V}$ is continuous when x_i=0 (i=1,2,...,n). For the cases that some of x_i (i=1,2,...,n) tend to zero, a similar conclusion can be obtained. Therefore, $\dot{V}$ is continuous and not positive, that is, the above Lyapunov function V for (3.11) is a smooth Lyapunov function.

To appreciate the simplicity of the construction of smooth Lyapunov functions as compared to non-smooth Lyapunov functions, we choose the same non-smooth Lyapunov function used by Shevitz and Paden (1994) for (3.11) as $\mathbf{V} = |\mathbf{x}_1| + |\mathbf{x}_2|$ for a simplified case of **n=2**. Such a Lyapunov function has negative derivative when both $\mathbf{x}_1$ and $\mathbf{x}_2$ are non-zero. Here, for the case that $\mathbf{x}_1 = \mathbf{0}$ and $\mathbf{x}_2 = \mathbf{0}$, that is, the discontinuity surface is the intersection of two discontinuity surfaces $\mathbf{x}_1 = \mathbf{0}$ and $\mathbf{x}_2 = \mathbf{0}$, in order to guarantee the stability, the following relationship must be proven:

$$\dot{\tilde{\mathbf{V}}}(\mathbf{x}, \mathbf{t}) := \bigcap_{\xi \in \partial \mathbf{V}} \xi^{\mathrm{T}} \mathbf{K}[\mathbf{f}](\mathbf{x}, \mathbf{t}) \leq \mathbf{0}$$

$\dot{\tilde{\mathbf{V}}}(\mathbf{x}, \mathbf{t})$ defined in Shevitz and Paden (1994) is the set of intersection of $\xi^{\mathrm{T}} \mathbf{K}[\mathbf{f}](\mathbf{x}, \mathbf{t})$ where ξ takes all values of set $\partial \mathbf{V}$. The generalized gradient, $\partial \mathbf{V}$, is a convex set which has the form $\overline{\mathbf{co}}\{(-1, 1)^{\mathrm{T}}, (1, 1)^{\mathrm{T}}, (-1,-1)^{\mathrm{T}}, (1,-1)^{\mathrm{T}}\}$ for this example. Filippov's differential inclusion, **K[f](x,t)** is also a convex set as

$$\overline{\mathbf{co}}\{-(\mathbf{R}_{11} + \mathbf{R}_{12}, \mathbf{R}_{21} + \mathbf{R}_{22})^{\mathrm{T}}, \; -(\mathbf{R}_{11} - \mathbf{R}_{12}, \mathbf{R}_{21} - \mathbf{R}_{22})^{\mathrm{T}}, \; (\mathbf{R}_{11} - \mathbf{R}_{12}, \mathbf{R}_{21} - \mathbf{R}_{22})^{\mathrm{T}}, \; (\mathbf{R}_{11} + \mathbf{R}_{12}, \mathbf{R}_{21} + \mathbf{R}_{22})^{\mathrm{T}}\}$$

Where the $\mathbf{R}_{ij}$ $(\mathbf{i}, \mathbf{j} = \mathbf{1,2})$ are the values when $\mathbf{x}_1 \to \mathbf{0}$ and $\mathbf{x}_2 \to \mathbf{0}$. To prove that $\dot{\tilde{\mathbf{V}}}(\mathbf{x}, \mathbf{t}) \leq \mathbf{0}$ requires the knowledge of convex analysis and is not always easy.

This example shows that a non-smooth Lyapunov function can be avoided by making parts of the gradient of the Lyapunov function, which corresponds to the discontinuous terms in the inner product, zero on the discontinuity surfaces. The example also shows that though in Shevitz and Paden's work (1994), the restriction of differentiability of Lyapunov functions is weakened as compared with smooth Lyapunov functions, the

difficulty in determining the sign of $\dot{\tilde{V}}(x,t)$ is introduced. From our experience, when the discontinuity surface is the intersection of several discontinuity surfaces, the task of determining the sign of the derivatives of non-smooth Lyapunov functions can be very difficult.

Example 2: Stability of a control system with friction (Cai and Song, 1993)

Consider a harmonic oscillator with stick-slip friction in the form of a state-space model

$$\begin{aligned} \dot{x}_1 &= x_2 \\ \dot{x}_2 &= -\frac{\Gamma_{fric}}{m} - \frac{k}{m}x_1 \end{aligned} \tag{3.12}$$

Γ_{fric} represents the stick-slip friction formulated by Cai and Song (1993) as follows:

$$\tau_{fric} = -\mathbf{sgn}(x_2)\tau_{slip} - \{1 - \mathbf{abs}[\mathbf{sgn}(x_2)]\}\tau_{stick}(\tau_{appl}) \tag{3.13}$$

where $\tau_{appl} = -\frac{k}{m}x_1$ and $\mathbf{sgn}(x_2)$ and τ_{stick} are defined as follows

$$\mathbf{sgn}(x_2) = \begin{cases} 1 & x_2 > 0 \\ 0 & x_2 = 0 \\ -1 & x_2 < 0 \end{cases}$$

$$\tau_{stick}(\tau_{appl}) = \begin{cases} \tau_{appl} & \mathbf{abs}(\tau_{appl}) < \tau_{max} \\ \tau_{max} & \mathbf{abs}(\tau_{appl}) \geq \tau_{max} \end{cases}$$

It is noted that τ_{fric} is a discontinuous function and the absolute value of τ_{fric} is bounded within $[0, \max\{\tau_{slip}, \tau_{max}\}]$. The right-hand side of (3.12) is discontinuous for $x_2 = 0$, but it is Lebesgue measurable and bounded. The existence and uniqueness of Filippov's solution to (3.12) have been proven by Filippov (1964). A Lyapunov function for (3.12) is

constructed as $V(x_1,x_2)=\frac{1}{2}mx_2^2+\frac{1}{2}kx_1^2$ which is continuous, positive and definite. Its derivative with respect to time, $\dot{V}$, is

For $x_2 \neq 0$

$$\dot{V} = mx_2\dot{x}_2 + kx_1x_2 = -\tau_{slip}x_2\,\mathrm{sgn}(x_2) = -\tau_{slip}|x_2| < 0$$

For $x_2 \to 0$

$$\dot{V}(x_1,0) = \lim_{x2\to 0^+}\dot{V} = \lim_{x2\to 0^-}\dot{V} = \lim_{x2\to 0}\lim_{\Delta t\to 0}\frac{V(t+\Delta t)-V(t)}{\Delta t} = m\lim_{x2\to 0}\lim_{\Delta t\to 0}x_2\frac{\Delta x_2}{\Delta t} = 0$$

It is known that $\dot{x}_2$ is not continuous but bounded (condition for the existence of Filippov's solution). It should be noted that though $\dot{x}_2$ is not continuous at $x_2 = 0$, $x_2\dot{x}_2$ is uniquely defined and continuous. Therefore, $\dot{V}$ is uniquely defined and is continuous, negative and semi-definite. Based on the above discussion, V is a smooth Lyapunov function for the non-smooth system shown in (3.12).

Example 3: Variable structure control of robot manipulators (Stepanenko and Su, 1993)

Consider the sliding mode equation, describing variable structure control of robot manipulators (Stepanenko and Su, 1993) as follows:

$$D\dot{s} = \Phi\psi - \Phi\alpha - Bs - K_1 s - K_2\,\mathrm{sgn}(s) \qquad (3.14)$$

where matrix D is the symmetric, bounded, positive definite inertia matrix; matrix Φ is the regressor matrix; matrix B represents the centripetal and Coriolis torques; K_1 and K_2 are positive definite design matrices. $s=0$ is the general sliding manifold, $\mathrm{sgn}(s)$ is the sign function and $\psi \in R^m$ is the vector of switching functions defined below:

$$\psi_i = -\overline{\alpha}_i\,\mathrm{sgn}\left(\sum_{j=1}^{n} s_j\Phi_{ji}\right)$$

System (3.14) describes a variable structure control of robot manipulators with nonlinear sliding manifolds and the robustness of the controller with respect to a class of state-dependent uncertainties was also analyzed (Stepanenko and Su, 1993). The right-hand side of (3.14) is discontinuous when the solution trajectory crosses the sliding manifold $\mathbf{S}$ or ψ_i changes its sign. The Lyapunov function for system (3.14) can be constructed as $\mathbf{V(s)} = \frac{1}{2}\mathbf{s}^T\mathbf{Ds}$ which is continuous, positive and definite. Its derivative with respect to time is

$$\dot{\mathbf{V}} = \mathbf{s}^T(\Phi\psi - \Phi\alpha - \mathbf{K}_1\mathbf{s} - \mathbf{K}_2\,\mathbf{sgn(s)})$$

It can be easily proven that $\dot{\mathbf{V}}$ is never positive in the continuous region. We prove here that $\dot{\mathbf{V}}$ is continuous when $\mathbf{s} = \mathbf{0}$ and when ψ_i is not continuous.

Case 1: $\mathbf{s} = \mathbf{0}$, that is the solution trajectory approaches to the sliding manifold.

$$\lim_{\mathbf{s}\to 0^+} \dot{\mathbf{V}} = \lim_{\mathbf{s}\to 0^+} \mathbf{s}^T[\Phi\psi - \Phi\alpha - \mathbf{K}_1\mathbf{s} - \mathbf{K}_2\,\mathbf{sgn(s)}] = \mathbf{0}$$

Note that the right-hand side of the system (3.14) (shown in the bracket of the above equation) is bounded due to the existence of Filippov's solution. Thus $\dot{\mathbf{V}} = \mathbf{0}$ as $\mathbf{s} \to \mathbf{0}^+$. Following the same procedure, it can be proven that $\lim_{\mathbf{s}\to 0^-} \dot{\mathbf{V}} = \mathbf{0}$. From the expression of $\dot{\mathbf{V}}$, we have $\dot{\mathbf{V}} = \mathbf{0}$. Therefore, $\dot{\mathbf{V}}$ is continuous when $\mathbf{s} = \mathbf{0}$.

Case 2: ψ_i is not continuous, that is $\lambda_i = \sum_{j=1}^{n} \mathbf{s}_j\Phi_{ji} \to \mathbf{0}$.

$$\lim_{\lambda_i\to 0^+} \dot{\mathbf{V}} = \lim_{\lambda_i\to 0^+} \mathbf{s}^T(\Phi\psi - \Phi\alpha - \mathbf{K}_1\mathbf{s} - \mathbf{K}_2\,\mathbf{sgn(s)})$$

$$= \lim_{\lambda_i\to 0^+} \{-\mathbf{s}^T\mathbf{K}_1\mathbf{s} - \mathbf{s}^T\mathbf{K}_2\,\mathbf{sgn(s)} - \sum_{i=1}^{m}\alpha_i\sum_{j=1}^{n}\mathbf{s}_j\Phi_{ji} - \sum_{i=1}^{m}\overline{\alpha}_i\left|\sum_{j=1}^{n}\mathbf{s}_j\Phi_{ji}\right|\}$$

The first three terms are continuous, the last term which is related to λ_i tends to zero. Thus, we have

$$\lim_{\lambda_i \to 0^+} \dot{V} = \lim_{\lambda_i \to 0^-} \dot{V} = \lim_{\lambda_i \to 0^+} \{-s^T K_1 s - s^T K_2 \, \mathrm{sgn}(s) - \sum_{i=1}^{m} \alpha_i \sum_{j=1}^{n} s_j \Phi_{ji}\} = \dot{V}(\lambda_i = 0)$$

Therefore, $\dot{V}$ is a continuous function, and the Lyapunov function shown above is a smooth Lyapunov function for system (3.14).

In summary, the main difficulty in construction of non-smooth Lyapunov functions is the evaluation of its derivative on the discontinuity surfaces which leads to the determination of the intersection of infinite convex sets. Such a limitation may cause the Lyapunov stability analysis of some non-smooth systems impractical. The above examples show that smooth Lyapunov functions can be constructed for some non-smooth systems in a simpler way. The approach to derive a smooth Lyapunov function for a non-smooth system is the same as its smooth counterpart except that parts of the gradient of the Lyapunov function corresponding to the discontinuous term in the rate of the state vector are such that the production of the discontinuous term of the rate of state vectors and the corresponding parts of the gradient of the smooth Lyapunov function must be zero on the discontinuity surfaces. For some cases, such as the first two examples, the corresponding parts of the gradient of the Lyapunov functions are set to be zero directly. It is shown from the above examples, the requirement of keeping the zero-production of the discontinuous terms of the rate of state vector and the corresponding parts of the gradient of Lyapunov functions can be easily satisfied. Thus, smooth Lyapunov functions can be easier to use for some non-smooth systems. Note that the presented method is not the replacement of the previous work (Shevitz and Paden, 1994), but rather a complementary

study. For some non-smooth systems, non-smooth Lyapunov functions appears to be the only choices.

3.4 Development of the extended integral method

In this section, the generalized integral method is extended, with the main objective of reducing the sensitivity of the method to the form of the state-space model. This extension is achieved by simply allowing all the state variables, including their time derivatives, to be incorporated in each weighting function. As a result of this inclusion, the compatibility requirements imposed on the state-space models are relaxed due to the fact that the choice of a less compatible state-space model can be compensated through proper choice of the weighting functions. This treatment, as will be demonstrated, will lead to a less restrictive and more easily constructed Lyapunov function. It is also noted that most of the techniques of constructing Lyapunov functions are developed for autonomous systems which exclude many engineering systems. The extended method can be applied to both autonomous and non-autonomous systems, including those with time as an explicit variable.

3.4.1 Derivation of Lyapunov functions: an extended integral method

Consistent with the generalized integral method developed by Chin (1987b), we consider a nonlinear dynamic system represented by the following general state-space model:

$$\dot{x}_i = f_i(t,x_1,..,x_n) \qquad i = 1,2,...,n \qquad (3.15)$$

Equation (3.15) implies that the system under study can be either autonomous or non-autonomous. Function $f_i(t,x_1,..,x_n)$ can be either continuous or discontinuous. Rewriting this equation in the following form

$$L_i = \dot{x}_i - f_i(t,x_1,..,x_n) = 0 \tag{3.16}$$

we then define the following integral

$$I_i = \int_0^t w_i(t,x_1,..,x_n,\dot{x}_1,..,\dot{x}_n)L_i dt = 0 \tag{3.17}$$

where $w_i(t,x_1,..,x_n,\dot{x}_1,..,\dot{x}_n)$ represents a continuous weighting function of time and some or all the state variables and their time derivatives. For the case of discontinuous $f_i(t,x_1,..,x_n)$, the production of $w_i(t,x_1..,x_n,\dot{x}_1..,\dot{x}_n)f_i(t,x_1..,x_n)$ must be continuous to guarantee that I_i can be integrated. Equation (3.17) is now summed over **i=1,2,...n,**

$$I = \sum_{i=1}^{n} I_i = 0 \tag{3.18}$$

which alternately can be rearranged as follows:

$$F(t,x_1,\ldots,x_n) + \int_0^t G(t,x_1,\ldots,x_n)dt = 0 \tag{3.19}$$

Comparing (3.19) with the following equation

$$V(t,x_1,..,x_n) + \int_0^t -\dot{V}(t,x_1,..,x_n)dt = 0$$

one can easily write the following relations:

$$V(t,x_1,..,x_n) = F(t,x_1,..,x_n)$$
$$\dot{V}(t,x_1,..,x_n) = -G(t,x_1,..,x_n)$$

if $\mathbf{F}(t,x_1,..,x_n)$ is positive definite and $-\mathbf{G}(t,x_1,..,x_n)$ is negative definite or at least semi-definite, we can then claim that for the system represented by (3.15), $\mathbf{V}(t,x_1,..,x_n)$ is the Lyapunov function. The function $w_i(t,x_1,..,x_n,\dot{x}_1,..,\dot{x}_n)$ should be determined such that the conditions imposed on **F** and **-G** are satisfied.

The reason (3.18) is rearranged to form (3.19) lies in the fact that although it is relatively easy to develop a positive definite function for nonlinear systems, for example, energy functions, it may be difficult to prove the negativeness of the time derivative of such a function, especially if the time derivative is calculated from the function directly. In (3.19), the time derivative of **F** is given as (**-G**) which incorporates weighting functions. The weighting functions are then adjusted to result in a negative (**-G**).

The extended integral method includes most of Chin's methods. Several cases can be demonstrated. Note that

$$w_i(t,x_1,..,x_n,\dot{x}_1,..,\dot{x}_n)=\sum_{k=1}^{n} g_{ik}(x_k) \qquad (3.20)$$

will lead to Chin's generalized integral method where $g_{ik}(x_k)$ is a function of only one state variable x_k (Chin 1987b). Chin's intrinsic method is also a special case of the extended integral method. This is proven in the following way:

Assuming

$$w_{k+1}(t,x_1,..,x_n,\dot{x}_1,..,\dot{x}_n)=\dot{x}_k \qquad k+1\le n$$
$$w_i(t,x_1,..,x_n,\dot{x}_1,..,\dot{x}_n)=0 \qquad i\ne k+1,\ i=1,..,n$$

The integral **I** in (3.18) is written as follows:

$$\mathbf{I} = \int_0^t \dot{x}_k (\dot{x}_{k+1} - f_{k+1}(x_1,..,x_n))dt$$
$$= \int_0^t \dot{x}_k \dot{x}_{k+1} dt - \int_0^t \dot{x}_k f_{k+1}(x_1,..,x_n)dt \qquad (3.21)$$

Note that

$$\dot{x}_k = f_k(x_1,..,x_n)$$

Thus,

$$\mathbf{I} = \int_0^{x_{k+1}} f_k(x_1,..,x_n)\dot{x}_{k+1}dt - \int_0^{x_k} f_{k+1}(x_1,..,x_n)\dot{x}_k dt = 0$$

which is equivalent to

$$\int_0^{x_{k+1}} f_k(x_1,..,x_n)dx_{k+1} = \int_0^{x_k} f_{k+1}(x_1,..,x_n)dx_k \qquad (3.22)$$

(3.22) is identical to (11) of Chin's intrinsic method (Chin 1988).

3.4.2 Examples of the application of the extended integral method

In this case study, the extended integral method is used, for the first time, to derive a Lyapunov function for a generalized nonlinear system described by:

$$\dot{x}_1 = x_2$$
$$\dot{x}_2 = -D(x_1,x_2,x_3)x_2 - ax_3 - h(x_1)$$
$$\dot{x}_3 = gx_2 - bx_3 \qquad (3.23)$$

where **a**, **b** and **g** are positive constants, $D(x_1,x_2,x_3)$, $h(x_1)$ are continuous and differentiable functions. System (3.23) is generalized from the state-space model describing a power system. Lyapunov functions have been constructed for the specific form of system (3.23) by Mukherjee and Bhattacharyya (1972), Miyagi and Taniguchi (1980) and Chin (1987b). The above construction is relatively less constructive and is only valid for the specific cases. It will be shown that using the extended integral method, the construction of a Lyapunov function for system (3.23) is easier and more systematic.

Identical Lyapunov functions to the previous ones can be constructed using the extended integral method and none of the previous construction can be used for system (3.23).

Following the extended integral method, the Lyapunov function is constructed by choosing the following weighting functions

$$\begin{aligned} w_1 &= 0 \\ w_2 &= gx_2 + ax_3 \\ w_3 &= x_3 - \frac{D(x_1,x_2,x_3)}{b}x_2 \end{aligned} \tag{3.24}$$

The integrals are calculated as follows:

$$I_1 = 0$$

$$\begin{aligned} I_2 &= \int_0^t s_2 L_2 dt \\ &= \int_0^t (x_3 + gx_2)(\dot{x}_2 + D(x_1,x_2,x_3)x_2 + ax_3 + h(x_1))dt \\ &= \frac{1}{2}gx_2^2 + g\int_0^{x_1} h(x_1)dt + g\int_0^t (ax_2x_3 + D(x_1,x_2,x_3)x_2^2)dt \\ &\quad + \int_0^t x_3(\dot{x}_2 + D(x_1,x_2,x_3)x_2 + ax_3 + h(x_1))dt \end{aligned}$$

$$\begin{aligned} I_3 &= \int_0^t s_3 L_3 dt \\ &= \int_0^t (ax_3 - \frac{D(x_1,x_2,x_3)}{b}x_2)(\dot{x}_3 - gx_2 + bx_3)dt \\ &= \frac{1}{2}ax_3^2 + a\int_0^t (-gx_2x_3 + bx_3^2)dt - \frac{1}{b}\int_0^t D(x_1,x_2,x_3)x_2(\dot{x}_3 - gx_2 + bx_3)dt \end{aligned}$$

Therefore

$$\begin{aligned} I &= g\int_0^{x_1} h(x_1)dx_1 + \frac{1}{2}gx_2^2 + \frac{1}{2}ax_3^2 + \int_0^t gD(x_1,x_2,x_3)(1+\frac{1}{b})x_2^2 + (ab+a)x_3^2 dt \\ &\quad + \int_0^t x_3\dot{x}_2 dt - \int_0^t \frac{D(x_1,x_2,x_3)}{b}x_2\dot{x}_3 dt + \int_0^t x_3 h(x_1)dt \end{aligned}$$

Rewriting equations (3.23) in the following form:

$$\begin{aligned} -D(x_1,x_2,x_3)x_2 &= \dot{x}_2 + ax_3 + h_{(x_1)} \\ \dot{x}_3 &= gx_2 - bx_3 \end{aligned} \tag{3.25}$$

and substituting equations (3.25) into the integral **I:**

$$\begin{aligned}
\mathbf{I} &= g\int_0^{x_1} h(x_1)dx_1 + \frac{1}{2}gx_2^2 + \frac{1}{2}ax_3^2 + \int_0^t gD(x_1,x_2,x_3)(1+\frac{1}{b})x_2^2 + a(b+1)x_3^2 dt \\
&\quad + \int_0^t x_3\dot{x}_2 dt + \frac{1}{b}\int_0^t \dot{x}_3(\dot{x}_2 + ax_3 + h(x_1))dt + \int_0^t x_3 h(x_1)dt \\
&= g\int_0^{x_1} h(x_1)dx_1 + \frac{1}{2}gx_2^2 + \frac{1}{2}ax_3^2 + \int_0^t gD(x_1,x_2,x_3)(1+\frac{1}{b})x_2^2 + a(b+1)x_3^2 dt \\
&\quad + \int_0^t x_3\dot{x}_2 dt + \frac{1}{b}\int_0^t (gx_2 - bx_3)(\dot{x}_2 + h(x_1))dt + \frac{a}{2b}x_3^2 + \int_0^t x_3 h(x_1)dt \\
&= g(1+\frac{1}{b})\int_0^{x_1} h(x_1)dx_1 + \frac{1}{2}g(1+\frac{1}{b})x_2^2 + \frac{1}{2}a(1+\frac{1}{b})x_3^2 \\
&\quad + \int_0^t gD(x_1,x_2,x_3)(1+\frac{1}{b})x_2^2 + a(b+1)x_3^2 dt
\end{aligned}$$

F, G, V and $\dot{\mathbf{V}}$ are derived as follows:

$$\begin{aligned}
\mathbf{V} &= (1+\frac{1}{b})^{-1}\mathbf{F} = g\int_0^{x_1} h_{(x_1)}dx_1 + \frac{1}{2}gx_2^2 + \frac{1}{2}ax_3^2 \\
-\dot{\mathbf{V}} &= (1+\frac{1}{b})^{-1}\mathbf{G} = gD_{(x_1,x_2)}x_2^2 + abx_3^2
\end{aligned} \qquad \textbf{(3.26)}$$

It follows that in order to keep $\dot{\mathbf{V}}$ negative and at least semi-definite, $\mathbf{D}(x_1,x_2,x_3)$ must be a non-negative, continuous and differentiable function. **V** is positive definite only for $\mathbf{V} \le \mathbf{V}_{max}$ where $\mathbf{V}_{max}$ is the Lyapunov function for the family of the closed hyper-surfaces of **V** in the phase plane (Mukherjee and Bhattacharyya 1972). $\mathbf{V}_{max}$ can be found by solving for the zeros of the gradient of **V** and then substituting these values into **V**. For the Lyapunov function shown by equations (3.26), $\mathbf{V}_{max}$ is as follows:

$$\mathbf{V}_{max} = g\int_0^{\tilde{x}_1} h(x_1)dx_1$$

where $\mathbf{h}(\tilde{\mathbf{x}}_1) = \mathbf{0}$. Hence, the conditions for the stability are that there exists $\tilde{\mathbf{x}}_1$ such that $\mathbf{h}(\tilde{\mathbf{x}}_1) = \mathbf{0}$ and that $\mathbf{D}(x_1,x_2,x_3) \ge \mathbf{0}$.

The Lyapunov function for the above general system is thus constructed. Next we consider three special cases for which Lyapunov functions were previously derived by others.

Special case 1: Chin (1987b): Assuming

$$\mathbf{D}(x_1, x_2, x_3) = \mathbf{D}(x_1)$$

The general Lyapunov function shown in equations (3.26) is reduced to:

$$\mathbf{V} = (1+\frac{1}{b})^{-1}\mathbf{F} = g\int_0^{x_1} \mathbf{h}(x_1)dx_1 + \frac{1}{2}gx_2^2 + \frac{1}{2}ax_3^2$$

$$\dot{\mathbf{V}} = -(1+\frac{1}{b})^{-1}\mathbf{G} = -(g\mathbf{D}(x_1)x_2^2 + abx_3^2)$$

The restrictions are that $\mathbf{D}(x_1) \geq 0$ and that there exists $\tilde{x}_1$ such that $\mathbf{h}(\tilde{x}_1) = 0$. The Lyapunov function for the above system was also derived by Chin (1987b) as follows:

$$2\mathbf{V} = \frac{a}{g}x_3^2 + (x_2 + \alpha'\mathbf{D}_1(x_1))^2 + \alpha'(1-\alpha')\mathbf{D}_1^2(x_1) + 2\int_0^{x_1}\mathbf{h}(x_1)dx_1$$

$$+ 4\int_0^t (\alpha'(1-\alpha')(\mathbf{h}(x_1) - \frac{\alpha' ag}{4b}\mathbf{D}(x_1))\mathbf{D}(x_1)\mathbf{D}_1(x_1))^{\frac{1}{2}}dx_1$$

where

$$\mathbf{D}_1(x_1) = \int_0^{x_1}\mathbf{D}(x_1)dx_1$$

and α' is defined as a function of **a** and **g**. The conditions for stability are :

$$0 \leq \alpha' \leq 1$$

$$\mathbf{D}(x_1) > 0$$

$$\mathbf{D}_1(x_1)\mathbf{h}(x_1) \geq \frac{\alpha' ag}{4b}\mathbf{D}_1^2(x_1) > 0$$

It is evident that the restrictions imposed on the system for the Lyapunov function derived by the extended integral method are fewer than those in Chin's derivation. Furthermore, Chin's generalized integral method is unlikely to be applicable for the

general case, described by equations (3.23), because the weighting function w_3 used in the extended integral method is a function of $D(x_1,x_2,x_3)x_2$ which is not allowed in Chin's integral method.

Special case 2: Mukherjee and Bhattacharyya (1972): Equations (3.23) can describe a power system with governor action but without flux decay given the following conditions:

$$D(x_1) = D = \text{constant} \geq 0$$
$$h(x_1) = \frac{c}{2} f(x_1)$$

where $f(x_1)$ is a continuous and differentiable function. The general Lyapunov function shown in (3.26) is reduced to:

$$V = \frac{2}{g} V = c\int_0^{x_1} f(x_1)dx_1 + x_2^2 + \frac{a}{g}x_3^2$$
$$\dot{V} = -\frac{2}{g}\dot{V} = -(Dx_2^2 + \frac{ab}{g}x_3^2)$$

which is identical to the Lyapunov function derived by Mukherjee and Bhattacharyya (1972).

Special case 3: Miyagi and Taniguchi (1980), Chin (1987b): Further we assume

$$a = 1$$
$$h(x_1) = \sin(x_1 + \delta_0) - \sin(\delta_0)$$

This model also represents a power system. The Lyapunov function in (3.26) is reduced to

$$V = g\int_0^{x_1} h(xdx_1 + \frac{1}{2}gx_2^2 + \frac{1}{2}x_3^2$$
$$\dot{V} = -[gDx_2^2 + bx_3^2] \qquad (3.27)$$

The above Lyapunov function requires no restrictions on the system for this case. The Lyapunov function for this case was also derived by Miyagi and Taniguchi (1980) and by Chin (1987) as follows:

$$2V(x_1,x_2,x_3)=\frac{x_3^2}{g}+(x_2+\alpha' Dx_1)^2+\alpha'(1-\alpha')D^2x_1^2 + 2\int_0^{x_1} h(x_1)dx_1+\frac{\alpha' D}{bg}(x_3-gx_1)^2 + 4\int_0^{x_1}(\alpha'(1-\alpha')D^2)^{\frac{1}{2}}(x_1h(x_1))^{\frac{1}{2}}dx_1$$

In order to keep the Lyapunov function positive definite and its time derivative negative and semi-definite, the following conditions have to be satisfied:

$$0\le\alpha'\le 1$$
$$x_1h(x_1)>0$$

This case study shows that the extended method is more general and includes methods previously thought distinct (Wu *et al.* 1995) and the restrictions imposed on the nonlinear system are fewer when the extended method is used. The derivation of the Lyapunov function for equations (3.23) shows that the Lyapunov function can still be derived for the less compatible state-space model by adjusting the form of the weighting functions. This ability to adjust is extremely useful for those engineering systems described by state-space models that are rather difficult to change or to manipulate.

3.5 Summary

It has been proven mathematically that Lyapunov's second method can be extended to the stability of non-smooth dynamic systems. Such extension makes the stability analysis of non-smooth systems possible using Lyapunov's stability theory directly. The main

purpose of the extension of Lyapunov's second method is to form the foundation of construction of smooth Lyapunov functions for non-smooth systems because the evaluation of the derivative of non-smooth Lyapunov functions on the discontinuity surfaces can be extremely difficult.

The method of construction of smooth Lyapunov functions for non-smooth dynamic systems has also been proposed in which the key step is to keep zero-production of the discontinuous terms of the rate of the state vector and the corresponding parts of the gradient of the smooth Lyapunov functions as the solution trajectories (solution in the sense of Filippov) approach the discontinuity surfaces. It has been shown by the examples that smooth Lyapunov functions can be constructed for some non-smooth systems making the stability analysis of non-smooth dynamic systems easier.

Finally, an extension of Chin's generalized integral method of developing Lyapunov functions has been presented. This extension was desired in order to remove the restrictions on the compatibility between the state-space models and Lyapunov functions so that the more commonly used state-space models could be utilized to analyze the stability of systems using Lyapunov's second method. In the extended integral method, a more general form of weighting functions is allowable in the formulation of Lyapunov functions and it was demonstrated that the restriction on the form of the state-space models can be substantially reduced, even eliminated. This elimination of restrictions is due to the fact that the choice of the less compatible state-space model can be compensated through proper choice of the weighting functions. In order to demonstrate the generality of the extended integral method, it was shown that either the previously

developed techniques are simply special cases of the extended integral method proposed here or the previous examples can be handled by using the extended method. In the presented example, similar or less restrictive Lyapunov functions were derived using the extended method. More examples are shown in Wu *et al.* (1995).

The specific significance with regard to the work presented in this chapter is the fact that two theoretical limitations, Lyapunov's stability of non-smooth systems and construction of Lyapunov functions, have been removed or reduced. The methods developed in this chapter not only allow Lyapunov stability theory to be applied to the stability of the base-excited inverted pendulum but also valid for more general engineering systems as shown in the previous examples.

CHAPTER FOUR

LYAPUNOV FEEDBACK CONTROL OF A BASE-EXCITED INVERTED PENDULUM WITH ONE DEGREE OF ROTATIONAL FREEDOM

4.1 Introduction

Study of dynamics and control of inverted pendulums is important from both theoretical and practical viewpoints since an inverted pendulum is a typical example of an unstable system (Mori *et al.*, 1976). The inverted pendulum studied in this chapter has one degree of rotational freedom and the base point can move freely in the vertical plane. As discussed before, the inclusion of the base point accelerations makes a mathematical model of the control system non-autonomous and furthermore, with the horizontal acceleration, the dynamic system does not have an equilibrium point. Such a dynamic system is regarded as a system under constantly acting perturbations which can not be treated by Lyapunov's second method directly.

In this chapter, a methodology is developed to study the problem of stabilizing a single degree-of-rotational-freedom inverted pendulum in which the base point can move in the vertical plane with the only restriction of having continuous accelerations. Though a single-degree-of-rotational-freedom inverted pendulum is oversimplified to model the human trunk movement, it is chosen mainly for the purpose to demonstrate the development of the methodology.

4.2 Inverted pendulum model

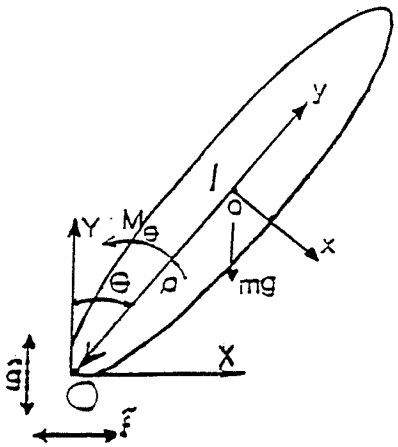

Figure 4.1 Single degree-of-freedom inverted pendulum model.

The inverted pendulum model is shown in Figure 4.1. **OXY** is the inertial coordinate system with **X** in the horizontal direction and **Y** in the vertical direction. The rotation is described by θ. The motion of the base point is described by its components in the **X** and **Y** directions which are shown as $\tilde{f}(t)$ and $\tilde{g}(t)$, respectively. The formulation of the dynamic equations can be carried out by a variety of methods. The final state-space equations are

$$\dot{x}_1 = x_2$$
$$\dot{x}_2 = \frac{m\rho}{I}(g + \ddot{\tilde{g}}(t))\sin x_1 + \frac{m\rho}{I}\ddot{\tilde{f}}(t)\cos x_1 + \frac{M_\theta}{I} \qquad (4.1)$$

where $x_1 = \theta$, $x_2 = \dot{x}_1 = \dot{\theta}$, **m** is the mass of the inverted pendulum, **g** is the gravitational acceleration, ρ is the distance between the base point and the center of mass, **I** is the moment of inertia about the base point and M_θ is the control torque applied at the base point.

4.2.1 Development of piecewise continuous control strategy based on total stability theorem

The following control algorithm is designed for system (4.1) and is discussed below:

$$\mathbf{M_\theta = -k_1 x_1 - k_2 x_2 - m\rho g x_1 - m\rho G_0\, sgn(x_2)|x_1| + M_f} \qquad (4.2)$$

where $\mathbf{k_1}$ and $\mathbf{k_2}$ are the proportional and derivative control gains, respectively. Function $\mathbf{sgn(x_2)}$ is defined as follows

$$\mathbf{sgn}(\gamma) = \begin{cases} 1 & \text{when } \gamma > 0 \\ 0 & \text{when } \gamma = 0 \\ -1 & \text{when } \gamma < 0 \end{cases}$$

$\mathbf{G_0 \geq |\ddot{\tilde{g}}(t)|}$. $\mathbf{M_f}$ is a part of the control torque which counteracts the effect from the horizontal base point acceleration. The term $\mathbf{sgn(x_2)|x_1|}$ in (4.2) is equivalent to $\mathbf{sgn(x_1x_2)x_1}$. The design of the term $\mathbf{sgn(x_1x_2)x_1}$ is, to a certain extent, based on physical considerations. When the inverted pendulum falls away from the vertical, meaning that $\mathbf{x_1x_2 > 0}$, extra torque is needed to push the inverted pendulum back. When the inverted pendulum moves towards the upright position, meaning that $\mathbf{x_1x_2 < 0}$, the torque corresponding to this term slows down the motion to prevent the overshoot. Substituting (4.2) into equations (4.1),

$$\begin{aligned} \dot{x}_1 &= x_2 \\ \dot{x}_2 &= c_0(g + \ddot{\tilde{g}}(t))\sin x_1 + c_0 \ddot{\tilde{f}}(t)\cos x_1 - \frac{k_2}{I}x_2 - \frac{k_1}{I}x_1 \\ &\quad - c_0 g x_1 - c_0 G_0 |x_1| sgn(x_2) + \frac{M_f}{I} \end{aligned} \qquad (4.3)$$

where $\mathbf{c_0 = \frac{m\rho}{I}}$.

The resultant effect of the horizontal acceleration and the control action on the pendulum is shown as $\frac{m\rho}{I}\ddot{\tilde{f}}(t)\cos x_1 + \frac{M_f}{I}$. For the case of $x_1 = 0$ and $x_2 = 0$, the above term becomes $\frac{m\rho}{I}\ddot{\tilde{f}}(t) + \frac{M_f}{I} \neq 0$ for general horizontal acceleration $\ddot{\tilde{f}}(t)$. Therefore, system (4.3) is a non-autonomous control system under constantly acting perturbation. Equations (4.3) do not have an equilibrium point. The unperturbed system for (4.3) is chosen as

$$\dot{x}_1 = x_2 \tag{4.4a}$$

$$\dot{x}_2 = \frac{m\rho}{I}(g + \ddot{\tilde{g}}(t))\sin x_1 - \frac{k_2}{I}x_2 - \frac{k_1}{I}x_1 - c_0 g x_1 - c_0 G_0 |x_1| \operatorname{sgn}(x_2) \tag{4.4b}$$

which represents an inverted pendulum system with only the vertical base point motion. According to theorem of total stability, the uniform and asymptotic stability of (4.4) must be proven in order to guarantee the trajectory of (4.3) to remain arbitrarily close to the equilibrium point.

The right-hand side of (4.4b) is discontinuous, indicating that the conventional solution theory is no longer valid. Before proceeding to the stability analysis of the control system described by equations (4.4), the existence and uniqueness of the solution must be studied.

Existence-uniqueness of the solutions

The basic results of Filippov's solution theory for discontinuous differential equations (Filippov, 1960, 1979 and 1988) are applied here to define a solution concept for the piecewise continuous dynamic system described by equations (4.4). The following discontinuity surface is first defined:

$$S := \{x_1, x_2 : s(x_1, x_2) = x_2 = 0\}$$

The discontinuity surface **S** divides the solution domain Ω into two regions; $\Omega^+ := \{x_1, x_2 : x_2 > 0\}$ and $\Omega^- := \{x_1, x_2 : x_2 < 0\}$. The conditions for the existence and the continuation of Filippov's solution, such that the right-hand sides of equations (4.4) are measurable and bounded, are all satisfied. Thus, according to Theorems 4 and 5 of Filippov (1960), the existence and continuation of the Filippov solution are guaranteed.

To prove the uniqueness of the solution, further conditions need to be satisfied. Following the guideline given by Filippov (1960) summarized in Section (2.1), functions $\mathbf{f}^-$ and $\mathbf{f}^+$ are first defined as the right-hand sides of equations (4.4) in the regions Ω^- and Ω^+, respectively:

$$\mathbf{f}^- = \begin{Bmatrix} x_2 \\ -c_0 g(x_1 - \sin x_1) + c_0 (G_0 |x_1| + \ddot{\tilde{g}}(t) \sin x_1) - \frac{k_1}{I} x_1 - \frac{k_2}{I} x_2 \end{Bmatrix}$$

$$\mathbf{f}^+ = \begin{Bmatrix} x_2 \\ -c_0 g(x_1 - \sin x_1) + c_0 (-G_0 |x_1| + \ddot{\tilde{g}}(t) \sin x_1) - \frac{k_1}{I} x_1 - \frac{k_2}{I} x_2 \end{Bmatrix}$$

Consistent with the notation used by Filippov shown in Section 2.1, vector **h** which is defined as $\mathbf{h} = (\mathbf{f}^+ - \mathbf{f}^-)$ for all points on the discontinuity surface **S**, is constructed as follows:

$$\mathbf{h} = \begin{Bmatrix} 0 \\ -2c_0 G_0 |x_1| \end{Bmatrix} \tag{4.5}$$

Note that on the discontinuity surface **S**, we have $x_2 = 0$ and the normal to the discontinuity surface is denoted by the unit vector $\mathbf{N}_s$ shown as

$$\mathbf{N_s} = \begin{Bmatrix} \dfrac{\partial s(x_1, x_2)}{\partial x_1} \\ \dfrac{\partial s(x_1, x_2)}{\partial x_2} \end{Bmatrix} = \begin{Bmatrix} 0 \\ 1 \end{Bmatrix} \tag{4.6}$$

From (4.5) and (4.6), it is obvious that the vector **h** is directed along the normal to the discontinuity surface when the trajectory approaches it. The scalar, $\mathbf{h_N}$, defined as the projection of **h** on the normal to the discontinuity surface **S**, is

$$\mathbf{h_N} = \mathbf{N_s^T} \cdot \mathbf{h} = \{0 \quad 1\} \begin{Bmatrix} 0 \\ -2c_0 G_0 |x_1| \end{Bmatrix} = -2c_0 G_0 |x_1| < 0 \tag{4.7}$$

Equations (4.5), (4.6) and (4.7) guarantee the uniqueness of the Filippov solution to equations (4.4) according to Lemma 7 of Filippov (1960) shown in Section 2.1.

To further explore the properties of the solution on the discontinuity surface **S**, $\mathbf{f_N^+}$ and $\mathbf{f_N^-}$ are calculated below:

$$\mathbf{f_N^+} = \mathbf{f^+} \cdot \mathbf{N_s} = -c_0 g(x_1 - \sin x_1) + c_0 (G_0 |x_1| + \ddot{\tilde{g}}(t) \sin x_1) - \frac{k_1}{I} x_1$$

$$\mathbf{f_N^-} = \mathbf{f^-} \cdot \mathbf{N_s} = -c_0 g(x_1 - \sin x_1) + c_0 (G_0 |x_1| + \ddot{\tilde{g}}(t) \sin x_1) - \frac{k_1}{I} x_1$$

where $x \in S$. If $k_1 \geq 2m\rho G_0$ all the time, then $f_N^+ > 0$ & $f_N^- > 0$ when $x_1 < 0$ and $f_N^+ < 0$ & $f_N^- < 0$ when $x_1 > 0$. Therefore, according to Lemma 9 of Filippov (1960) in Section 2.1, the solution goes through the discontinuity surface with an isolated point on the discontinuity surface **S**.

Stability verification

The stability of the system (4.4) is proven here using the extended Lyapunov's second method. A smooth Lyapunov function is constructed employing the integral method (see

Chin 1987, Wu *et al.* 1995). Following the integral method, equations (4.4) are written in the following form:

$$\dot{x}_i - Y_i = 0 \qquad i = 1,2$$

where Y_i is the right hand side of equations (4.4). Defining the following weighting functions $w_i(x_1, x_2)$, $i = 1,2$:

$$w_1(x_1, x_2) = 0$$
$$w_2(x_1, x_2) = x_2$$

The integral defined by Chin (1987) is now constructed

$$\begin{aligned} I &= \int_0^t x_2(\dot{x}_2 - Y_2)dt \\ &= \frac{1}{2}x_2^2 + \frac{k_1}{2I}x_1^2 - c_0\int_0^t x_2 g(\sin x_1 - x_1)dt - c_0\int_0^t x_2(\ddot{\tilde{g}}(t)\sin\theta - G_0\,\mathrm{sgn}(x_2)|x_1|)dt + \frac{k_2}{I} \\ &= 0 \end{aligned}$$

Defining

$$M = \frac{1}{2}x_2^2 + \frac{k_1}{2I}x_1^2 \tag{4.8a}$$

The above equation can be restated as

$$M + \int_0^t N dt = 0$$

where

$$N = \frac{k_2}{I}x_2^2 + c_0 g x_2(x_1 - \sin x_1) + c_0 x_2(G_0\,\mathrm{sgn}(x_2)|x_1| - \ddot{\tilde{g}}(t)\sin x_1) \tag{4.8b}$$

The Lyapunov function candidate is now constructed;

$$V = M + c_0 g(\frac{1}{2}x_1^2 + \cos x_1 - 1) \tag{4.9}$$

Note that $c_0 g(\frac{1}{2}x_1^2 + \cos x_1 - 1)$ is a continuous and positive definite function. Thus, V is a continuous and positive definite function. The derivative of the Lyapunov function candidate with respect to time is

$$\dot{V} = -\sum_{i=1}^{2} J_i \tag{4.10}$$

where

$$J_1 = c_0[G_0 \operatorname{sgn}(x_2)|x_1|x_2 - x_2\ddot{\tilde{g}}(t)\sin x_1]$$
$$J_2 = \frac{k_2}{I}x_2^2$$

Note that $x_2 \operatorname{sgn}(x_2)$ is positive and continuous. Therefore, $\dot{V}$ is continuous, i.e., V is a smooth function. In order to validate V as a Lyapunov function for the control system, its derivative with respect to time must be negative and at least semi-definite. It is now proven that J_1 is never negative. Knowing that the following,

$$x_2 \operatorname{sgn}(x_2) = |x_2|$$
$$|x_1| \geq |\sin x_1| \qquad \text{for } -\pi \leq x_1 \leq \pi$$

Thus,

$$|x_1|x_2 \operatorname{sgn}(x_2) \geq |x_2 \sin x_1|$$

Since $G_0 \geq |\ddot{\tilde{g}}(t)|$,

$$G_0|x_1|x_2 \operatorname{sgn}(x_2) \geq |\ddot{\tilde{g}}(t)x_2 \sin x_1|$$

which leads to

$$J_1 = G_0|x_1|x_2 \operatorname{sgn}(x_2) - \ddot{\tilde{g}}(t)x_2 \sin x_1 \geq 0$$

Since $\mathbf{J}_2$ is never negative, thus $\dot{\mathbf{V}} \leq \mathbf{0}$ and the control system (4.4) is stable in the sense of Lyapunov. Moreover, the above proof is independent of the state variables and the Lyapunov function is not dependent of time explicitly. Therefore, the control system is globally and uniformly stable.

The asymptotic stability of (4.4) can be proven using a Lyapunov-like theorem (Slotine and Li, 1991) since LaSalle's principle is valid only for autonomous systems. It is obvious that $\mathbf{V(t,\ x)}$ is lower bounded; that $\dot{\mathbf{V}}\mathbf{(t,x)}$ is negative semi-definite and uniformly continuous with respect to time $\mathbf{t}$. Therefore, $\dot{\mathbf{V}}\mathbf{(t,x)} \rightarrow \mathbf{0}$ as $\mathbf{t} \rightarrow \infty$ according to the Lyapunov-like theorem. Since $\mathbf{J}_1$ and $\mathbf{J}_2$ are not negative, we have $\mathbf{J}_1 \rightarrow \mathbf{0}$ and $\mathbf{J}_2 \rightarrow \mathbf{0}$ as $\mathbf{t} \rightarrow \infty$. From the form of $\mathbf{J}_1$ and $\mathbf{J}_2$, it can be concluded that $\mathbf{x}_2 \rightarrow \mathbf{0}$. Assuming that as $\mathbf{t} \rightarrow \infty$, $\mathbf{x}_1 \neq \mathbf{0}$, that is the system (4.4) is not asymptotically stable, it can be found that $\dot{\mathbf{x}}_2 \neq \mathbf{0}$ which conflicts with the fact that $\mathbf{x}_2 = \mathbf{0}$ as $\mathbf{t} \rightarrow \infty$. Therefore, the control system described by (4.4) is uniformly, globally and asymptotically stable at the equilibrium point. Furthermore, according to the theorem of total stability, the system shown by (4.3) can be stabilized about the upright position arbitrarily closely under the condition that the disturbance is 'small'.

In order to guarantee the total stability of the system, control torque $\mathbf{M}_f$ must be designed so that $\mathbf{M}_f + \mathbf{c}_0\ddot{\tilde{\mathbf{f}}}\mathbf{(t)cosx}_1$ has low magnitude which requires accurate measurement of $\mathbf{c}_0$ and $\ddot{\tilde{\mathbf{f}}}\mathbf{(t)}$. Such a restriction makes the control strategy impractical. In the next section, a method to remove such a restriction on the control law is presented.

4.2.2 Development of an improved control strategy

In this section, a control strategy is to be developed in which the restriction of low perturbation is removed. Though total stability cannot be proven rigorously, it is guaranteed that the trajectory of the dynamic system under constantly acting perturbation can be bounded in a controlled region around the equilibrium point. The following control algorithm is now proposed and discussed:

$$\mathbf{M_\theta = -k_1 x_1 - k_2 x_2 - m\rho g x_1 - m\rho G_0\, sgn(x_2)|x_1| - m\rho F_0\, sgn(x_2)} \qquad \textbf{(4.11)}$$

where $\mathbf{k_1}$ and $\mathbf{k_2}$ are the proportional and derivative control gains, respectively. $\mathbf{F_0 = |\ddot{\tilde{f}}(t)|}$ and $\mathbf{G_0 = |\ddot{\tilde{g}}(t)|}$ or $\mathbf{|\ddot{\tilde{f}}(t)|_{max}}$ and $\mathbf{|\ddot{\tilde{g}}(t)|_{max}}$, respectively. The design of the term $\mathbf{F_0\, sgn(x_2)}$ in (4.11) will be discussed later.

Substituting (4.11) into equations (4.1),

$$\mathbf{\dot{x}_1 = x_2} \qquad \textbf{(4.12a)}$$

$$\mathbf{\dot{x}_2 = c_0(g + \ddot{\tilde{g}}(t))\sin x_1 + c_0 \ddot{\tilde{f}}(t)\cos x_1 - \frac{k_2}{I}x_2 - \frac{k_1}{I}x_1 - c_0 g x_1 - c_0 G_0 |x_1| sgn(x_2) - c_0 F_0\, sgn(x_2))} \qquad \textbf{(4.12b)}$$

where $\mathbf{c_0 = \frac{m\rho}{I}}$. The right-hand side of (4.12b) is discontinuous. Following exactly the same procedure shown in Section 4.2.1, the existence and uniqueness of the solution of equations (4.12) can be proven (not detailed here).

Since system (4.12) does not have an equilibrium point and the perturbation $\mathbf{c_0 \ddot{\tilde{f}}(t)\cos x_1 - c_0 F_0\, sgn(x_2)}$ may not be small, Lyapunov's second method and total stability theory cannot be applied to study the stability of system shown by equations (4.12). In this section, we derive a scalar function, $\mathbf{V_s}$, that satisfies all the conditions of a

Lyapunov function. Such a scalar function can serve as a measure of the boundness of the stability region. By the property of the monotonic decrease in the positive-definite scalar function, the boundness of the trajectory can then be studied.

Following the exact same procedure for the construction of a Lyapunov function as was used for system shown by equation (4.4), the scalar function for (4.12) is constructed as follows

$$V_s = M + c_0 g(\frac{1}{2}x_1^2 + \cos x_1 - 1) \tag{4.13}$$

Function M is defined in (4.8a). The scalar function V_s is a smooth and positive definite function. The derivative of such a function candidate with respect to time is

$$\dot{V}_s = -\sum_{i=1}^{3} J_i \tag{4.14}$$

where

$$J_1 = c_0[G_0 \operatorname{sgn}(x_2)|x_1|x_2 - x_2\ddot{\tilde{g}}(t)\sin x_1]$$
$$J_2 = c_0[F_0 x_2 \operatorname{sgn}(x_2) - x_2\ddot{\tilde{f}}(t)\cos x_1]$$
$$J_3 = \frac{k_2}{I}x_2^2$$

As proven before, J_i $(i = 1,2,3)$ are never negative, that is $\dot{V}_s \leq 0$. Thus, for system (4.12), a scalar function has been constructed which satisfies all conditions imposed on a Lyapunov function. According to Barbalat's lemma (Slotine and Li, 1991), $\dot{V}_s(t,x) \to 0$ as $t \to \infty$. Referring to equation (4.14), we have $x_2 \to 0$ as $t \to \infty$. Therefore, as time increases, the system shown by equations (4.12) stays offset from the equilibrium point.

The design of the term $-m\rho F_0 \operatorname{sgn}(x_2)$ in (4.11) merits some discussion at this stage. The effect of the motion of the base point on the system stability is shown in the form of

$m\rho\ddot{\tilde{f}}(t)\cos x_1$ in the dynamic equations described in equations (4.1). The design of the term $-m\rho F_0\,\mathrm{sgn}(x_2)$ in the control algorithm can counteract such a nonlinear effect and can validate the scalar function. It is always of the opposite sign of $x_2 = \dot{\theta}$, meaning that the control term slows down the motion to suppress the overshoot.

It was proven above that there exists an offset of the states. Such an offset is caused by the fact that $-m\rho F_0\,\mathrm{sgn}(x_2)$ in (4.11) is always in the opposite direction of x_2 and is independent of x_1. To reduce this offset, the control strategy can be improved by adding a nonlinear compensation torque as follows:

$$M_\theta^* = M_\theta - K\tanh(\alpha x_1) \tag{4.15}$$

where M_θ is given in (4.11), $K \geq m\rho\left|\ddot{\tilde{f}}(t)\right|_{max}$ and α is a positive constant. The plot of $\tanh(\alpha x_1)$ versus x_1 with different values of α is shown in Figure 4.2. It is seen that as $\alpha \to \infty$, the value of the hyperbolic function $\tanh(\alpha x_1)$ tends to $\mathrm{sgn}(x_1)$. Note that the addition of this nonlinear term does not alter the existence and uniqueness of the solution described before since $\tanh(\alpha x_1)$ is a continuous function.

The scalar function, V_s^*, for the compensated control system described by equations (4.12) can be constructed by following a procedure of extended integral method. The new scalar function is

$$V_s{}^* = V_s + \frac{K}{\alpha I}\ln[\cosh(\alpha x_1)] \tag{4.16}$$

where V_s is given in (4.13). $V_s{}^*$ is smooth, positive and definite. Similar to $\dot{V}_s$ in (4.14), it can be proven that the derivative of $V_s{}^*$ with respect to time, $\dot{V}_s{}^*$, is always negative semi-definite and tends to zero as $t \to \infty$. Therefore, the control system has the same

stability property as that of (4.12), but the offset can be controlled to be within a permitted level.

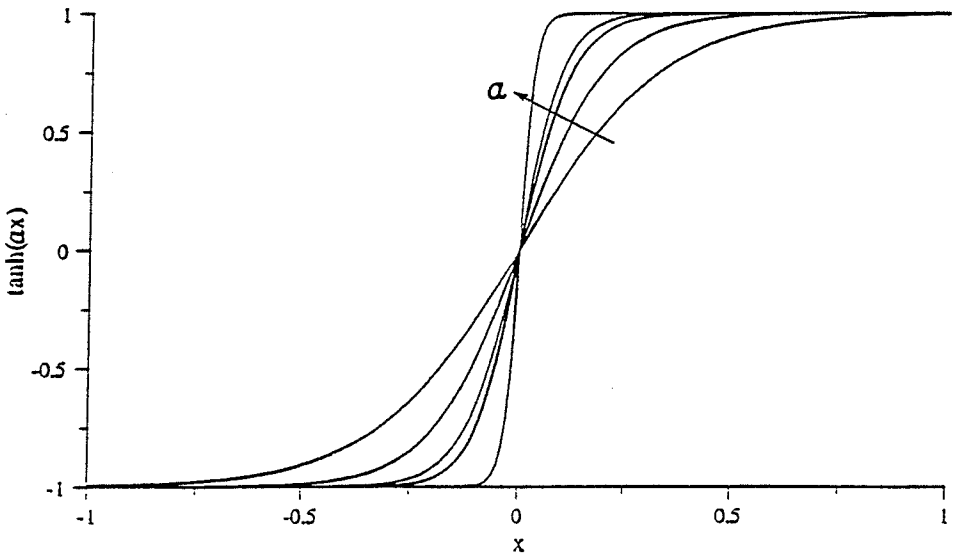

Figure 4.2 Plot of $\tanh(\alpha x)$ with different values of α.

4.3 Robustness analysis

In this section, the robustness of the control system to the parameter $c_1 = m\rho$ and the acceleration measurements $\ddot{\tilde{f}}(t)$ and $\ddot{\tilde{g}}(t)$ required by the control laws, is analyzed. Consider the system described by equations (4.1) with the control algorithm shown in (4.15) and assuming that c_1 is estimated as c_1^e :

$$c_1^e = c_1 + \gamma c_1 > 0$$

Here $\gamma > -1$ since c_1^e cannot be negative. The control algorithm shown in (4.15) becomes

$$\begin{aligned} M_\theta = &-k_1 x_1 - k_2 x_2 - c_1^e g x_1 - c_1^e G_0 \operatorname{sgn}(x_2)|x_1| \\ &- c_1^e F_0 \operatorname{sgn}(x_2) - c_1^e \left|\ddot{\tilde{f}}(t)\right|_{max} \tanh(\alpha x_1) \end{aligned} \qquad (4.17)$$

The scalar function is modified as below:

$$V_s^e = M + \frac{c_1^e}{2I} g x_1^2 + \frac{c_1}{I} g(\cos x_1 - 1) + \frac{c_1^e}{\alpha I} \left| \ddot{\tilde{f}}(t) \right|_{max} \ln(\cosh(\alpha x_1)) \qquad (4.18)$$

where M is given in (4.8a). The derivative of the above function with respect to time is

$$\dot{V}_s^e = -\sum_{i=1}^{3} J_i^e$$

where

$$J_1^e = \frac{c_1^e}{I} G_0 |x_1| \operatorname{sgn}(x_2) x_2 - \frac{c_1}{I} x_2 \ddot{\tilde{g}}(t) \sin x_1$$

$$J_2^e = \frac{c_1^e}{I} F_0 x_2 \operatorname{sgn}(x_2) - \frac{c_1}{I} x_2 \ddot{\tilde{f}}(t) \cos x_1$$

$$J_3^e = \frac{k_2}{I} x_2^2$$

Following the same procedure detailed in Section 4.2, it can be proven that in order to guarantee J_i^e $(i = 1,2)$ to be positive and at least semi-definite, the following condition must be satisfied:

$$\gamma \geq 0 \qquad (4.19)$$

The above condition indicates that the torque determined from a control algorithm which overestimates the physical parameter c_1 can keep the inverted pendulum stable around the upright position.

The base point accelerations $\ddot{\tilde{f}}(t)$ and $\ddot{\tilde{g}}(t)$ are also the inputs to the control strategy. In practice, it is not always easy to accurately measure these accelerations. Assuming that actual accelerations $\ddot{\tilde{f}}(t)$ and $\ddot{\tilde{g}}(t)$ and the measured ones $\ddot{\tilde{f}}^e(t)$ and $\ddot{\tilde{g}}^e(t)$ are related to each other by the following relations:

$$\ddot{\tilde{f}}^e(t) = \ddot{\tilde{f}}(t) + \chi\ddot{\tilde{f}}(t)$$
$$\ddot{\tilde{g}}^e(t) = \ddot{\tilde{g}}(t) + \lambda\ddot{\tilde{g}}(t)$$

where χ and λ can be any functions of time. The control strategy shown in (4.15) is written as

$$\begin{aligned} M_\theta = &-k_2x_2 - k_1x_1 - m\rho g x_1 - m\rho G_0^e \operatorname{sgn}(x_2)|x_1| \\ &- m\rho F_0^e \operatorname{sgn}(x_2) - m\rho\left|\ddot{\tilde{f}}(t)\right|_{max}^e \tanh(\alpha x_1) \end{aligned} \qquad (4.20)$$

where $F_0^e = \left|\ddot{\tilde{f}}^e(t)\right|$ and $G_0^e = \left|\ddot{\tilde{g}}^e(t)\right|$ or $F_0^e = \left|\ddot{\tilde{f}}^e(t)\right|_{max}$ and $G_0^e = \left|\ddot{\tilde{g}}^e(t)\right|_{max}$. The scalar function for the control system with the controller shown in (4.20) is constructed as follows:

$$V_s^e = M + c_0 g\left(\frac{1}{2}x_1^2 + \cos x_1 - 1\right) + \frac{m\rho}{\alpha I}\left|\ddot{\tilde{f}}(t)\right|_{max}^e \ln(\cosh(\alpha x_1)) \qquad (4.21)$$

Its time derivative is:

$$\dot{V}_s^e = -\sum_{i=1}^{3} J_i^e$$

where

$$\begin{aligned} J_1^e &= c_0[G_0^e \operatorname{sgn}(x_2)|x_1|x_2 - x_2\ddot{\tilde{g}}(t)\sin x_1] \\ J_2^e &= c_0[F_0^e x_2 \operatorname{sgn}(x_2) - x_2\ddot{\tilde{f}}(t)\cos x_1] \\ J_3^e &= \frac{k_2}{I}x_2^2 \end{aligned}$$

Note that $c_0 = \dfrac{m\rho}{I}$.

It can be easily shown that in order to keep J'_i $(i = 1,2)$ positive, the following conditions must be satisfied

$$\lambda \geq 0 \qquad \chi \geq 0 \qquad (4.22)$$

The above analysis indicates that the system stability is guaranteed as far as c_1 and the absolute values of $\ddot{\tilde{f}}(t)$ and $\ddot{\tilde{g}}(t)$ are overestimated in the control strategies.

4.4 Approximating the discontinuous terms with continuous functions

The control algorithms shown in (4.2), (4.11) and (4.15) contain discontinuous terms. The implementation of such discontinuous controllers is not desirable from the practical viewpoint (see discussions by Slotine and Sastry, 1983 and Corless, 1993). In this section, the effect of replacing these discontinuous terms with continuous functions is to be studied. Equation (4.15) is therefore written as follows:

$$M_\theta = -k_2 x_2 - k_1 x_1 - m\rho g x_1 - m\rho \hat{G}_0 E|x_1| - m\rho \hat{F}_0 E - K \tanh(\alpha x_1) \qquad (4.23)$$

where E is a continuous function of state x_2 and time t. $\hat{G}_0$, $\hat{F}_0$ and K are chosen as follows:

$$\hat{F}_0 = F_0 + \varepsilon_1 \qquad \hat{G}_0 = G_0 + \varepsilon_2 \qquad K = 2m\rho\left|\ddot{\tilde{f}}(t)\right|_{max}$$

where ε_1 and ε_2 are positive constants required by the stability analysis for this case. Following the integral method, the scalar function candidate is constructed for the above continuous control system:

$$V = M + c_0 g\left(\frac{1}{2}x_1^2 + \cos x_1 - 1\right) + \frac{K}{\alpha I}\ln(\cosh(\alpha x_1)) \qquad (4.24)$$

where M is given in (4.8a). Function V is positive definite. Its derivative with respect to time is

$$\dot{V} = -\sum_{i=1}^{3} J_i$$

where J_i (i=1, 2, 3) is given below:

$$J_1 = c_0\hat{G}_0 E|x_1|x_2 - c_0\ddot{\tilde{g}}(t)x_2 \sin x_1$$
$$J_2 = c_0\hat{F}_0 E x_2 - c_0 x_2 \ddot{\tilde{f}}(t)\cos x_1$$
$$J_3 = \frac{k_2}{I}x_2^2 \qquad (4.25)$$

By examining J_1 and J_2, it is seen that it is impossible to find a continuous function that guarantees both J_1 and J_2 to be positive all the time. For example, in order to keep J_1 positive, two conditions must be satisfied. Firstly, E must be an odd function of x_2, and secondly, $|E| \geq 1$. The only function that meets these two conditions is $E=\text{sgn}(x_2)$ which is not continuous. Therefore, it is unlikely that one can design a continuous control algorithm with the above quadratic Lyapunov-type function that decreases monotonically. With this background we construct a quasi Lyapunov function that may increase in certain regions, but the amount of increase is controlled to be lower than the amount of decrease in the adjacent regions. A similar idea of using such a non- monotonically decreasing quasi Lyapunov function to prove the system stability was discussed by Reissig (1959, 1960) and Hahn (1963) which was briefly explained in Section 2.2.4.

Assume the following continuous function for E ,

$$E_1 = \tanh[p(t)x_2] \qquad (4.26)$$

where p is a bounded, continuous and positive function of time t. The algorithm shown in (4.23) establishes a continuous control under the condition of the base point acceleration being also continuous. Knowing that J_3 in (4.25) is never negative, we first focus on J_1. When $x_1 = 0$ or $x_2 = 0$, $J_1 = 0$. For $x_1 \neq 0$ and $x_2 \neq 0$, J_1 can be rewritten as follows:

$$J_1 = c_0(\hat{G}_0|x_1|x_2 \tanh[p(t)x_2] - \ddot{\tilde{g}}(t)x_2 \sin x_1)$$
$$= c_0\hat{G}_0|x_1x_2|(\tanh[p(t)|x_2|] \pm \frac{\ddot{\tilde{g}}(t)}{\hat{G}_0}\frac{\sin x_1}{x_1})$$
$$\geq c_0\hat{G}_0|x_1x_2|(\tanh[p(t)|x_2|] - \frac{|\ddot{\tilde{g}}(t)|}{\hat{G}_0}\frac{\sin x_1}{x_1})$$

Note that $x_2 \tanh[p(t)x_2]$ is a continuous and even function of x_2, i.e.,

$$x_2 \tanh[p(t)x_2] = |x_2| \tanh[p(t)|x_2|]$$

Also, $\frac{\sin x_1}{x_1} \geq 0$, and $0 < \frac{|\ddot{\tilde{g}}(t)|}{\hat{G}_0} < \delta < 1$, where δ is a constant, the value of which depends on ε_2. In order to guarantee $J_1 \geq 0$, the following condition must be satisfied:

$$\tanh[p(t)|x_2|] - \frac{|\ddot{\tilde{g}}(t)|}{\hat{G}_0}\frac{\sin x_1}{x_1} \geq 0$$

Thus,

$$|x_2| \geq \frac{1}{2p(t)} \ln \frac{1 + \frac{|\ddot{\tilde{g}}(t)|}{\hat{G}_0}\frac{\sin x_1}{x_1}}{1 - \frac{|\ddot{\tilde{g}}(t)|}{\hat{G}_0}\frac{\sin x_1}{x_1}} \tag{4.27}$$

Note that the right-hand side of inequality (4.27) is bounded for $-\pi \leq x_1 \leq \pi$ since $0 < \frac{|\ddot{\tilde{g}}(t)|}{\hat{G}_0} < \delta < 1$. Similarly, in order to keep $J_2 > 0$, one may arrive at the following relation:

$$|x_2| \geq \frac{1}{2p(t)} \ln \frac{1 + \frac{|\ddot{\tilde{f}}(t)|}{\hat{F}_0}|\cos x_1|}{1 - \frac{|\ddot{\tilde{f}}(t)|}{\hat{F}_0}|\cos x_1|} \tag{4.28}$$

with a bounded right hand side for x of $-\pi \le x_1 \le \pi$.

Inequalities (4.27) and (4.28) are not always satisfied. For example, when $x_2 = \dot{\theta}$ changes sign, there exists a region that violates inequalities (4.27) or (4.28), and function **V** in (4.24) may increase. It is first proven that the state trajectory does not stay for infinite time period in the region where **V** may increase. The proof by contradiction can be developed. Suppose without loss of generality that the state trajectory stays in the region $\mathbf{R_s} := \{ x_1, x_2 : x_1 > x_{cr} > 0\}$ where **V** might increase for an infinite time period. The state x_{cr} is the angular displacement such that when $x_1 > x_{cr}$, inequalities (4.27) or (4.28) is violated which further causes $\dot{V}$ to be positive. Note that $\mathbf{R_s} \subset \mathbf{R_1} + \mathbf{R_2}$ where

$$\mathbf{R_1} := \{x_1, x_2 : x_1 > x_{cr} \ \& \ x_2 > 0\}$$

and

$$\mathbf{R_2} := \{x_1, x_2 : x_1 > x_{cr} \ \& \ x_2 < 0\}$$

With a proper choice of **p(t)** in (4.26), x_2 (representing the velocity) can be kept bounded within ε (a small positive constant). Three cases are possible.

Case One: The trajectory stays in sub-region $\mathbf{R_1}$. In this case, x_2 is positive and bounded within ε; x_1 keeps increasing and the acceleration in such a region becomes,

$$\dot{x}_2 = -c_0 g(x_1 - \sin x_1) + c_0 \ddot{\tilde{g}}(t) \sin x_1 + c_0 \ddot{\tilde{f}}(t) \cos x_1 - \frac{K}{I} \tanh \alpha x_1 - \frac{k_1}{I} x_1$$
$$- c_0 \hat{G}_0 E |x_1| - c_0 \hat{F}_0 E - \frac{k_2}{I} x_2$$

Since x_2 is low, the control torque is mainly dependent on the angular displacement x_1. If $k_1 > m\rho(|\ddot{\tilde{g}}(t)| + \hat{G})$ and **K** and α are chosen such that $-K \tanh \alpha x_1$ can counteract the

effect of the term $c_0\ddot{\tilde{f}}(t)$, $\dot{x}_2$ is approximately proportional to $-x_1$ and $\dot{x}_2$ has the opposite sign of x_2. Therefore, x_2 can not remain positive for infinite time, that is the trajectory can not stay permanently in the region for which $x_1 > x_{cr}$ & $0 < x_2 < \varepsilon$. Note that by increasing **K** and α, the magnitude of $\dot{x}_2$ increases, thus x_2 approaches to zero faster.

Case Two: x_2 changes the sign and the trajectory stays in the sub-region $\mathbf{R}_2$. In this case, $x_2 < 0$ and $\dot{x}_2$ has the same sign as x_2. Therefore, x_2 increases satisfying inequalities (4.27) and (4.28).

Case Three: The trajectory oscillates in the region of $\mathbf{R}_1 + \mathbf{R}_2$. This case is impossible since x_2 does not change sign in the region $\mathbf{R}_2$.

It is thus proven that the trajectories stay in the regions in which **V** might increase for only a finite time period. Note that functions **p(t)**, **K** and α play important roles in controlling the size of such sub-regions. Increasing **p(t)** enlarges the region in which the quasi Lyapunov function decreases. Subsequently, the region in which the quasi Lyapunov function increases will be reduced by adjusting the nonlinear compensation torque (controlled by **K** and α). Therefore, by a proper choice of **K**, α and **p(t)**, the size of these sub-regions can be controlled so that the amount of increase in **V** is always less than the amount of decrease in **V** in the adjacent regions. This way **V** can experience an overall decrease until the state trajectories reach a small region about the upright position.

In summary, the quasi Lyapunov function shown in (4.24) does not decrease monotonically which conflicts with the requirements of standard Lyapunov functions. However, it is guaranteed that the amount of increase in the quasi Lyapunov function is

always lower than the amount of decrease in the adjacent regions. Thus, the quasi Lyapunov function decreases overall. The robustness analysis shown in Section 4.3 can also be applied to the continuous control system shown in equations (4.1) and (4.23), and the same conclusion as that in Section 4.3 can be drawn, that is, the system stability is largely insensitive to the uncertainties of some physical parameters and of the measurement in the base point accelerations.

4.5 Numerical examples

Three numerical examples are presented in this section. The first example compares the performance of the three control laws presented in this thesis. Three control laws are piecewise continuous control; piecewise continuous control with compensation and continuous control. The second example demonstrates the behavior of the quasi Lyapunov function pertaining to the continuous control law. Finally, the last example examines the robustness of the continuous control algorithm in the presence of uncertainty in the parameter estimations or measurements.

In these examples the pendulum was given an initial angle of **0.3 rad**, and the base point was allowed to move in both **X** and **Y** directions according to the following profiles:

$$\ddot{\tilde{f}}(t) = 3.2\sin(2\pi t) \quad (m/sec^2)$$
$$\ddot{\tilde{g}}(t) = 1.2\sin(2\pi t) \quad (m/sec^2)$$

The above accelerations approximate the hip motion of a human being during walking. The values of parameters pertaining to the pendulum chosen to resemble the human upper body are, **m=36.86kg**, **I= 5.9kgm^2** and **ρ=0.29m**. The proportional and derivative control gains were chosen as **k_1=121.5** and **k_2=9.15**, respectively. The simulations were

performed using ACSL (*A*dvanced *C*ontinuous *S*imulation *L*anguage) running on a 486 personal computer system.

The response to different controllers are shown in Figure 4.3. The state trajectories tend to zero rapidly and all control systems are clearly stable (Figure 4.3-a. The response to the piecewise continuous control system exhibits a steady-state error (Figure 4.3-b). The addition of the nonlinear compensation torque (with α=**8.0**) as in (4.10) reduced such an error. The response belonging to the continuous control system contains slightly larger oscillations about the upright position as compared to those related to the discontinuous compensated controllers. However, the continuous control system is stabilized in a region about the upright position and the amplitudes of the oscillations tend to reduce with time. Note that in this example $\mathbf{p(t)}$ was chosen as $\mathbf{5(0.01+0.4t)}$, ε_1 and ε_2 were chosen as 5% of the amplitude of the base point accelerations in (4.18).

The control torques produced from the continuous control strategy and the compensated piecewise continuous control algorithm are plotted in Figure 4.4. The control torques determined from the piecewise continuous control algorithm exhibit chattering. It is also seen that both controllers are active during the steady-state case. Such torques are necessary to counteract the effect of base point motion.

The Lyapunov function corresponding to the response of the continuous control, shown in Figure 4.3-a, is plotted in Figure 4.5. As is seen in a certain time period, the quasi Lyapunov function increases. The amount of the increase is, however, lower than the decrease in the adjacent regions and the function decreases overall.

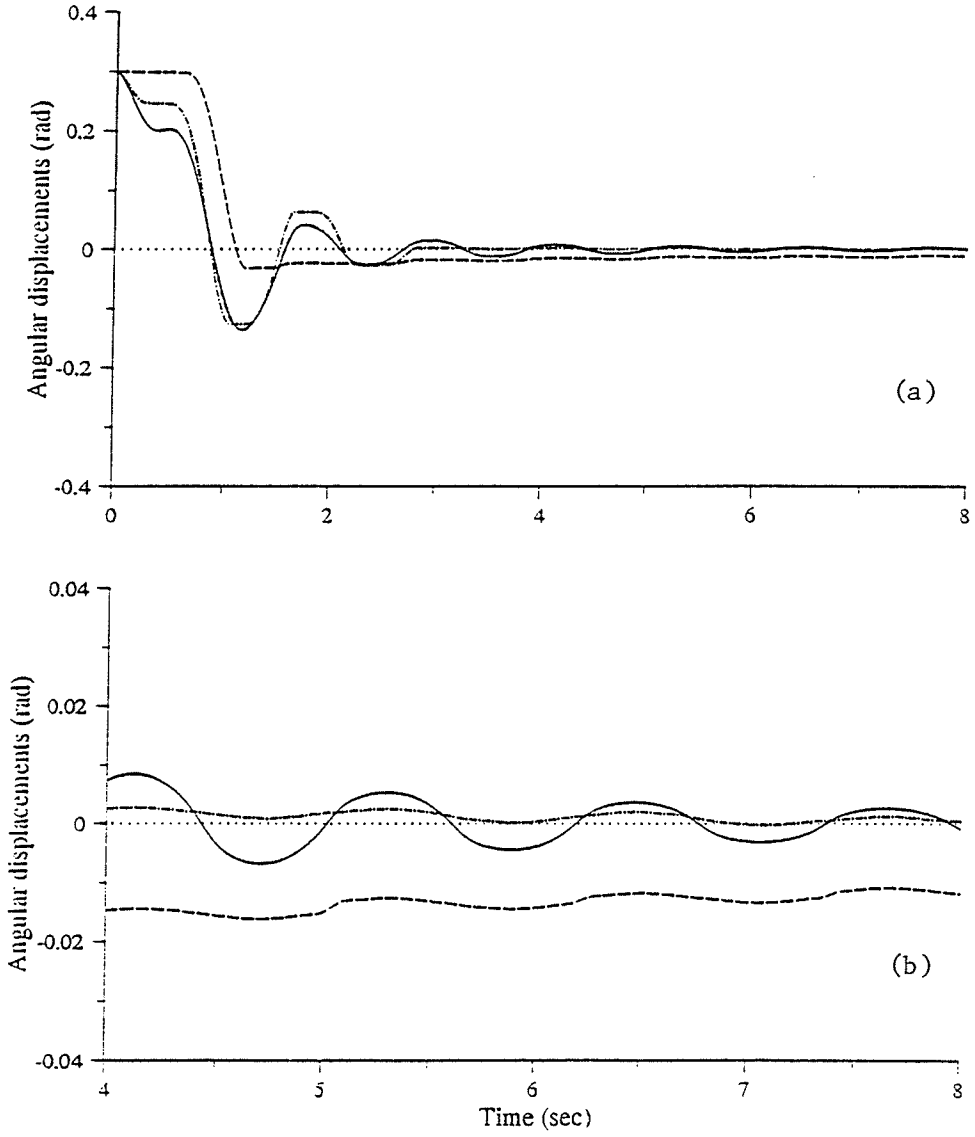

Figure 4.3 *(a)* Angular displacement responses; (----- non-compensated control system; - · - · - compensated control system; —— continuous control system).

(b) A close-up of responses.

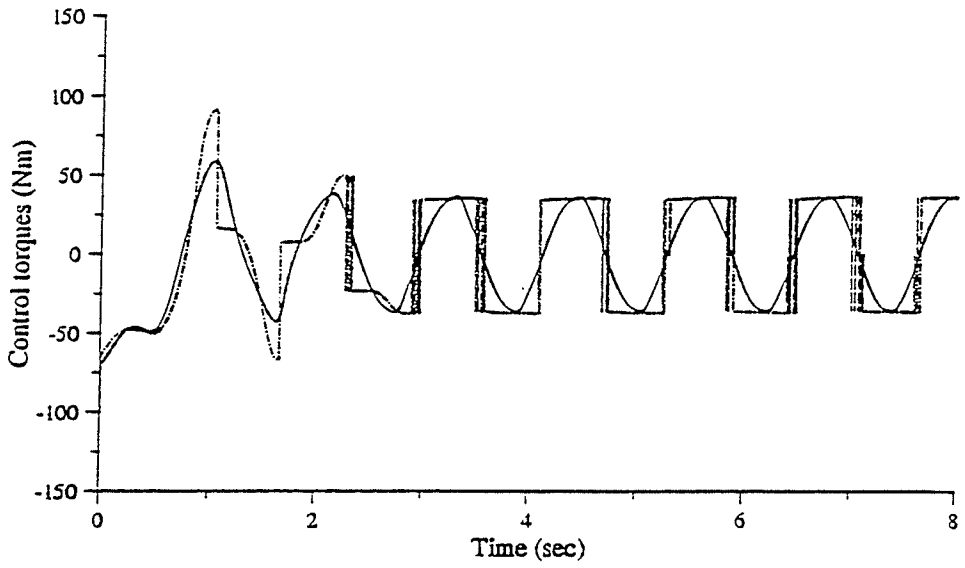

Figure 4.4 Control torques pertaining to Figure 4.3.

(- - - discontinuous control system; —— continuous control system.)

The last example examines the robustness of the proposed control strategies. The response to the continuous control algorithm has been chosen for demonstration. The responses for the case in which $\mathbf{c_1 = m\rho}$ was overestimated (about 60%) by the controller and the one in which an accurate value of $\mathbf{c_1}$ was used are shown Figure 4.6. The corresponding control torques are shown in Figure 4.7. It is seen that both state trajectories converge to zero and the range of the control torque for overestimated $\mathbf{c_1}$ is slightly higher. The response of the continuous controller and the control torques, when the accelerations were overestimated as $\mathbf{F_0 = 1.5\left|\ddot{\tilde{f}}(t)\right|}$ and $\mathbf{G_0 = 1.25\left|\ddot{\tilde{g}}(t)\right|}$, are compared in Figure 4.8 and Figure 4.9. Overestimating the base point acceleration (see Figure 4.8) resulted in a higher control torque and both state trajectories converge to zero state.

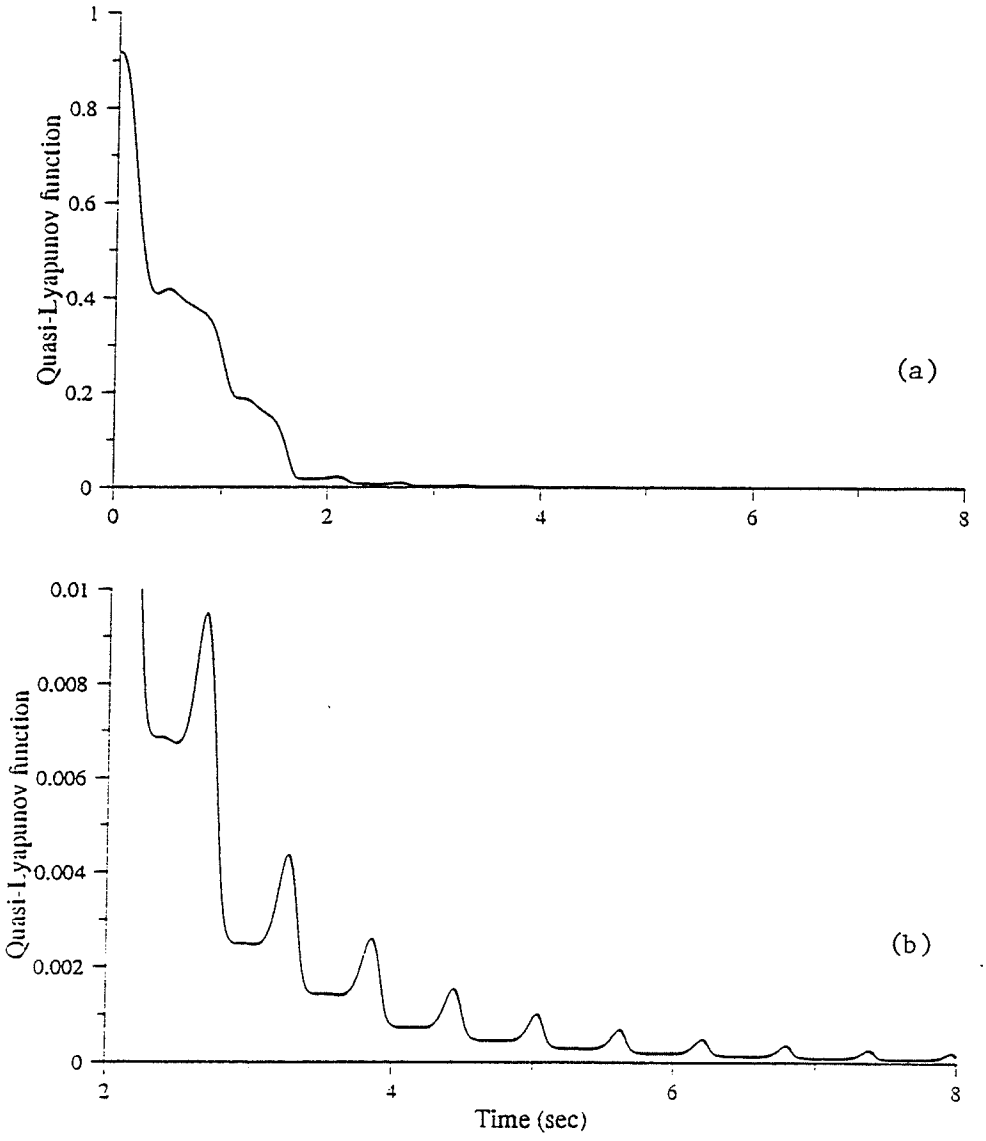

Figure 4.5 *(a)* Quasi-Lyapunov function pertaining to the continuous control strategy *(b)* Close-up of the Lyapunov function.

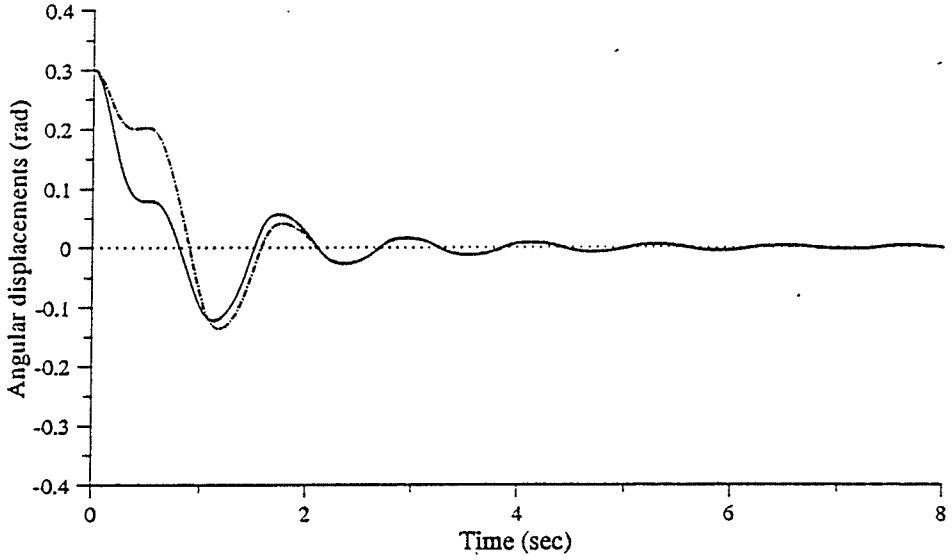

Figure 4.6 Response of the continuous controller with $c_1^e = 1.6m\rho$ (——) as compared with the case in Figure 4, where $c_1^e = m\rho$ (- · - · -).

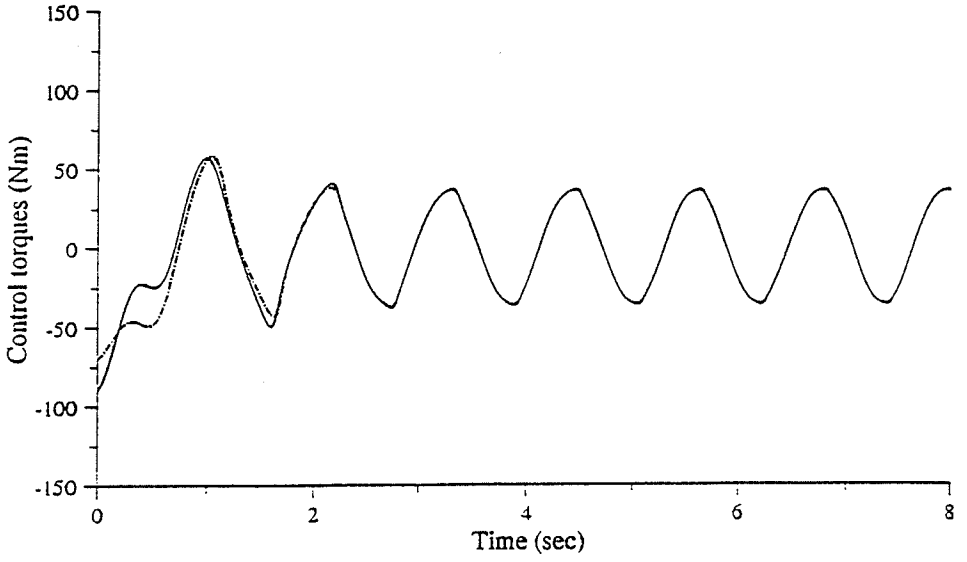

Figure 4.7 Control torques pertaining to Figure 4.6.

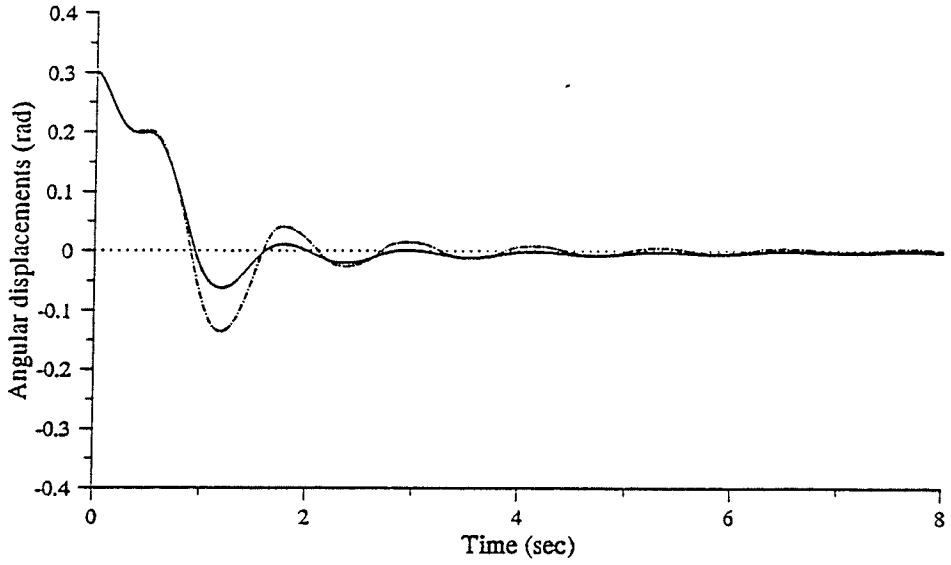

Figure 4.8 *(a)* Response of continuous controller with over-estimated base point accelerations (——) as compared with the accurate ones (----);

(b) A close-up of responses.

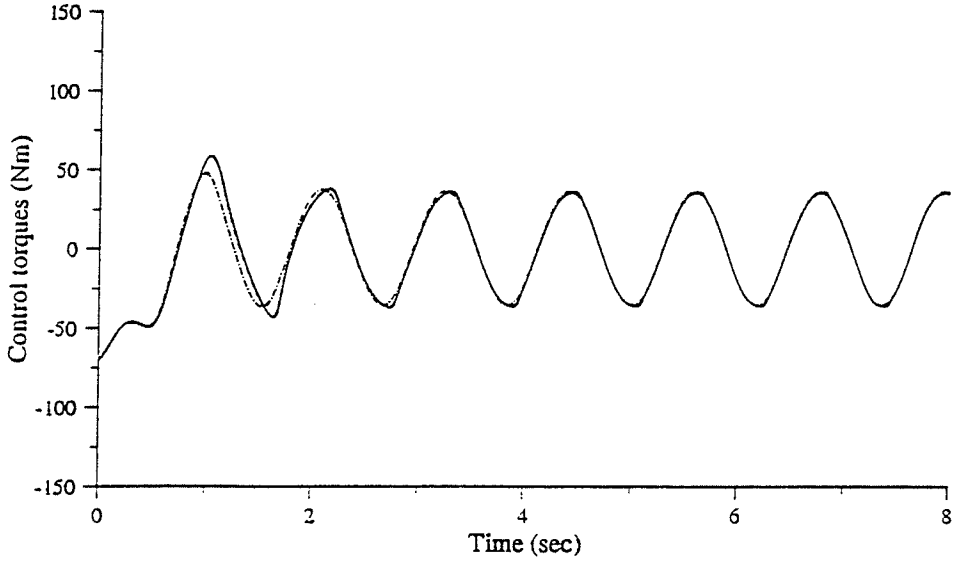

Figure 4.9 Control torques pertaining to Figure 4.8.

4.6 Summary

A methodology was developed in this chapter to study the problem of stabilizing a single degree-of-rotational-freedom inverted pendulum in which the base point can move in the vertical plane with the only restriction of having continuous accelerations. Though a single-degree-of-rotational-freedom inverted pendulum is oversimplified to model the human trunk movement, it is chosen mainly for the purpose to demonstrate the development of the methodology. As discussed before, such a pendulum model represents a system under constantly acting perturbations. The undisturbed system is chosen as the inverted pendulum with only vertical base point motion. It was found in the course of the work that the discontinuous controller is inevitable in order to validate a Lyapunov function. Thus, the dynamic systems are non-smooth due to the discontinuous controllers. Filippov's solution theory (1960, 1979 and 1988) is used to define the solution concept for the proposed control system, and the existence-uniqueness of Filippov's solution is proven. It is then shown, using the extended Lyapunov's second method for non-smooth systems, that such a control law can achieve the uniform, global and asymptotic stability of the undisturbed control system. Under the condition of small perturbations, total stability of the disturbed control system (the pendulum system including the horizontal acceleration) can be guaranteed, that is, the trajectory of the control system with the horizontal base point movement can be arbitrarily close to the upright position (Slotine and Li, 1991). However, such a condition of small perturbation requires accurate measurements on the horizontal base point acceleration and some physical parameters. To remove such a restriction, another improved control strategy is designed which guarantees

the solution to be closely bounded to the equilibrium point. In the course of stability analysis of the improved control system, it is observed that steady-state errors may appear in the response. In order to reduce such errors, a continuous compensation torque is further added in the control strategy. Such a nonlinear compensation torque has been adapted from the technique originally suggested by Cai and Song (1993) to compensate the effect of coulomb friction at the manipulators' joints.

The discontinuous terms in the control strategy were then replaced by some continuous functions to avoid chattering of the control actions and to better represent the actual implementation of the developed controller. A quasi Lyapunov function was constructed for the continuous control system, and it was shown that there exist some regions in which the quasi Lyapunov function may increase; however, the amount of increase in the function in the regions can be controlled to be lower than the amount of decrease in their adjacent regions. This allows the pendulum to be practically stabilized within a region around the upright position. Such an idea, though not used very often, has been helpful for engineering problems (Hahn, 1963). The robustness of the control system to those physical parameters and measurement uncertainties was also examined and it was shown that the system stability is largely insensitive to the physical parameters, as well as the uncertainty in the acceleration measurements of the base point. Finally, the above findings were demonstrated through numerical simulations.

CHAPTER FIVE

LYAPUNOV STABILITY CONTROL OF A BASE-EXCITED INVERTED PENDULUM WITH TWO DEGREES OF ROTATIONAL FREEDOM

5.1 Introduction

The method developed in the previous chapter is extended here. The control and stability of a base-excited inverted pendulum with two degrees of rotational freedom will be studied. The self-rotation of the inverted pendulum is restricted and the base point can move in the three dimensional space with no restrictions on the motion except that the accelerations of the base point must be continuous. It is shown that the proof of uniqueness of the solution is more challenging when the discontinuity surface is the intersection of two discontinuity surfaces. Also as will be shown, the complexity of the problem increases dramatically as the degrees of freedom increases.

Analogous to the previous chapter, a piecewise continuous control strategy is first developed for the undisturbed system, that is the inverted pendulum system with only vertical base point movement since the inverted pendulum system does not have a single equilibrium point. The existence and uniqueness of Filippov's solution are proven. It is then shown, using the extended Lyapunov's second method and Lyapunov-like analysis, that the proposed control law can achieve the uniform, global and asymptotic stability of the undisturbed pendulum system about the upright position. Based on the total stability theorem, the trajectory of the disturbed system, i.e. the inverted pendulum system with general base point motion, can be bounded arbitrarily close to the upright position under the condition of small perturbations. Such a condition of small perturbations requires

accurate measurement of horizontal base point accelerations and some physical parameters. To remove such a condition, an improved control strategy is designed which guarantees the trajectory of the inverted pendulum system with general base point motion can be bounded within a controlled region about the upright position.

To better reflect the actual implementation scenario, the discontinuous control terms are approximated by a class of continuous functions. It is then found that given such a continuous control law, the practical stability can be guaranteed and can be proven using the generalized Lyapunov analysis.

5.2 The pendulum model

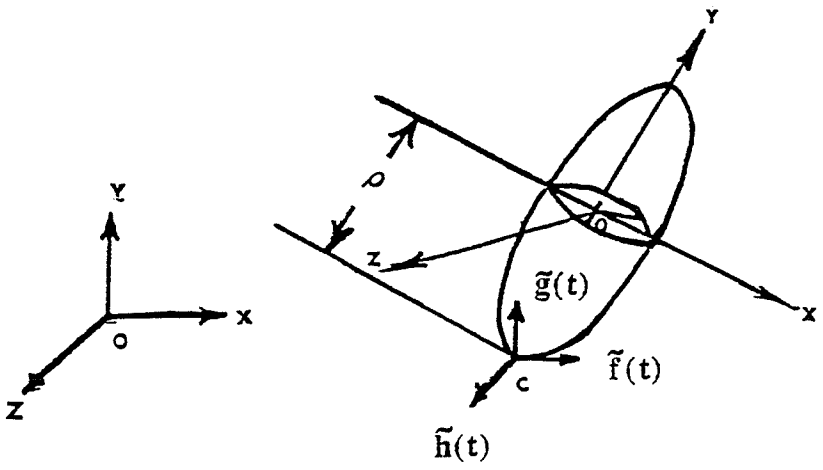

Figure 5.1 Inverted pendulum model with two degrees of rotational freedom

The inverted pendulum model is shown in Figure 5.1. **OXYZ** is the inertial coordinate system with **X** in the horizontal direction, **Y** in the vertical direction and **Z** forming a right-handed orthogonal coordinate system. The body coordinate system is denoted by **oxyz** and is attached to the center of mass **o**. It is oriented along three principal axes of the inverted pendulum. **OXYZ** and **oxyz** coincide at the initial time. The rotations are described by the

ZXY type of Euler angles (Murray *et al.*, 1994). The motion of the base point is described by $\tilde{\mathbf{f}}(t)$, $\tilde{\mathbf{g}}(t)$ and $\tilde{\mathbf{h}}(t)$ in the inertial coordinate system. The dynamic equations derived using the Lagrangian method are shown as follows:

$$\ddot{\theta} = \frac{1}{(1-\mu\sin^2\psi)}(\mu\sin(2\psi)\dot{\theta}\dot{\psi} + c_0(g+\ddot{\tilde{g}}(t))\sin\theta\cos\psi - c_0\ddot{\tilde{f}}(t)\cos\psi\cos\theta + \frac{1}{A}M_\theta)$$

$$\ddot{\psi} = -\frac{1}{2}\mu\sin(2\psi)\dot{\theta}^2 + c_0(g+\ddot{\tilde{g}}(t))\sin\psi\cos\theta - c_0\ddot{\tilde{h}}(t)\cos\psi$$

$$+ c_0\ddot{\tilde{f}}(t)\sin\theta\sin\psi + \frac{1}{A}M_\psi \qquad (5.1)$$

where

$$A = I_0 + m\rho^2 \qquad \mu = 1 - \frac{I_y}{A} \qquad c_0 = \frac{m\rho}{A}$$

$I_x = I_z = I_0 > I_y$. Note that for an inverted pendulum $0 < \mu < 1$.

5.2.1 Development of a piecewise continuous control strategy

The control algorithm which determines the stabilizing torques for the inverted pendulum is designed as follows:

$$M_\theta = -(k_\theta + m\rho g)\theta - K_{d\theta}\dot{\theta} - m\rho G_0\,\mathrm{sgn}(\dot{\theta})|\theta| - K_1\tanh(\alpha_1\theta) + M_f$$

$$M_\psi = -(k_\psi + m\rho g)\psi - K_{d\psi}\dot{\psi} - m\rho G_0\,\mathrm{sgn}(\dot{\psi})|\psi|$$

$$- K_2\tanh(\alpha_2\psi) + M_h \qquad (5.2)$$

where $\mathrm{sgn}(\dot{\theta})$ and $\mathrm{sgn}(\dot{\psi})$ are sign functions defined in Section 4.2.1. G_0 is taken as $|\ddot{\tilde{g}}(t)|$ or $|\ddot{\tilde{g}}(t)|_{max}$. The choice of using the maximum absolute values requires less information about the base point motion but it may demand larger control efforts. The first choice of taking the current accelerations requires a knowledge of the base point motion at all times. The terms related to K_i and α_i (i=1,2) are the compensation torques with the hyperbolic function $\tanh(\alpha x) = \frac{e^{\alpha x} - e^{-\alpha x}}{e^{\alpha x} + e^{-\alpha x}}$ as before.

The resultant effects of the horizontal accelerations and the control action on the pendulum are shown as $M_h + c_0\ddot{\tilde{h}}(t)\cos\psi$ and $M_f + c_0\ddot{\tilde{f}}(t)\cos\theta\cos\psi$. For the case of $\theta = \psi = 0$, the above terms become $M_h + c_0\ddot{\tilde{h}}(t) \neq 0$ and $M_f + c_0\ddot{\tilde{f}}(t) \neq 0$. Therefore, the control system described by (5.1) and (5.2) does not have an equilibrium point. The undisturbed system is chosen as the inverted pendulum with only the vertical base point motion. To guarantee the total stability of the control system of (5.1) and (5.2), the uniform and asymptotic stability of the undisturbed system must be proven. Assuming that the state-space vector $x = \{x_1, x_2, x_3, x_4\}$, where $x_1 = \theta$ and $x_2 = \psi$, the state space model of the undisturbed system is

$$\dot{x}_1 = x_3 \tag{5.3a}$$

$$\dot{x}_2 = x_4 \tag{5.3b}$$

$$\dot{x}_3 = \frac{1}{1-\mu\sin^2 x_2}(\mu x_3 x_4 \sin(2x_2) + c_0(g+\ddot{\tilde{g}}(t))\sin x_1 \cos x_2 - (\frac{k_\theta}{A} + c_0 g)x_1 - \frac{K_{d\theta}}{A}x_3 - c_0 G_0\, \mathrm{sgn}(x_3)|x_1| - \frac{K_1}{A}\tanh(\alpha_1 x_1)) \tag{5.3c}$$

$$\dot{x}_4 = -\frac{1}{2}\mu x_3^2 \sin(2x_2) + c_0(g+\ddot{\tilde{g}}(t))\sin x_2 \cos x_1 - (\frac{k_\psi}{A} + c_0 g)x_2 - c_0 G_0\, \mathrm{sgn}(x_4)|x_2| - \frac{K_{d\psi}}{A}x_4 - \frac{K_2}{A}\tanh(\alpha_2 x_2) \tag{5.3d}$$

The right-hand sides of (5.3c) and (5.3d) are discontinuous, which violates the conventional solution theory, indicating that the existence and uniqueness of the solutions can not be guaranteed. Before proceeding with the stability analysis of the control system shown by (5.3), the existence and uniqueness of the solution to (5.3) must be studied.

5.2.2 Existence and uniqueness of the solution

Filippov's theory (1964, 1979) is applied to prove the existence and uniqueness of the solutions to the proposed control system described by (5.3). The conditions for existence and continuity of the Filippov's solution, such as the right-hand sides of (5.3) are measurable and bounded, are all satisfied. Thus, the existence and continuity of the solutions to (5.3) are guaranteed. The discontinuity surface for (5.3) is one of the following three cases:

$$\textbf{Case 1} \quad S_1^3 := \{x: x_3 = 0 \ \& \ x_4 \neq 0\}$$
$$\textbf{Case 2} \quad S_1^3 := \{x: x_4 = 0 \ \& \ x_3 \neq 0\}$$
$$\textbf{Case 3} \quad S_1^2 := \{x: x_3 = x_4 = 0\}$$

Note that the discontinuity surface S_1^2 is the intersection of the surfaces for Case 1 and 2. It is obvious that the vector-valued function of the right-hand side of (5.3) is continuous up to the discontinuity surfaces. The discontinuity surfaces described by the above relations are smooth and they are independent of time **t.**

For the case of single discontinuity surface, the uniqueness of the solution can be proven following the same procedure as the one in the previous chapter and if $k_\theta \geq 2m\rho G_{0max}$ for Case I and $k_\psi \geq 2m\rho G_{0max}$ for Case II, the solution goes through the discontinuity surface with an isolated point on it.

In Case 3, the discontinuity surface is the intersection of two surfaces. The uniqueness of Filippov's solution has been studied only when the discontinuity surface is the single surface (Slotine and Sastry, 1983 and Southwood *et al.*, 1993). To the best of author's knowledge, the uniqueness of Filippov's solution has not been analyzed when the discontinuity surface is the intersection of several surfaces. In this work, the uniqueness of

Filippov's solution is to be proven rigorously when the solution trajectory approaches the intersection of discontinuity surfaces.

For case 3, the solution region Ω is divided into four regions described as follows:

$$\Omega_1 := \{x;\ x_3 > 0\ \&\ x_4 > 0\}$$
$$\Omega_2 := \{x;\ x_3 > 0\ \&\ x_4 < 0\}$$
$$\Omega_3 := \{x;\ x_3 < 0\ \&\ x_4 > 0\}$$
$$\Omega_4 := \{x;\ x_3 < 0\ \&\ x_4 < 0\}$$

The above four regions are bounded by smooth surfaces denoted by S_i^p shown below:

$$S_1^3 := \{x;\ x_3 = 0\ \&\ x_4 > 0\} \quad S_2^3 := \{x;\ x_3 = 0\ \&\ x_4 < 0\}$$
$$S_3^3 := \{x;\ x_3 > 0\ \&\ x_4 = 0\} \quad S_4^3 := \{x;\ x_3 < 0\ \&\ x_4 = 0\}$$
$$S_5^2 := \{x;\ x_3 = 0\ \&\ x_4 = 0\}$$

Note that the superscript **p** is the dimension of the surface and the subscript **i** is the number of the surface. The vectors parallel to the **p**-dimensional tangent to S_i^p at point $x \in S_i^2$, are

$$P_1^3 = \begin{Bmatrix} \tilde{x}_1 - x_1 \\ \tilde{x}_2 - x_2 \\ 0 \\ \tilde{x}_4 \end{Bmatrix}_{\tilde{x}4>0} \quad P_2^3 = \begin{Bmatrix} \tilde{x}_1 - x_1 \\ \tilde{x}_2 - x_2 \\ 0 \\ \tilde{x}_4 \end{Bmatrix}_{\tilde{x}4<0} \quad P_3^3 = \begin{Bmatrix} \tilde{x}_1 - x_1 \\ \tilde{x}_2 - x_2 \\ \tilde{x}_3 \\ 0 \end{Bmatrix}_{\tilde{x}3>0} \quad P_4^3 = \begin{Bmatrix} \tilde{x}_1 - x_1 \\ \tilde{x}_2 - x_2 \\ \tilde{x}_3 \\ 0 \end{Bmatrix}_{\tilde{x}3<0}$$

$$P_1^4 = \begin{Bmatrix} \tilde{x}_1 - x_1 \\ \tilde{x}_2 - x_2 \\ \tilde{x}_3 \\ \tilde{x}_4 \end{Bmatrix}_{\substack{\tilde{x}3>0 \\ \tilde{x}4>0}} \quad P_2^4 = \begin{Bmatrix} \tilde{x}_1 - x_1 \\ \tilde{x}_2 - x_2 \\ \tilde{x}_3 \\ \tilde{x}_4 \end{Bmatrix}_{\substack{\tilde{x}3>0 \\ \tilde{x}4<0}} \quad P_3^4 = \begin{Bmatrix} \tilde{x}_1 - x_1 \\ \tilde{x}_2 - x_2 \\ \tilde{x}_3 \\ \tilde{x}_4 \end{Bmatrix}_{\substack{\tilde{x}3<0 \\ \tilde{x}4>0}} \quad P_4^4 = \begin{Bmatrix} \tilde{x}_1 - x_1 \\ \tilde{x}_2 - x_2 \\ \tilde{x}_3 \\ \tilde{x}_4 \end{Bmatrix}_{\substack{\tilde{x}3<0 \\ \tilde{x}4<0}}$$

$$P_5^2 = \begin{Bmatrix} \tilde{x}_1 - x_1 \\ \tilde{x}_2 - x_2 \\ 0 \\ 0 \end{Bmatrix}$$

where $\tilde{x}$ is on the p-dimensional surface tangential to S_i^p.

Now $F_i^p(t,x)$ is calculated according to Filippov (1979)

$$F_1^3 = \overline{co}\left\{\begin{bmatrix} 0 \\ 0 \\ B \pm c_0 G_0 |x_1| \\ C - c_0 G_0 |x_2| \end{bmatrix}\right\} \quad F_2^3 = \overline{co}\left\{\begin{bmatrix} 0 \\ 0 \\ B \pm c_0 G_0 |x_1| \\ C + c_0 G_0 |x_2| \end{bmatrix}\right\} \quad F_3^3 = \overline{co}\left\{\begin{bmatrix} 0 \\ 0 \\ B - c_0 G_0 |x_1| \\ C \pm c_0 G_0 |x_2| \end{bmatrix}\right\}$$

$$F_4^3 = \overline{co}\left\{\begin{bmatrix} 0 \\ 0 \\ B + c_0 G_0 |x_1| \\ C \pm c_0 G_0 |x_2| \end{bmatrix}\right\} \quad F_1^4 = \left\{\begin{bmatrix} 0 \\ 0 \\ B - c_0 G_0 |x_1| \\ C - c_0 G_0 |x_2| \end{bmatrix}\right\} \quad F_2^4 = \left\{\begin{bmatrix} 0 \\ 0 \\ B - c_0 G_0 |x_1| \\ C + c_0 G_0 |x_2| \end{bmatrix}\right\}$$

$$F_3^4 = \left\{\begin{bmatrix} 0 \\ 0 \\ B + c_0 G_0 |x_1| \\ C - c_0 G_0 |x_2| \end{bmatrix}\right\} \quad F_4^4 = \left\{\begin{bmatrix} 0 \\ 0 \\ B + c_0 G_0 |x_1| \\ C - c_0 G_0 |x_2| \end{bmatrix}\right\} \quad F_1^2 = \overline{co}\left\{\begin{bmatrix} 0 \\ 0 \\ B \pm c_0 G_0 |x_1| \\ C \pm c_0 G_0 |x_2| \end{bmatrix}\right\}$$

where $\overline{co}$ refers to the convex hull of a set and

$$B = \frac{1}{1 - \mu \sin^2 x_2}(c_0(g + \ddot{\tilde{g}}(t)) \sin x_1 \cos x_2 - (\frac{k_\theta}{A} + c_0 g)x_1)$$

$$C = c_0(g + \ddot{\tilde{g}}(t)) \sin x_2 \cos x_1 - (\frac{k_\psi}{A} + c_0 g)x_2$$

To prove the uniqueness of the solution to system (5.3) according to Theorem 1 of Filippov (1979), we need to prove that there is right-sided uniqueness up to the boundary of S_1^2 and one and only one of sets $K_i^m = F_i^m \cap P_i^m$ is non-empty. Condition (i) in Theorem 1 of Filippov (1979) is satisfied for the case studied here, that is, the trajectories of the system goes from set S_1^2 to another only a finite number of times.

The right-sided uniqueness of the solution on the intersection of discontinuity surfaces S_1^2 can be proven based on the definition given by Filippov (1979) directly. Assuming that

the initial value $x(t_0) = \{x_{10} \quad x_{20} \quad 0 \quad 0\}^T$ (Note that $x(t_0)$ is on the surface S_1^2.), the state-space equations become

$$\dot{x}_1 = \dot{x}_2 = 0$$

$$\dot{x}_3 = \frac{1}{(1-\mu \sin^2 x_2)}(c_0(g_0 + \ddot{\tilde{g}}(t))\sin x_1 \cos x_2 - (\frac{k_\theta}{A} + c_0 g)x_1)$$

$$\dot{x}_4 = c_0(g_0 + \ddot{\tilde{g}}(t))\sin x_2 \cos x_1 - (\frac{k_\psi}{A} + c_0 g)x_2$$

If $x_{10} = x_{20} = 0$, we have $\dot{x}_{10} = \dot{x}_{20} = 0$. Therefore, $x_3 = x_4 = 0$ and $x_1 = x_2 = 0$ at any time instant. Thus, the solution is unique on the intersection of discontinuity surface. If one of x_{10} and x_{20} is non-zero, for example, $x_{10} \neq 0$, we have $\dot{x}_3 \neq 0$. Therefore, at next time instant, $x_3 \neq 0$, that is the solution trajectory moves away from the intersection of the discontinuity surfaces. Thus, only one point of the solution trajectory is on the intersection of the discontinuity surfaces, i.e., the solution on the discontinuity surface S_1^2 is unique.

The method to prove that one and only one of sets $K_i^m = F_i^m \cap P_i^m$ is non-empty is based on the property of a convex set in normed linear spaces, that is, if two points belong to a convex set, every point on the segment connecting these two points also belongs to the same convex set. For the system studied in this work, the emptiness of sets K_i^4, K_i^3 and K_1^2 should be proven as follows.

(a) Consider sets K_i^4, **i=1,...,4,** if the signs of the state variables in the vector of sets F_i^4 are the same as those of set P_i^4, set K_i^4 is non-empty. Otherwise, set K_i^4 is empty.

(b) Consider sets K_i^3, $i = 1,...,4$, two vectors in sets F_i^3 represent two points in plane **ouv** with **u** and **v** as axes and **o** as the origin. In order to prove that set K_1^3, for example, is non-empty, we need to prove that i) the segment connecting two points has an

intersection with v axis and ii) such an intersection is on the positive v axis since set $\mathbf{P}_1^3$ has the form of $\{0 \quad \tilde{x}_4\}^T$, $\tilde{x}_4 > 0$.

(c) Consider set $\mathbf{K}_1^2$, four vectors in set $\mathbf{F}_1^2$ form a simplex in **ouv** plane. To prove set $\mathbf{K}_1^2$ is non-empty, we need to determine the intersections of the segments connecting any two points with **u** and **v** axes, respectively. If we can find at least two intersections on either **u** or **v** axis which are on two sides of the origin **o** or on the origin **o**, set $\mathbf{K}_1^2$ is non-empty since set $\mathbf{P}_1^2$ is a null set. Otherwise, set $\mathbf{K}_1^2$ is empty.

The proof that one and only one of the sets $\mathbf{K}_i^m$ is non-empty can be developed based on the relationship between $|\mathbf{B}|$ and $\mathbf{c}_0\mathbf{G}_0|\mathbf{x}_1|$, $|\mathbf{C}|$ and $\mathbf{c}_0\mathbf{G}_0|\mathbf{x}_2|$, respectively.

When $\begin{matrix}|\mathbf{B}| > \mathbf{c}_0\mathbf{G}_0|\mathbf{x}_1| \\ |\mathbf{C}| > \mathbf{c}_0\mathbf{G}_0|\mathbf{x}_2|\end{matrix}$, functions $\mathbf{B} \pm \mathbf{c}_0\mathbf{G}_0|\mathbf{x}_1|$ are of the same sign and so are functions $\mathbf{C} \pm \mathbf{c}_0\mathbf{G}_0|\mathbf{x}_2|$ which indicates that the segments connecting any two points in sets $\mathbf{F}_i^3(\mathbf{t},\mathbf{x})$ and $\mathbf{F}_1^2(\mathbf{t},\mathbf{x})$ cannot intersect with either axis **u** or **v**. According to the forms of $\mathbf{P}_i^p(\mathbf{t},\mathbf{x})$ **p=2, 3**, all sets $\mathbf{K}_i^3(\mathbf{t},\mathbf{x})$ and $\mathbf{K}_1^2(\mathbf{t},\mathbf{x})$ are empty. Only one of $\mathbf{K}_i^4(\mathbf{t},\mathbf{x})$ is non-empty. For example, set $\mathbf{K}_1^4(\mathbf{t},\mathbf{x})$ is non-empty when $\mathbf{B} > \mathbf{0}$ and $\mathbf{C} > \mathbf{0}$. Therefore, condition (iii) of Theorem 1 of Filippov (1979) is satisfied. For the case when $\begin{matrix}|\mathbf{B}| = \mathbf{c}_0\mathbf{G}_0|\mathbf{x}_1| \\ |\mathbf{C}| > \mathbf{c}_0\mathbf{G}_0|\mathbf{x}_2|\end{matrix}$ and $\mathbf{B} > \mathbf{c}_0\mathbf{G}_0|\mathbf{x}_1|$ $|\mathbf{C}| = \mathbf{c}_0\mathbf{G}_0|\mathbf{x}_2|$, a similar conclusion can be drawn.

When $\begin{matrix}|B| \le c_0 G_0 |x_1| \\ |C| \le c_0 G_0 |x_2|\end{matrix}$, we have $\begin{matrix}B - c_0 G_0 |x_1| \le 0 \\ B + c_0 G_0 |x_1| \ge 0\end{matrix}$ and $\begin{matrix}C - c_0 G_0 |x_2| \le 0 \\ C + c_0 G_0 |x_2| \ge 0\end{matrix}$. We prove that $K_1^2(t,x)$ is a null set. By observing sets P_1^2 and F_1^2 and by choosing $\tilde{x}_1 = \tilde{x}_2 = 0$, we need to prove that $\{0 \quad 0\}^T \in \overline{co}\left(B \pm c_0 G_0 |x_1| \quad C \pm c_0 G_0 |x_2|\right)^T$. Set F_1^2 forms a simplex (rectangular for this case) in plane **ouv**. Four vertexes of such a simplex are located in four quadrants, respectively. Therefore, the origin o belongs to set F_1^2 and set $K_1^2(t,x)$ is a null set. It can also be seen that all sets $K_i^3(t,x)$ and $K_i^4(t,x)$ are empty by observing $F_i^p(t,x)$ and $P_i^p(t,x)$, **p=3, 4**. Therefore, condition (iii) of Theorem 1 of Filippov (1979) is satisfied.

In the above proof, the properties (empty or non-empty) of sets $K_i^p(t,x)$ are discussed and it was found that one and only one of sets $K_i^p(t,x)$ can be empty. Empty sets $K_i^p(t,x)$ mean empty sets $H_i^p(t,x)$ which is the set of the vectors of $K_i^p(t,x)$ at the point on the edge (boundary) of S_i^p. Thus, we conclude that the uniqueness of the solution to (5.3) is verified when the discontinuity surface is the intersection of two surfaces according to Filippov (1979). If the conditions that k_θ and k_ψ are greater than $2m\rho G_{0\max}$, only Case 1 is possible.

5.2.3 Stability verification

The stability of the control system (5.3) may now be verified using the extended Lyapunov's second method. Following the extended integral method, we consider the integral shown below:

$$\Gamma = \sum_{i=1}^{4} \Gamma_i = \sum_{i=1}^{4} \int_0^t w_i(x_1,..,x_4,)(\dot{x}_i - Y_i)dt = 0$$

where Y_i (i=1,2,3,4) are the right-hand sides of (5.3) and the weighting functions $w_i(x_1,x_2,x_3,x_4)$ are chosen as follows:

$$w_1(x_1,..,x_4) = 0$$
$$w_2(x_1,..,x_4) = 0$$
$$w_3(x_1,..,x_4) = (1-\mu\sin^2 x_2)x_3$$
$$w_4(x_1,..,x_4) = x_4$$

Therefore

$$\Gamma_1 = \Gamma_2 = 0$$

$$\Gamma_3 = \int_0^t x_3(1-\mu\sin^2 x_2)(\dot{x}_3 - f_3)dt$$
$$= \frac{1}{2}(1-\mu\sin^2 x_2)x_3^2 - \frac{1}{2}\int_0^t \mu x_3^2 x_4 \sin(2x_2)dt - c_0 g\int_0^t (x_3 \sin x_1 \cos x_2 - x_1 x_3)dt$$
$$- c_0\int_0^t (x_3\ddot{g}(t)\sin x_1 \cos x_2 - G_0 x_3\,\mathrm{sgn}(x_3)|x_1|)dt + \frac{K_{d\theta}}{A}\int_0^t x_3^2 dt + \frac{k_\theta}{2A}x_1^2$$
$$+ \frac{K_1}{A}\int_0^t x_3 \tanh(\alpha_1 x_1)dt$$

$$\Gamma_4 = \int_0^t x_4(\dot{x}_4 - f_4)dt$$
$$= \frac{1}{2}x_4^2 + \frac{k_\psi}{2A}x_2^2 + \frac{1}{2}\int_0^t \mu x_3^2 x_4 \sin(2x_2)dt - c_0 g\int_0^t (x_4 \sin x_2 \cos x_1 - x_2 x_4)dt$$
$$- c_0\int_0^t x_4(\ddot{g}(t)\sin x_2 \cos x_1 - G_0\,\mathrm{sgn}(x_4)|x_2|)dt + \frac{K_{d\psi}}{A}\int_0^t x_4^2 dt$$
$$+ \frac{K_2}{A}\int_0^t x_4 \tanh(\alpha_2 x_2)dt$$

Considering

$$\Gamma = \sum_{i=1}^{4}\Gamma_i = M + \int_0^t N dt + \text{constant} = 0$$

M and **N** are found as:

$$M = \frac{k_\theta}{2A}x_1^2 + \frac{k_\psi}{2A}x_2^2 + \frac{1}{2}(1-\mu\sin^2 x_2)x_3^2 + \frac{1}{2}x_4^2 \qquad \textbf{(5.4a)}$$

$$N = -c_0(g+\ddot{\tilde{g}}(t))x_3 \sin x_1 \cos x_2 + (c_0 g x_1 + c_0 G_0 |x_1| \mathrm{sgn}(x_3))x_3$$
$$- c_0(g+\ddot{\tilde{g}}(t))x_4 \sin x_2 \cos x_1 + (c_0 g x_2 + c_0 G_0 |x_2| \mathrm{sgn}(x_4))x_4$$
$$+ \frac{K_{d\theta}}{A} x_3 + \frac{K_{d\psi}}{A} x_4 + \frac{K_1}{A} x_3 \tanh(\alpha_1 x_1) + \frac{K_2}{A} x_4 \tanh(\alpha_2 x_2) \qquad (5.4b)$$

The Lyapunov function candidate is now constructed:

$$V = M + c_0 g(\frac{1}{2}x_1^2 + \frac{1}{2}x_2^2 + \cos x_1 \cos x_2 - 1) + \sum_{i=1}^{2} \frac{K_i}{\alpha_i} \ln(\cosh(\alpha_i x_i)) \qquad (5.5)$$

Note that $(\frac{1}{2}x_1^2 + \frac{1}{2}x_2^2 + \cos x_1 \cos x_2 - 1) \geq 0$ and it is a definite function. The derivative of the Lyapunov function shown in (5.5) with respect to time is

$$\dot{V} = -(N - c_0 g(x_1 x_3 + x_2 x_4 - x_3 \sin x_1 \cos x_2 - x_4 \cos x_1 \sin x_2) = -\sum_{i=1}^{3} J_i$$

where

$$J_1 = c_0 x_3 (G_0 |x_1| \mathrm{sgn}(x_3) - \ddot{\tilde{g}}(t) \sin x_1 \cos x_2)$$
$$J_2 = c_0 x_4 (G_0 |x_2| \mathrm{sgn}(x_4) - \ddot{\tilde{g}}(t) \sin x_2 \cos x_1)$$
$$J_3 = \frac{K_{d\theta}}{A} x_3^2 + \frac{K_{d\psi}}{A} x_4^2$$

Note that $x_3 \,\mathrm{sgn}(x_3)$ and $x_4 \,\mathrm{sgn}(x_4)$ are continuous functions. It was proven in the previous chapter that J_k (k=1,2, 3) is never negative, that is $\dot{V}$ is negative and semi-definite. The above stability verification is independent of the states and V is not dependent of time t explicitly, therefore, the system is uniformly and globally stable in the sense of Lyapunov.

The asymptotic stability of (5.3) can be proven using a Lyapunov-like theorem. It is obvious that V(t, x) is lower bounded; $\dot{V}(t,x)$ is negative semi-definite and uniformly continuous with respect to time t. Therefore, $\dot{V}(t,x) \to 0$ as $t \to \infty$. Since J_1 to J_3 are

not negative, we have $J_1 \to 0$, $J_2 \to 0$ and $J_3 \to 0$ as $t \to \infty$. From the form of J_1, J_2 and J_3, it can be concluded that $x_3 \to 0$ and $x_4 \to 0$ as $t \to \infty$. Assuming that as $t \to \infty$, $x_1 \neq 0$ or $x_2 \neq 0$, that is the system (5.3) is not asymptotically stable, it can be found that $\dot{x}_3 \neq 0$ and $\dot{x}_4 \neq 0$ which conflicts with the fact that $x_3 = 0$ and $x_4 = 0$. Therefore, the control system described by (5.3) is uniformly, globally and asymptotically stable about the equilibrium point. Furthermore, according to the theorem of total stability, the disturbed system is totally stable, which means that the trajectories of the pendulum system with horizontal base point movements (disturbance) can be stabilized arbitrarily closely about the upright position under the condition that the disturbance is 'small'.

In order to guarantee the 'small' disturbance, control torque M_f and M_h must be designed so that $M_f + m\rho\ddot{\tilde{f}}(t)\cos x_1 \cos x_2$ and $M_h - m\rho\ddot{\tilde{h}}(t)\cos x_2$ have low magnitudes which requires accurate measurement of $m\rho$, $\ddot{\tilde{f}}(t)$ and $\ddot{\tilde{h}}(t)$. Such a restriction makes the control strategy impractical. In the next section, it is shown how such a restriction on the control law may be removed.

5.2.4 Development of an improved control strategy

In this section, a control strategy is to be developed in which the restriction of low perturbations is removed. The control algorithm which determines the stabilizing torques is designed as follows:

$$\begin{aligned} M_\theta &= -(k_\theta + m\rho g)\theta - K_{d\theta}\dot{\theta} - m\rho G_0 \operatorname{sgn}(\dot{\theta})|\theta| - m\rho F_0 \operatorname{sgn}(\dot{\theta}) - K_1 \tanh(\alpha_1\theta) \\ M_\psi &= -(k_\psi + m\rho g)\psi - K_{d\psi}\dot{\psi} - m\rho(G_0 + F_0)\operatorname{sgn}(\dot{\psi})|\psi| \\ &\quad - m\rho H_0 \operatorname{sgn}(\dot{\psi}) - K_2 \tanh(\alpha_2\psi) \end{aligned} \qquad (5.6)$$

where F_0, G_0 and H_0 are $\left|\ddot{\tilde{f}}(t)\right|$, $\left|\ddot{\tilde{g}}(t)\right|$ and $\left|\ddot{\tilde{h}}(t)\right|$ or $\left|\ddot{\tilde{f}}(t)\right|_{max}$, $\left|\ddot{\tilde{g}}(t)\right|_{max}$ and $\left|\ddot{\tilde{h}}(t)\right|_{max}$, respectively. Assuming the state space vector $x=\{x_1,x_2,x_3,x_4\}$, where $x_1=\theta$ and $x_2=\psi$, the state space model is

$$\dot{x}_1 = x_3 \tag{5.7a}$$

$$\dot{x}_2 = x_4 \tag{5.7b}$$

$$\begin{aligned}\dot{x}_3 = {} & \frac{1}{1-\mu\sin^2 x_2}(\mu x_3 x_4 \sin(2x_2) + c_0(g+\ddot{\tilde{g}}(t))\sin x_1 \cos x_2 - (\frac{k_\theta}{A}+c_0 g)x_1 \\ & -\frac{K_{d\theta}}{A}x_3 - c_0 G_0\, \mathrm{sgn}(x_3)|x_1| - c_0\ddot{\tilde{f}}(t)\cos x_1 \cos x_2 \\ & - c_0 F_0\, \mathrm{sgn}(x_3) - \frac{K_1}{A}\tanh(\alpha_1 x_1))\end{aligned} \tag{5.7c}$$

$$\begin{aligned}\dot{x}_4 = {} & -\frac{1}{2}\mu x_3^2 \sin(2x_2) + c_0(g+\ddot{\tilde{g}}(t))\sin x_2 \cos x_1 - (\frac{k_\psi}{A}+c_0 g)x_2 - c_0\ddot{\tilde{h}}(t)\cos x_2 \\ & -\frac{K_{d\psi}}{A}x_4 - c_0(G_0+F_0)\,\mathrm{sgn}(x_4)|x_2| + c_0\ddot{\tilde{f}}(t)\sin x_1 \sin x_2 \\ & - c_0 H_0 \mathrm{sgn}(x_4) - \frac{K_2}{A}\tanh(\alpha_2 x_2)\end{aligned} \tag{5.7d}$$

The right-hand sides of (5.7c) and (5.7d) are discontinuous which violates the conventional solution theory, indicating that the existence and uniqueness of the solutions cannot be guaranteed. Following the same procedure shown in Section 5.2.2, the existence and uniqueness of the solution to equations (5.7) can be proven.

Since system (5.7) does not have an equilibrium point and the perturbation $M_f + m\rho\ddot{\tilde{f}}(t)\cos x_1 \cos x_2$ and $M_h - m\rho\ddot{\tilde{h}}(t)\cos x_2$ may not be small, Lyapunov's second method and total stability theory cannot be applied to study the stability of system (5.7). Similar to Section 4.2.2, we develop a scalar function, V_s, that satisfies all the conditions of Lyapunov function. Such a scalar function can serve as a measure of the boundness of the solution trajectory of (5.7). By the property of the monotonic decrease

in the positive definite scalar function, the boundness of the trajectory can be studied. As in Section 4.2.2, the scalar function for system (5.7) is now constructed:

$$V_s = M + c_0 g(\frac{1}{2}x_1^2 + \frac{1}{2}x_2^2 + \cos x_1 \cos x_2 - 1) + \sum_{i=1}^{2} \frac{K_i}{\alpha_i A} \ln(\cosh(\alpha_i x_i)) \qquad (5.8)$$

The derivative of the scalar function shown in (5.8) with respect to time is

$$\dot{V}_s = -(N - c_0 g(x_1 x_3 + x_2 x_4 - x_3 \sin x_1 \cos x_2 - x_4 \cos x_1 \sin x_2) - \sum_{i=1}^{2} \frac{K_i}{A} \tanh(\alpha_i x_i)$$

$$= -\sum_{i=1}^{6} J_i$$

where

$$J_1 = c_0 x_3 (G_0 |x_1| \operatorname{sgn}(x_3) - \ddot{g}(t) \sin x_1 \cos x_2)$$

$$J_2 = c_0 x_4 (G_0 |x_2| \operatorname{sgn}(x_4) - \ddot{g}(t) \sin x_2 \cos x_1)$$

$$J_3 = c_0 x_4 (F_0 \operatorname{sgn}(x_4) |x_2| - \ddot{f}(t) \sin x_1 \sin x_2)$$

$$J_4 = c_0 x_3 (F_0 \operatorname{sgn}(x_3) + \ddot{f}(t) \cos x_1 \cos x_2)$$

$$J_5 = c_0 x_4 (H_0 \operatorname{sgn}(x_4) + \ddot{h}(t) \cos x_2)$$

$$J_6 = \frac{K_{d\theta}}{A} x_3^2 + \frac{K_{d\psi}}{A} x_4^2$$

Following the same procedure shown in 4.2.2, it can be proven that J_K **(k=1, ..., 6)** is non-negative for all values of x_i **(i=1, 2, 3, 4)**. Therefore, $\dot{V}$ is negative and semi-definite. According to Barbalat's lemma (Slotine and Li, 1991), $\dot{V}_s(t,x) \to 0$ as $t \to \infty$ and we have $x_3 \to 0$ and $x_4 \to 0$ as $t \to \infty$. Therefore, as time increases, the system (5.7) can be stabilized around the upright position with an offset, and the offset can be controlled to be within a permitted level by the compensation torques $K_1 \tanh(\alpha_1 \theta)$ and $K_2 \tanh(\alpha_2 \psi)$.

5.3 Robustness Analysis of the Control System

In this section, the robustness of the control system to the parameter $c_1 = m\rho$ and the acceleration measurements $\ddot{\tilde{f}}(t)$, $\ddot{\tilde{g}}(t)$ and $\ddot{\tilde{h}}(t)$ required by the control law, is analyzed. Consider the system with the control algorithm (5.6) and assuming that c_1 is estimated as c_1^e :

$$c_1^e = c_1 + \gamma c_1 > 0$$

where $\gamma > -1$ since c_1^e cannot be negative. The control algorithm then becomes

$$\begin{aligned} M_\theta &= -K_{d\theta}\dot{\theta} - (k_\psi + c_1^e g)\theta - c_1^e G_0 |\theta| \operatorname{sgn}(\dot{\theta}) - c_1^e F_0 \operatorname{sgn}(\dot{\theta}) - K_1 \tanh(\alpha_1 x_1) \\ M_\psi &= -K_{d\psi}\dot{\psi} - (k_\psi + c_1^e g)\psi - c_1^e (F_0 + G_0)|\psi| \operatorname{sgn}(\dot{\psi}) \\ &\quad - c_1^e H_0 \operatorname{sgn}(\dot{\psi}) - K_2 \tanh(\alpha_2 x_2) \end{aligned} \tag{5.9}$$

The scalar function for the control system with the control strategy of (5.9) is shown below:

$$V_s = M + \frac{c_1^e}{2A} g(x_1^2 + x_2^2) + \frac{1}{2} c_0 g(\cos x_1 \cos x_2 - 1) + \sum_{i=1}^{2} \frac{K_i}{\alpha_i A} \ln(\cosh(\alpha_i x_i))$$

The derivative of the above scalar function with respect to time is

$$\begin{aligned} \dot{V}_s &= -(N - \frac{c_1^e}{A} g(x_1 x_3 + x_2 x_4 - x_3 \sin x_1 \cos x_2 - x_4 \cos x_1 \sin x_2) - \sum_{i=1}^{2} \frac{K_i}{A} \tanh(\alpha_i x_i) \\ &= -\sum_{i=1}^{6} J_i \end{aligned}$$

where

$$J_1 = x_3\left(\frac{c_1^e}{A}G_0|x_1|\,\mathrm{sgn}(x_3) - c_0\ddot{\tilde{g}}(t)\sin x_1\cos x_2\right)$$

$$J_2 = x_4\left(\frac{c_1^e}{A}G_0|x_2|\,\mathrm{sgn}(x_4) - c_0\ddot{\tilde{g}}(t)\sin x_2\cos x_1\right)$$

$$J_3 = x_4\left(\frac{c_1^e}{A}F_0\,\mathrm{sgn}(x_4)|x_2| - c_0\ddot{\tilde{f}}(t)\sin x_1\sin x_2\right)$$

$$J_4 = x_3\left(\frac{c_1^e}{A}F_0\,\mathrm{sgn}(x_3) + c_0\ddot{\tilde{f}}(t)\cos x_1\cos x_2\right)$$

$$J_5 = x_4\left(\frac{c_1^e}{A}H_0\,\mathrm{sgn}(x_4) + c_0\ddot{\tilde{h}}(t)\cos x_2\right)$$

$$J_6 = \frac{K_{d\theta}}{A}x_3^2 + \frac{K_{d\psi}}{A}x_4^2$$

It can be proven that the system stability is guaranteed under the following condition

$$\gamma \geq 0 \tag{5.10}$$

Similar to the above discussion, the base point accelerations $\ddot{\tilde{f}}(t)$, $\ddot{\tilde{g}}(t)$ and $\ddot{\tilde{h}}(t)$ are also the inputs to the control strategy. In reality, it is difficult to measure the accelerations accurately. Assuming actual acceleration $\ddot{\tilde{f}}(t)$, $\ddot{\tilde{g}}(t)$ and $\ddot{\tilde{h}}(t)$ and those measured $\ddot{\tilde{f}}^e(t)$, $\ddot{\tilde{g}}^e(t)$ and $\ddot{\tilde{h}}^e(t)$ are related to each other as follows:

$$\ddot{\tilde{f}}^e(t) = \ddot{\tilde{f}}(t) + \gamma\ddot{\tilde{f}}(t)$$
$$\ddot{\tilde{g}}^e(t) = \ddot{\tilde{g}}(t) + \lambda\ddot{\tilde{g}}(t)$$
$$\ddot{\tilde{h}}^e(t) = \ddot{\tilde{h}}(t) + \kappa\ddot{\tilde{h}}(t)$$

where γ, λ and κ can be functions of time. The control strategy is then

$$M_\theta = -K_{d\theta}\dot{\theta} - (k_\theta + c_1 g)\theta - c_1 G_0^e|\theta|\,\mathrm{sgn}(\dot{\theta}) - c_1 F_0^e\,\mathrm{sgn}(\dot{\theta})$$
$$M_\psi = -K_{d\psi}\dot{\psi} - (k_\psi + c_1 g)\psi - c_1(F_0^e + G_0^e)|\psi|\,\mathrm{sgn}(\dot{\psi}) - c_1 H_0^e\,\mathrm{sgn}(\dot{\psi}) \tag{5.11}$$

where $F_0^e = \left|\ddot{\tilde{f}}^e(t)\right|$, $G_0^e = \left|\ddot{\tilde{g}}^e(t)\right|$ and $H_0^e = \left|\ddot{\tilde{h}}^e(t)\right|$. Following the same procedure shown in Section 5.2.4, the same scalar function shown in (5.8) can be used. The derivative of the scalar function shown in (5.8) with respect to time is

$$\dot{V}_s = -(N - c_0 g(x_1 x_3 + x_2 x_4 - x_3 \sin x_1 \cos x_2 - x_4 \cos x_1 \sin x_2) - \sum_{i=1}^{2} \frac{K_i}{A} \tanh(\alpha_i x_i)$$

$$= -\sum_{i=1}^{6} J_i$$

where

$$J_1 = c_0 x_3 (G_0^e |x_1| \operatorname{sgn}(x_3) - \ddot{\tilde{g}}(t) \sin x_1 \cos x_2)$$

$$J_2 = c_0 x_4 (G_0^e |x_2| \operatorname{sgn}(x_4) - \ddot{\tilde{g}}(t) \sin x_2 \cos x_1)$$

$$J_3 = c_0 x_4 (F_0^e \operatorname{sgn}(x_4) |x_2| - \ddot{\tilde{f}}(t) \sin x_1 \sin x_2)$$

$$J_4 = c_0 x_3 (F_0^e \operatorname{sgn}(x_3) + \ddot{\tilde{f}}(t) \cos x_1 \cos x_2)$$

$$J_5 = c_0 x_4 (H_0^e \operatorname{sgn}(x_4) + \ddot{\tilde{h}}(t) \cos x_2)$$

$$J_6 = \frac{K_{d\theta}}{A} x_3^2 + \frac{K_{d\psi}}{A} x_4^2$$

To keep $\dot{V} \le 0$, the following conditions must be satisfied

$$\gamma \ge 0 \qquad \lambda \ge 0 \qquad \kappa \ge 0 \qquad (5.12)$$

Therefore, the system stability is not effected as long as the acceleration values are over estimated.

The above sensitivity analysis shows that the system stability is largely insensitive to the variation of the physical parameter c_1 and the measurement error in base point accelerations. Theoretically, as long as c_1^e and the measured base point accelerations are overestimated, the system stability is not effected, but they should be chosen carefully in simulation by considering overshoot avoidance, convergence speed, as well as the amount of applied control torque.

5.4 Approximating the perturbations with continuous terms

The control algorithms shown in (5.2) and (5.6) contain perturbation terms. The implementation of such discontinuous control strategies is not desirable from the practical viewpoint as was explained in Section 1.2.4. In this section, the effect of replacing the perturbation terms with continuous functions is studied. Equations (5.6) are therefore written as follows:

$$\begin{aligned}\mathbf{M}_\theta &= -(\mathbf{k}_\theta + \mathbf{m}\rho\mathbf{g})\theta - \mathbf{K}_{d\theta}\dot{\theta} - \mathbf{m}\rho\hat{\mathbf{G}}_0\mathbf{E}_1|\theta| - \mathbf{m}\rho\hat{\mathbf{F}}_0\mathbf{E}_1 - \mathbf{K}_1\tanh(\alpha_1\theta)\\ \mathbf{M}_\psi &= -(\mathbf{k}_\psi + \mathbf{m}\rho\mathbf{g})\psi - \mathbf{K}_{d\psi}\dot{\psi} - \mathbf{m}\rho(\hat{\mathbf{F}}_0 + \hat{\mathbf{G}}_0)\mathbf{E}_2|\psi|\\ &\quad - \mathbf{m}\rho\hat{\mathbf{H}}_0\mathbf{E}_2 - \mathbf{K}_2\tanh(\alpha_2\psi)\end{aligned} \tag{5.13a}$$

where $\mathbf{E}_1$ and $\mathbf{E}_2$ are continuous functions of state $\mathbf{x}_3$, $\mathbf{x}_4$ and time $\mathbf{t}$. $\hat{\mathbf{F}}_0$, $\hat{\mathbf{G}}_0$ and $\hat{\mathbf{H}}_0$ are chosen as follows:

$$\begin{aligned}\hat{\mathbf{F}}_0 &= \mathbf{F}_0 + \varepsilon_1\\ \hat{\mathbf{G}}_0 &= \mathbf{G}_0 + \varepsilon_2\\ \hat{\mathbf{H}}_0 &= \mathbf{H}_0 + \varepsilon_3\end{aligned} \tag{5.13b}$$

where ε_i, $\mathbf{i} = \mathbf{1},\ \mathbf{2},\ \mathbf{3}$ are positive constants required by the generalized Lyapunov analysis for this case. Following the extended integral method, the quasi-Lyapunov function candidate is constructed for the continuous control system as follows:

$$\mathbf{V}_q = \mathbf{M} + \mathbf{c}_0\mathbf{g}\left(\frac{1}{2}\mathbf{x}_1^2 + \frac{1}{2}\mathbf{x}_2^2 + \cos\mathbf{x}_1\cos\mathbf{x}_2 - \mathbf{1}\right) + \sum_{i=1}^{2}\frac{\mathbf{K}_i}{\alpha_i\mathbf{A}}\ln(\cosh(\alpha_i\mathbf{x}_i)) \tag{5.14}$$

$\mathbf{M}$ is given by (5.4a). $\mathbf{V}_q$ is a positive and definite function. Its derivative with respect to time is

$$\dot{\mathbf{V}}_q = -\sum_{i=1}^{6}\mathbf{J}_i \tag{5.15}$$

where

$$J_1 = c_0 x_3 (\hat{G}_0 E_1 |x_1| - c_0 \ddot{\tilde{g}}(t) \sin x_1 \cos x_2)$$

$$J_2 = c_0 x_3 (\hat{F}_0 E_1 + c_0 \ddot{\tilde{f}}(t) \cos x_1 \cos x_2)$$

$$J_3 = c_0 x_4 (\hat{G}_0 E_2 |x_2| - c_0 x_2 \ddot{\tilde{g}}(t) \sin x_2 \cos x_1)$$

$$J_4 = c_0 x_4 (c_0 \hat{F}_0 E_2 |x_2| + \ddot{\tilde{f}}(t) \sin x_1 \sin x_2)$$

$$J_5 = c_0 x_4 (\hat{H}_0 E_2 + c_0 \ddot{\tilde{h}}(t) \cos x_2)$$

$$J_6 = \frac{K_{d\theta}}{A} x_3^2 + \frac{K_{d\psi}}{A} x_4^2$$

As discussed in the previous chapter, the only function that can keep J_1, for example, positive is $E_1 = \mathrm{sgn}(x_3)$ which is not continuous. Therefore, it is likely not possible to design a continuous control algorithm with a quadratic Lyapunov-type function that decreases monotonically. With this background, a quasi Lyapunov function is constructed that may increase in certain regions, but the amount of the increase is controlled to be lower than the amount of the decrease in the adjacent regions until the pendulum is stabilized within an acceptable region about the upright position. Such an acceptable region is denoted by $R_a = \{x: \|x\| < \varsigma\}$ where ς is a positive number. Assuming the following continuous function for E_1 and E_2,

$$E_1 = \tanh[p_1(t) x_3] \qquad E_2 = \tanh[p_2(t) x_4]$$

$p_1(t)$ and $p_2(t)$ are bounded, continuous and positive functions of time **t.** The algorithm shown in (5.13) then establishes a continuous control under the condition of the base point acceleration being also continuous. J_6 in (5.15) is never negative, we first focus on J_1. When $x_1 = 0$ or $x_3 = 0$, $J_1 = 0$. For $x_1 \neq 0$ and $x_3 \neq 0$, J_1 can be rewritten as follows:

$$J_1 = c_0(\hat{G}_0|x_1|x_3 \tanh[p(t)x_3] - \ddot{\tilde{g}}(t)x_3 \sin x_1 \cos x_2)$$

$$= c_0\hat{G}_0|x_1x_3|(\tanh[p(t)|x_3|] \pm \frac{\ddot{\tilde{g}}(t)}{\hat{G}_0}\frac{\sin x_1}{x_1}\cos x_2)$$

$$\geq c_0\hat{G}_0|x_1x_3|(\tanh[p(t)|x_3|] - \frac{|\ddot{\tilde{g}}(t)|}{\hat{G}_0}\frac{\sin x_1}{x_1})$$

Note that $x_3 \tanh[p(t)x_3]$ is a continuous and even function of x_3, i.e.,

$$x_3 \tanh[p(t)x_3] = |x_3| \tanh[p(t)|x_3|]$$

and $\frac{\sin x_1}{x_1} > 0$. In order to guarantee $J_1 \geq 0$, the following condition must be satisfied:

$$\tanh[p_1(t)|x_3|] - \frac{|\ddot{\tilde{g}}(t)|}{\hat{G}_0}\frac{\sin x_1}{x_1} \geq 0$$

Thus,

$$|x_3| \geq \frac{1}{2p_1(t)} \ln \frac{1 + \frac{|\ddot{\tilde{g}}(t)|}{\hat{G}_0}\frac{\sin x_1}{x_1}}{1 - \frac{|\ddot{\tilde{g}}(t)|}{\hat{G}_0}\frac{\sin x_1}{x_1}} = \beta_1 \qquad \textbf{(5.16a)}$$

Note that the right hand side of inequality (5.16a) is bounded for $-\pi \leq x_1 \leq \pi$ since $0 < \frac{|\ddot{\tilde{g}}(t)|}{\hat{G}_0} < \delta < 1$. Similarly, in order to keep J_2 positive, one may arrive at the following relation:

$$|x_3| \geq \frac{1}{2p_1(t)} \ln \frac{1 + \frac{|\ddot{\tilde{f}}(t)|}{\hat{F}_0}|\cos x_1|}{1 - \frac{|\ddot{\tilde{g}}(t)|}{\hat{G}_0}|\cos x_1|} = \beta_2 \qquad \textbf{(5.16b)}$$

If $x_3 \geq \max(\beta_1, \beta_2)$, J_1 and J_2 are positive. Following the same procedure, we have that if $x_4 \geq \max(\alpha_1, \alpha_2, \alpha_3)$ where

$$\alpha_1 = \frac{1}{2p_2(t)} \ln \frac{1 + \frac{|\ddot{\tilde{g}}(t)|}{\hat{G}_0} \left| \frac{\sin x_2}{x_2} \right|}{1 - \frac{|\ddot{\tilde{g}}(t)|}{\hat{G}_0} \left| \frac{\sin x_2}{x_2} \right|} \tag{5.16c}$$

$$\alpha_2 = \frac{1}{2p_2(t)} \ln \frac{1 + \frac{|\ddot{\tilde{f}}(t)|}{\hat{F}_0} \left| \frac{\sin x_2}{x_2} \right|}{1 - \frac{|\ddot{\tilde{f}}(t)|}{\hat{F}_0} \left| \frac{\sin x_2}{x_2} \right|} \tag{5.16d}$$

and

$$\alpha_3 = \frac{1}{2p_2(t)} \ln \frac{1 + \frac{|\ddot{\tilde{h}}(t)|}{\hat{H}_0} |\cos x_1|}{1 - \frac{|\ddot{\tilde{h}}(t)|}{\hat{H}_0} |\cos x_1|} \tag{5.16e}$$

In summary, if $x_3 \geq \beta$ and $x_4 \geq \alpha$, J_i, $(i = 1,\ldots,6)$ is positive, that is $\dot{V}_q \leq 0$. However, inequalities (5.16a)-(5.16e) are not always satisfied. For example when $x_3 = \dot{\theta}$ or $x_4 = \dot{\psi}$ changes sign, there exists regions that violate some of the inequalities from (5.16a) to (5.16e). Therefore, $\dot{V}_q$ might be positive in such regions. In order to guarantee that the quasi-Lyapunov, V_q, function experiences an overall decrease, we need to prove that (i) the state trajectories do not remain for infinite time period in the regions where V_q may increase, and (ii) the amount of the increase in V_q is lower than the amount of the decrease in the adjacent regions until the pendulum is stabilized within an acceptable region R_a about the upright position.

We first prove that both x_3 and x_4 must have low absolute values if $\dot{V}_q$ is positive, that is the summation of $\sum_{i=1}^{6} J_i$ is negative. From inequalities (5.16a) to (5.16e), if J_i, $(i = 1,\ldots,5)$ is negative, the states x_3 and x_4 can be bounded within κ (a small positive constant) with a proper choice of functions $p_1(t)$ and $p_2(t)$. Suppose that inequality (5.16a) or (5.16b) is violated, that is x_3 has low absolute value, and J_1 or J_2 is negative which further causes $\dot{V}_q$ $(= -\sum_{i=1}^{6} J_i)$ positive. Since $\sum_{i=1}^{6} J_i$ is negative and J_6 is always positive, x_4 must have a low absolute value.

We now prove that the state trajectories do not stay for infinite time period in the region where V_q may increase. The proof can proceed by contradiction. It is assumed that, without the loss of generality, the state trajectory stays in a region $R_s := \{ x: x_1 > x_{1cr} > \varsigma > 0\}$ where V_q might increase for an infinite time period. The state x_{1cr} is the angular displacement such that when $x_1 > x_{1cr}$, inequality (5.16a) or (5.16b) is violated which further causes $\dot{V} > 0$. Note that $x_{1cr} > \varsigma$ that is $R_s \not\subset R_a$. R_a is the acceptable region within which the control system is stabilized. $R_s \subset R_1 + R_2$ where

$$R_1 := \{x: x_1 > x_{cr} \ \& \ x_3 > 0\}$$

and

$$R_2 = \{x: x_1 > x_{cr} \ \& \ x_3 < 0\}$$

Three cases are possible.

Case One: the trajectory stays in region R_1. In this case, x_3 is positive and bounded within κ; x_1 keeps increasing and the acceleration in such a region becomes,

$$\dot{x}_3 = \frac{1}{1-\mu\sin^2 x_2}(-c_0 g(x_1 - \sin x_1 \cos x_2) - (\frac{k_\theta}{A}x_1 - c_0\ddot{\tilde{g}}(t)\sin x_1 \cos x_2)$$
$$-\frac{K_1}{A}\tanh(\alpha_1 x_1) - c_0\ddot{\tilde{f}}(t)\cos x_1 \cos x_2$$
$$+\mu x_3 x_4 \sin(2x_2) - \frac{K_{d\theta}}{A}x_3 - c_0\hat{G}_0 E_1|x_1| - c_0\hat{F}_0 E_1) \qquad (5.17)$$

Note that it was proven that both x_3 and x_4 are bounded and have low absolute values. The term $\mu x_3 x_4 \sin(2x_2)$ is not significant. If $k_\theta > 2m\rho\hat{G}_0$, K_1 and α_1 are chosen such that $\frac{K_1}{A}\tanh(\alpha_1 x_1) + c_0\ddot{\tilde{f}}(t)\cos x_1 \cos x_2 > 0$. $\dot{x}_3$ is negative since it is proportional to $-x_1$. (Note that in region R_1, both x_1 and x_3 are positive.) Therefore, x_3 cannot remain positive for infinite time, that is the trajectory can not stay permanently in the region R_1 for which $x_1 > x_{cr}$ and $0 < x_3 < \kappa$. From (5.17) it can be seen that x_3 tends to zero faster by increasing K_1 and α_1.

Case Two: state x_3 changes sign and the trajectory stays in the region R_2. In this case, $-\kappa < x_3 < 0$ and $\dot{x}_3$ is still mainly determined by x_1 and has the same sign as x_3. Therefore, x_3 increases satisfying inequalities (5.16a) and (5.16b).

Case Three: the trajectory oscillates in the region of $R_1 + R_2$. This case is impossible since x_3 does not change sign in the region R_2.

A similar analysis can be done for the case when inequalities (5.16c) to (5.16e) are violated. From the above discussion, it can be concluded that the trajectories of x_1 and x_2 would not stay permanently in the region that $\dot{V}_q > 0$.

In the above proof, functions $p_1(t)$, $p_2(t)$ and the parameters in the compensated torques, such as α_1, α_2, K_1 and K_2, play important roles in controlling regions in which

$\mathbf{V_q}$ might increase. Increasing $\mathbf{p_1(t)}$ and $\mathbf{p_2(t)}$ enlarges the regions in which the quasi Lyapunov function decreases. Subsequently, the region in which the quasi Lyapunov function increases will be reduced by adjusting the nonlinear compensation torque (controlled by α_i and $\mathbf{K_i}$ **(i=1,2)**). Therefore, by a proper choice of α_i, $\mathbf{K_i}$ and $\mathbf{p_i(t)}$, **(i=1,2)**, the regions can be controlled so that the amount of increase in $\mathbf{V_q}$ is always less than the amount of decrease in **V** in the adjacent regions in the state space. This way $\mathbf{V_q}$ can be directed to overall decrease until the state trajectories stay within a small region about the upright position.

In summary the quasi Lyapunov function shown in (5.14) does not decrease monotonically which conflicts with the requirements of Lyapunov functions. However, it is guaranteed that the amount of increase of the quasi Lyapunov function is always lower than the amount of decrease in the adjacent regions. Thus, the quasi Lyapunov function is decreasing overall.

5.5 Simulation study

Three numerical examples are presented in this section. The first example compares the performance of the three control laws discussed in this thesis: *(1)* piecewise continuous control law without compensation; *(2)* piecewise continuous control law with compensation, and *(3)* continuous control law. The second example demonstrates the behavior of the quasi Lyapunov function pertaining to the continuous control law. Finally, the last example examines the robustness of the continuous control algorithm in the presence of uncertainty in the parameter estimations or measurements.

In these examples, the base point was allowed to move in **X, Y** and **Z** directions according to the following profiles:

$$\ddot{\tilde{f}}(t) = 2.5\sin(\pi t) \quad (m/sec^2)$$
$$\ddot{\tilde{g}}(t) = 1.5\sin(2\pi t) \quad (m/sec^2)$$
$$\ddot{\tilde{h}}(t) = 2.0\sin(\pi t) \quad (m/sec^2)$$

The initial conditions for the three examples are

$$\theta = 0.3 \ (rad) \qquad \psi = 0.5 \ (rad)$$
$$\dot{\theta} = 0.0 \ (rad/sec) \qquad \dot{\psi} = 0.0 \ (rad/sec)$$

The values of parameters pertaining to the pendulum are **m=36.86kg**, **ρ=0.29m**, **A= 6.0kgm^2** and $\mu = 0.942$. The proportional and derivative control gains were chosen as $k_\theta = k_\psi = 96.0$, $K_{d\theta} = 9.0$ and $K_{d\psi} = 6.0$, respectively.

The response to different controllers are shown in Figures 5.2 and 5.3. The state trajectories tend to zero rapidly and all control systems are clearly stable (Figures 5.2-a and 5.3-a). The response to the piecewise continuous control system without compensation exhibits an error (Figures 5.2-b and 5.3-b). The addition of the nonlinear compensation torque [with α_i=3.5 and K_i=169.0 (i=1,2) in equations (5.6)] reduced such an error. The response belonging to the continuous control system contains slightly larger oscillations about the upright position as compared to those related to the discontinuous controllers. However, the continuous control system was stabilized in a region about the upright position and the amplitudes of the oscillations tend to reduce with time. Note that in this example **p(t)** in (5.13a) was chosen as $p_1(t) = p_2(t) = 2 + 4.5t$ and, ε_1 and ε_2 in (5.13b) were chosen as **2%** of the amplitude of the base point accelerations.

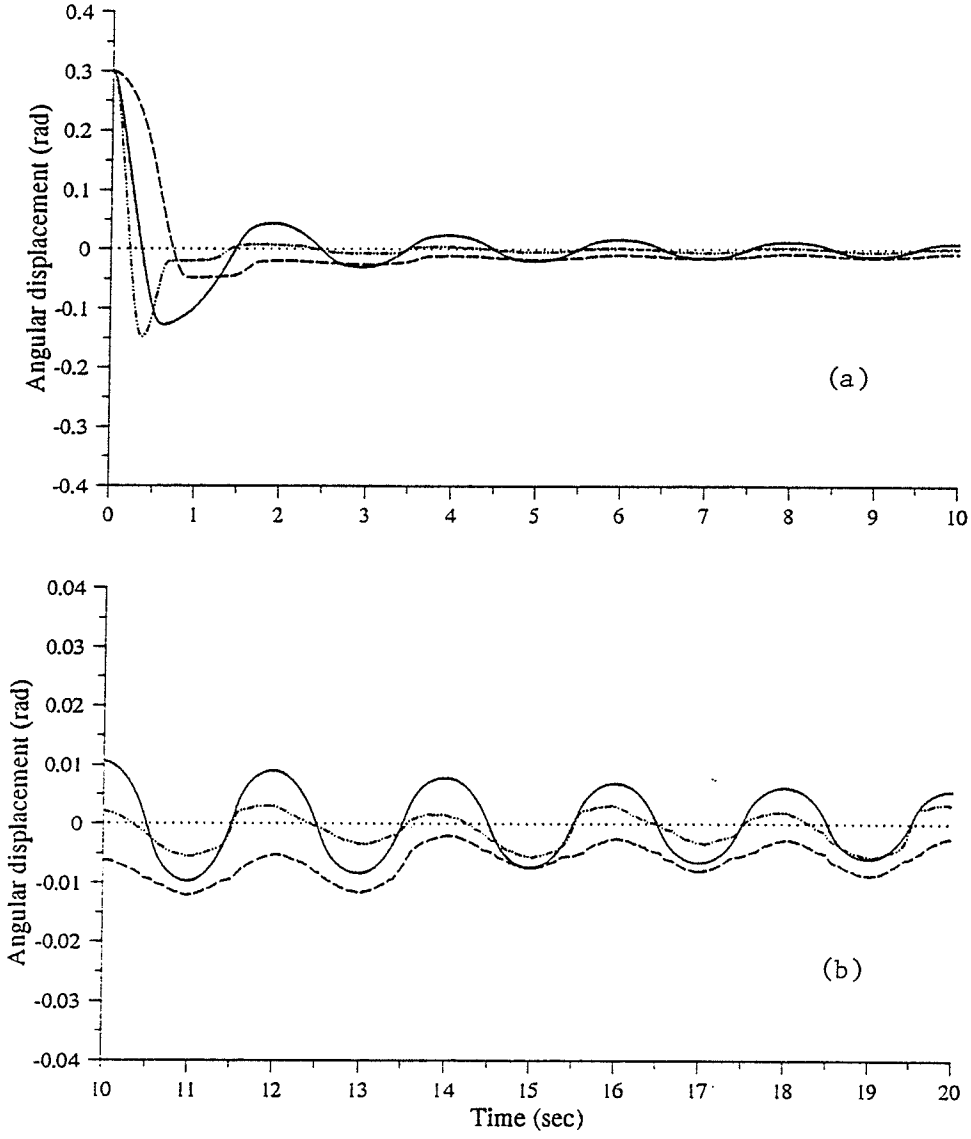

Figure 5.2 *(a)* Angular displacement responses (θ); (----- non-compensated control system; - - - - compensated control system; —— continuous control system).

(b) A close-up of responses.

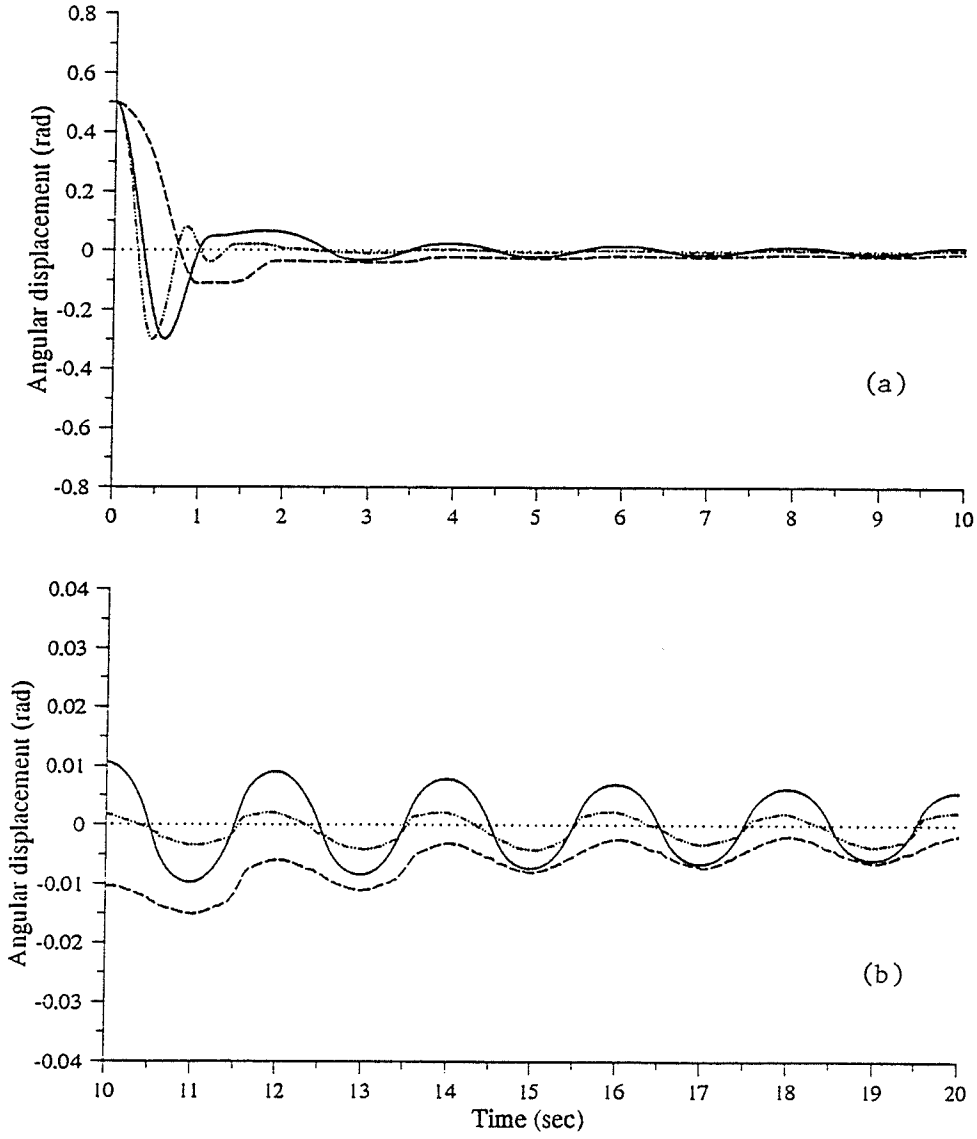

Figure 5.3 *(a)* Angular displacement responses (ψ); (----- non-compensated control system; - · - · - compensated control system; —— continuous control system).

(b) A close-up of responses

The control torques determined by the continuous control strategy and the compensated piecewise continuous control algorithm are plotted in Figure 5.4. The control torques determined from the piecewise continuous control algorithm exhibit chattering. It is also seen that in both cases the controllers are active during the steady-state case. Such torques are necessary to counteract the effect of the horizontal base point motions.

The quasi-Lyapunov function corresponding to the response of the continuous control, shown in Figure 5.4, is plotted in Figure 5.5. As is seen in the figure the quasi Lyapunov function increases during a certain time period,. The amount of the increase is, however, lower than the decrease in the adjacent regions and the function decreases overall.

The last example examines the robustness of the proposed control strategies. The response to the continuous control algorithm was chosen for demonstration. The responses for the case in which $\mathbf{c_1 = m\rho}$ was overestimated by about 50% by the controller was compared with the simulation in which an accurate value of $\mathbf{c_1}$ was used (see Figure 5.6). The corresponding control torques are shown in Figure 5.7. It is seen that both state trajectories converge to zero and the trajectories from the control system with overestimated $\mathbf{c_1}$ tend to zero states faster. The ranges of the control torques for the control system with an overestimated $\mathbf{c_1}$ is slightly higher during the transient stage for the presented example. The response of the continuous controller, when accelerations $\mathbf{F_0}$, $\mathbf{G_0}$ and $\mathbf{H_0}$ in (5.13) were chosen as $\mathbf{1.5}\left|\ddot{\tilde{f}}(t)\right|_{max}$, $\mathbf{1.2}\left|\ddot{\tilde{g}}(t)\right|_{max}$ and $\mathbf{1.5}\left|\ddot{\tilde{h}}(t)_{max}\right|$, respectively, are plotted in Figure 5.8. Overestimating the base point acceleration resulted, in this example, in a shorter settling time and smaller region within which the inverted pendulum

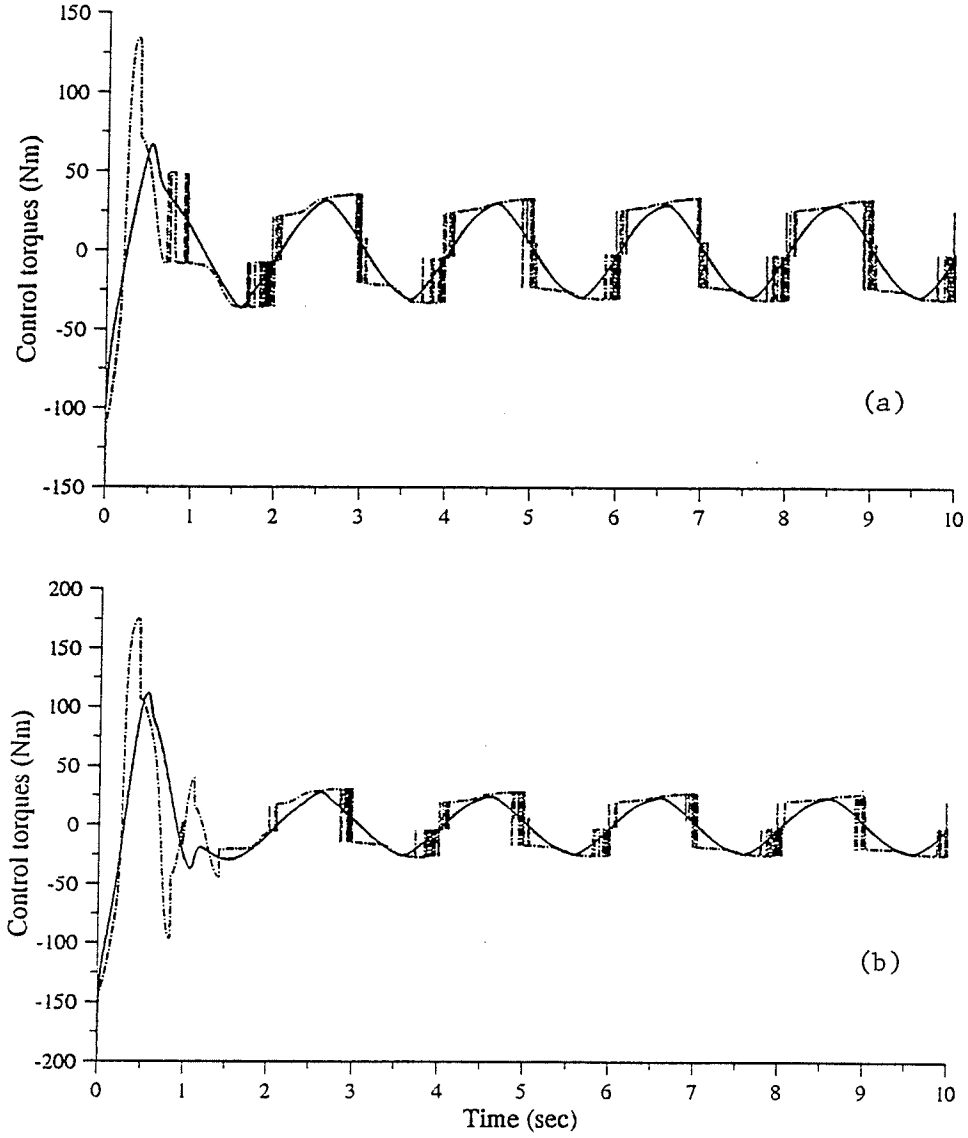

Figure 5.4 Control torques pertaining to Figure 5.2 and 5.3; (a) $\mathbf{M}_\theta$ and (b) $\mathbf{M}_\psi$.

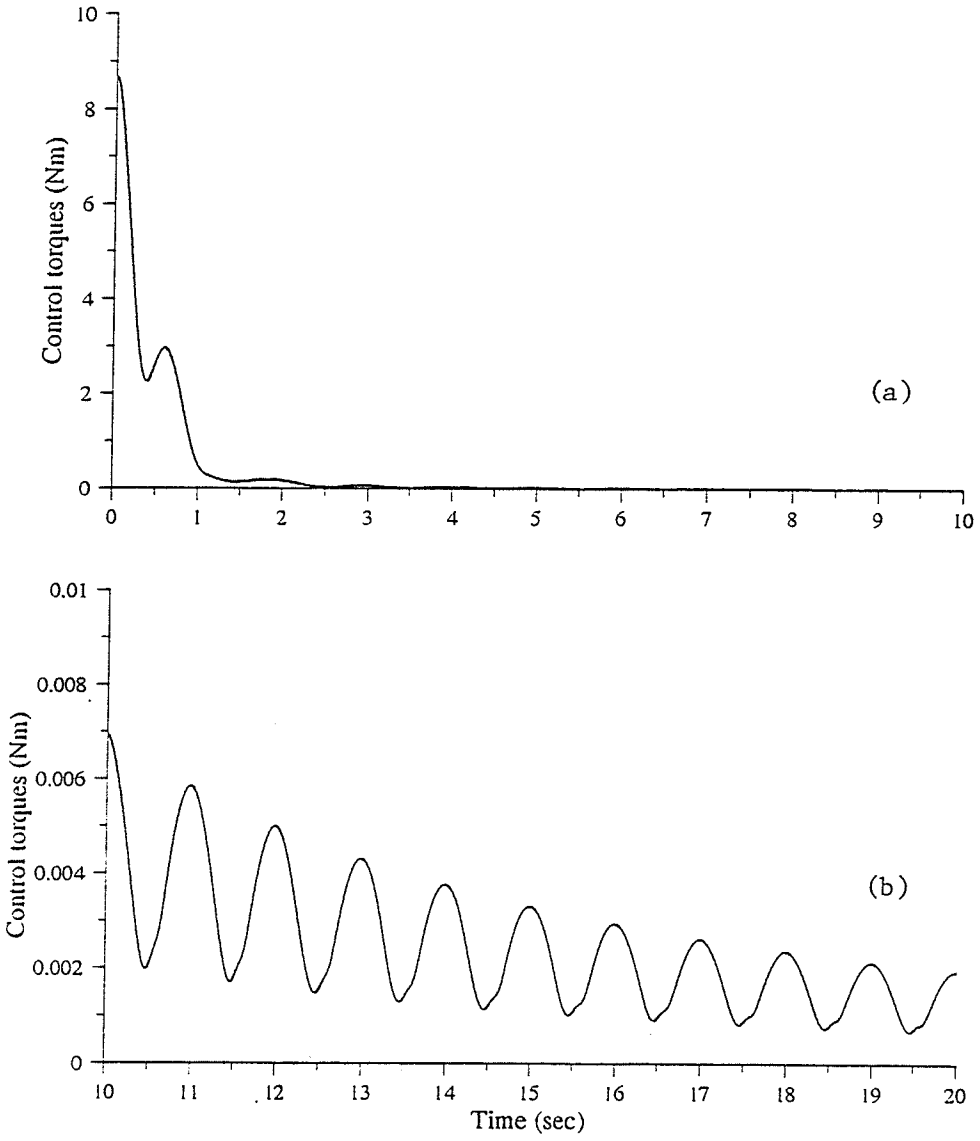

Figure 5.5 *(a)* Quasi Lyapunov function pertaining to the continuous control action

(b) Close-up of the quasi Lyapunov function.

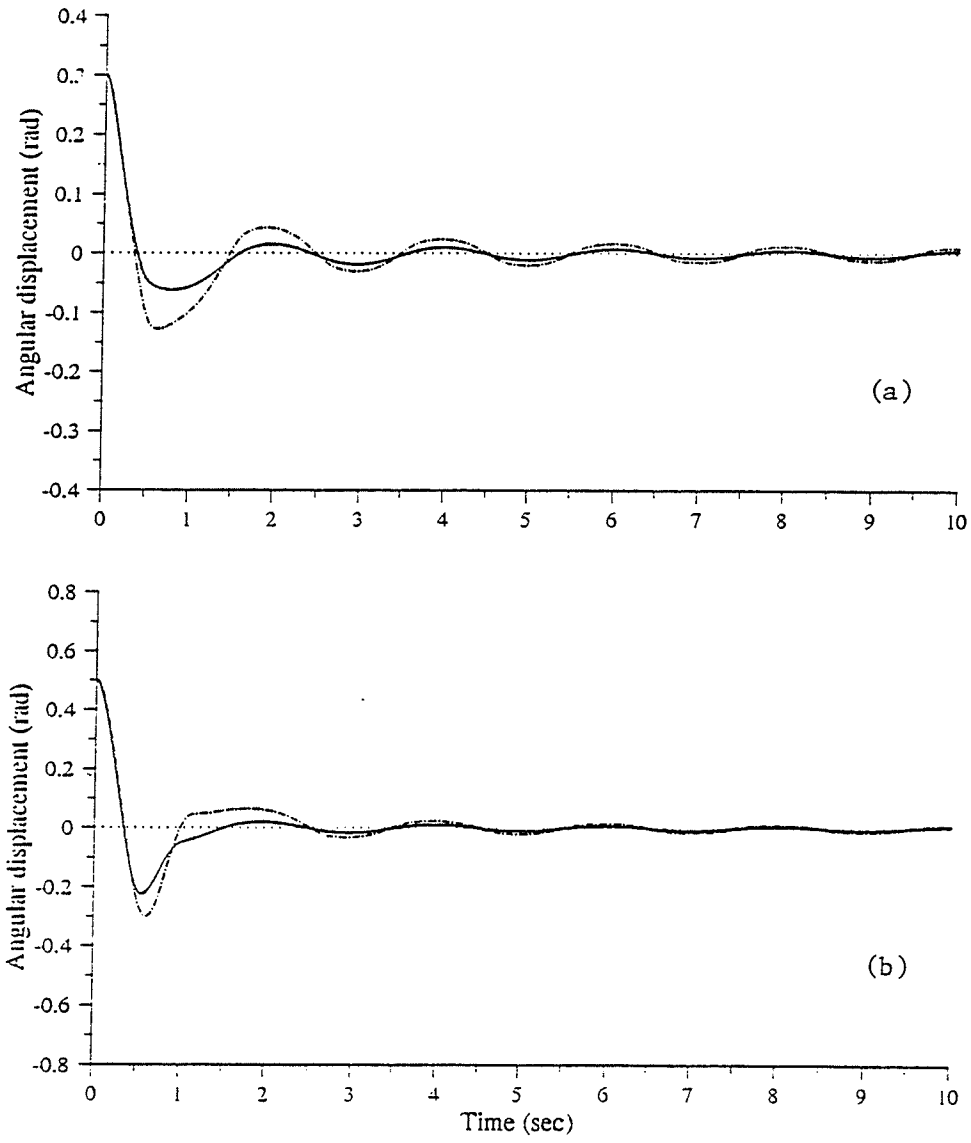

Figure 5.6 Responses of the continuous controller with over-estimated $\mathbf{c}_1$ (——) as compared to those with accurate $\mathbf{c}_1$ (- - - -), (**a**) θ and (**b**) ψ.

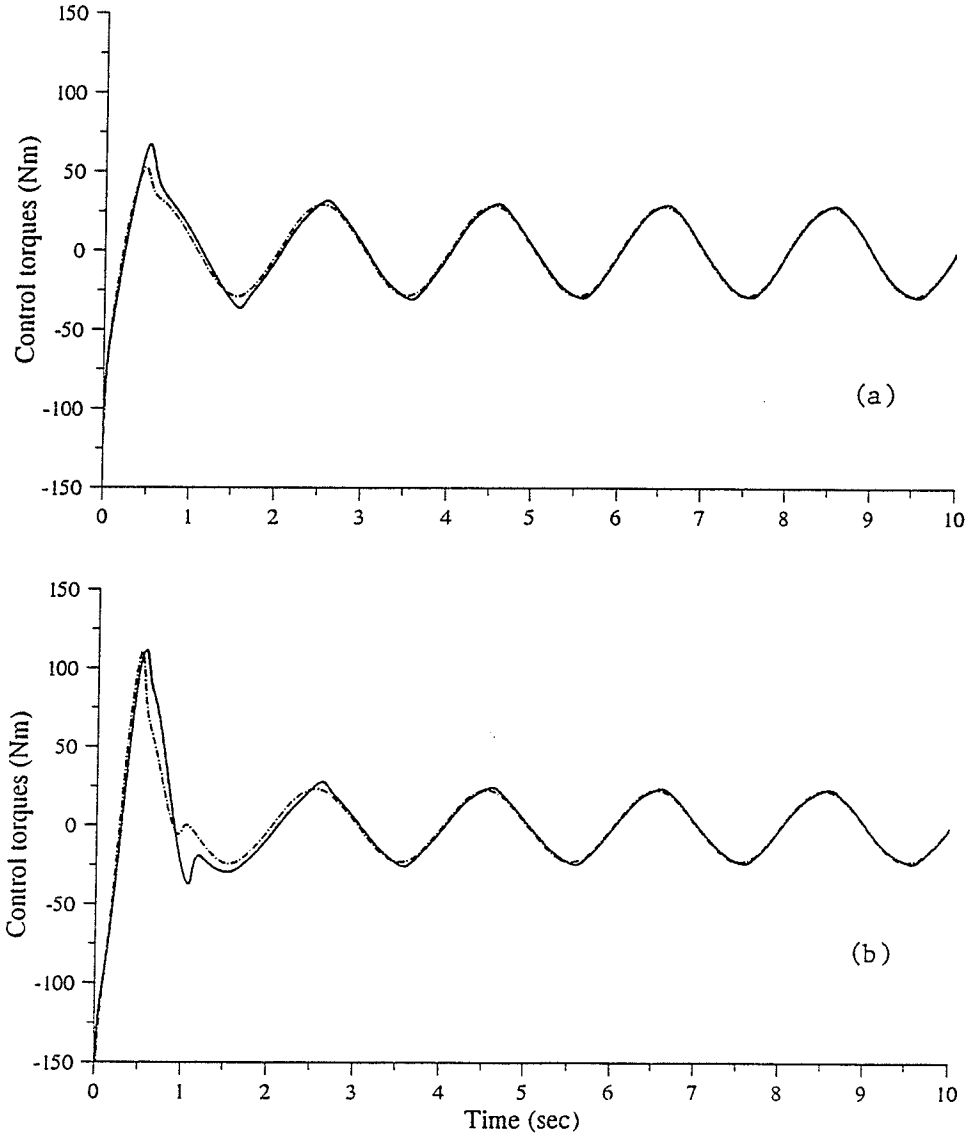

Figure 5.7 Control torques pertaining to Figure 5.6, (a) $\mathbf{M}_{\theta}$ and (b) $\mathbf{M}_{\psi}$.

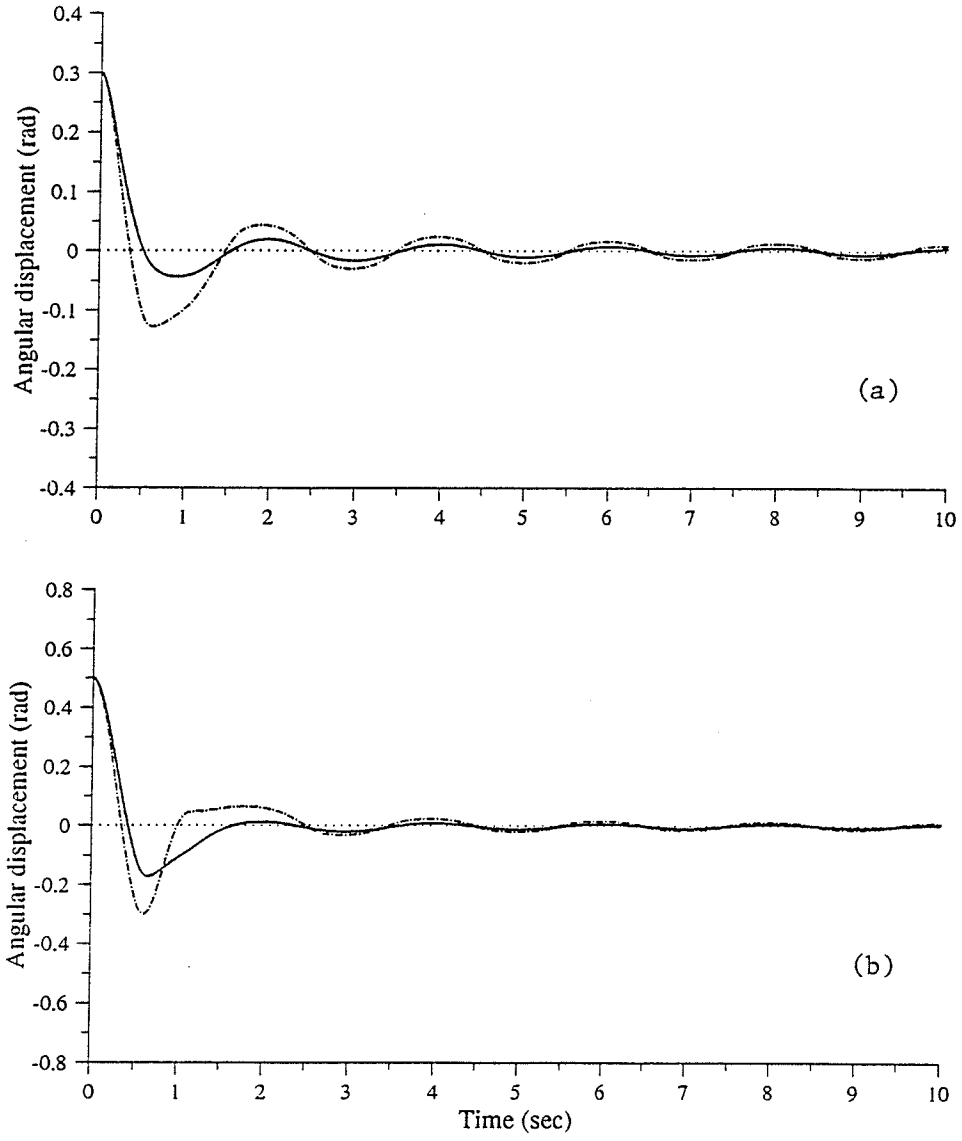

Figure 5.8 Responses of the continuous controller with over-estimated base point accelerations (——) as compared to those with accurate base point acceleration (—·—·—), (a) θ and (b) ψ.

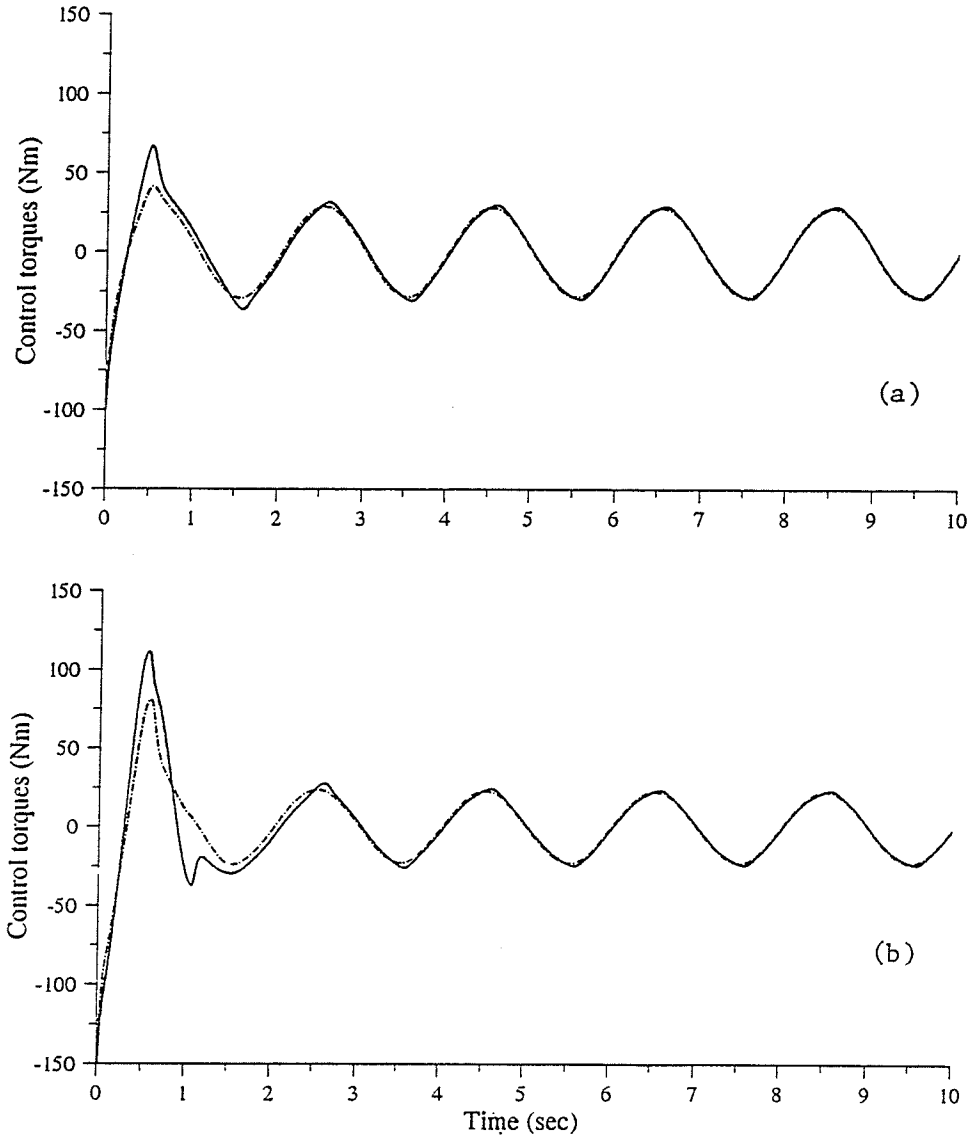

Figure 5.9 Control torques pertaining to Figure 5.8, (a) $\mathbf{M}_{\theta}$ and $\mathbf{M}_{\psi}$.

is stabilized. Overestimating the base point acceleration also resulted in higher corresponding control torques during the transient stage shown in Figure 5.9.

5.6 Summary

In this chapter, two piecewise continuous control strategies and a continuous control strategy were developed to stabilize an inverted pendulum with two degrees of rotational freedom and with a general three-dimensional base point motion. The first piecewise continuous controller guarantees the total stability of the inverted pendulum system about the upright position under the condition of small perturbations. The second piecewise continuous control strategy removes such a condition and can still keep the trajectories of the control system about the upright position within a controlled region. The continuous controller guarantees that the inverted pendulum can be stabilized in a controlled region around the upright position. The robustness of the proposed control systems with respect to those uncertainties in physical parameters and in measurement of the base point acceleration was also examined and it was shown that the system stability is largely insensitive to these classes of uncertainties.

Since the dynamic equations for the system contain discontinuous terms due to the piecewise continuous controller, the requirement of classical existence-uniqueness solution theory is violated. First, the existence and uniqueness of the solution to the proposed piecewise continuous control system was verified using the solution concept proposed by Filippov. Such a solution analysis is important for non-smooth dynamic systems which, in general, has not been studied rigorously, especially for the case when the discontinuity surface is the intersection of several discontinuity surfaces. The stability of the control

system was then verified using Lyapunov's second method and a Lyapunov-like theorem based on Barbalet's lemma. A smooth Lyapunov function was constructed using the extended integral method which removed restrictions on the control gains necessary in previous approach.

The discontinuous terms were then replaced by some continuous functions to avoid chattering of the control actions and to better represent the actual implementation of the developed controller. The control system can be stabilized in a region around the upright position by the continuous controller. A generalized Lyapunov analysis was employed to show that the pendulum can still be stabilized in a controlled region around the upright position.

The above findings were demonstrated through numerical simulations. The simulation results show that 1) the inverted pendulum system is successfully stabilized round the upright position by the proposed control strategies; 2) the system stability is largely insensitive to the uncertainties of some physical parameters and measurements of the base point accelerations and 3) though the quasi-Lyapunov function increases in certain time periods, the amount of increase is always lower than the amount of decrease in the adjacent regions. Thus, the quasi-Lyapunov function experiences an overall decrease.

CHAPTER SIX

APPLICATION OF THE INVERTED PENDULUM MODEL TO THE SIMULATION OF HUMAN TRUNK MOVEMENT DURING WALKING

6.1 Introduction

The mathematical model developed in the previous chapter is now applied to study the dynamics of the human upper body during walking. The objective is largely to advance the development of the mathematical model, not to simulate the direct detailed biological features of walking.

Most previous studies relevant to the human upper body focused on the use of inverse dynamics in which forces and torques are calculated based on the kinematics obtained through gait measurements (Cappozzo, 1982 and 1983; Thornton-Trump and Brodland, 1987; Mansour *et al.*, 1982; Stokes and Forssberg, 1989 and Mackinnon and Winter, 1993). In comparison, investigations of the upper body movement using the simulation approach (also referred to as direct dynamics) are sparse. In the study by Chow and Jacobson (1971, 1972), the unstable upright equilibrium of the trunk was investigated. A control effort was applied to stabilize the trunk which was modeled as an inverted pendulum. The base point of the pendulum was allowed to move to resemble the pelvis movement for normal gait, and the stability of the model was verified using Lyapunov's second method. The work is valuable in that the system stability was investigated which is an area where little work has been done in recent biomechanics research, yet the control strategy was simple enough to allow the interpretation of some muscular activities (Chow and Jacobson 1972). However, the problems of using the model for the simulation of the

upper body movements and for predicting the inter-segmental torques applied at the hip joints were not addressed. Additionally, their control strategy was designed for only prescribed base point motion in the vertical direction which imposes a limitation on the application of the model. Hemami and Katbab (1982) studied Chow and Jacobson's work in a more general context; self rotation (rotation about the longitudinal axis) was added and methods of preventing it were presented. Their model, however, did not include the base point motion when the stability was analyzed.

In this work, the dynamic model of the inverted pendulum developed in Chapter Five is used to simulate the upper body movement and to predict the hip torques for different gait patterns. The human upper body is simplified as an inverted pendulum with two degrees of rotational freedom about the base point. The base point is located at the bony landmark at the sacrum. The base point of the pendulum can move in three-dimensional space in a general way to resemble general gait patterns. The movement of the upper body is measured in the gait laboratory for the corresponding gait patterns. The simulated displacements of the gravity center of the upper body are compared with the measured ones and the control torques are compared with the trunk torques calculated from the kinematics of walking. The purpose of such a comparison is to establish the promise of the model for the further studies. Before the simulation results are presented, the inverse dynamic study of the upper body during walking is described below.

6.2 Mechanical model

The human upper body, consisting of the head, the trunk (the thorax and the pelvis) and the upper limbs, was simplified as one rigid link in this study. The inertial and

gravitational effects of the head and arms were included with those of the trunk. The head and swinging arms have certain influence on the trunk movements and the upper body dynamics (Cappozzo, 1983; Mackinnon and Winter, 1993). However, the first order dynamic features of the upper body, i.e., the magnitudes and the frequencies of the forces and the torques, are mainly decided by the trunk movements (Cappozzo 1983). Finally, although the relative motion between the thorax and the pelvis has been discussed in kinematic analyses (Thorstenson *et al.*, 1983 and Stokes and Forssberg, 1989), the trunk has been treated as one single link in most dynamic analyses (Onyshko and Winter, 1981; Cappozzo, 1983; Mackinnon and Winter, 1993 and Scheiner, 1993).

The kinematics of the trunk are described using the relative movement between the body coordinate system with respect to the inertial coordinate system. The axes of the body coordinate system were defined relative to three non-collinear reference points (the anatomical landmarks), such as first thoracic vertebral (T1), the bony landmark at the sacrum and the left crommion process. One axis was directed as the vector starting from the bony landmark at the sacrum and ending at T1. The second axis was perpendicular to the plane defined by the three anatomical references. The third axis was defined so that the set of axes formed a right handed system of reference. The origin of the body coordinate system was fixed at the estimated gravity center of the upper body. Three Euler angles, described in Appendix A, were used to described the rotations between the body coordinate system and the global coordinate system. The Euler angles were then calculated based on the displacements of the markers.

The self rotation was not included to simplify the model. Such a simplification is appealing in that only two equations are considered for the pendulum model and the coefficient matrices are less coupled (Chow and Jaconson, 1972). The effect of neglecting self-rotation on the resultant trunk torques applied at the hip joints is expected not to be significant. Stokes *et al.* (1989) reported that the pelvis and the thorax rotate about the vertical axis, but in opposite directions for most of the stride cycle. Similar observation was made by Vaughan and Sussman (1993). The reciprocal rotational movement of the thorax and the pelvis about the vertical axis tends to reduce the rotational momentum of the upper body (Stokes and Forssberg, 1989). Such a reciprocal rotation about the longitudinal axis is mainly controlled by internal oblique and external oblique, which is the internal action at the trunk segment. Moreover, the mass moment of inertia of the trunk about the longitudinal axis is much lower than those about the other two principal axes, resulting in a less dynamic effect (Cappozzo, 1983 and Hemami and Katbab 1982). Therefore, when considering the trunk as one link, it is an acceptable assumption to study the non-self-rotational case. The model, however, may not be adequate for certain severe pathological gaits in which the effect of self rotation is noticeable. In such cases, the model (including the control strategy) should be extended to include the self-rotation.

Finally, the human trunk was considered to be supported at one base point in this work, rather than two points representing the two hip joints. To consider the upper body alone, a one base point model must be used (Cappozzo, 1983 and Mackinnon and Winter, 1993). In order to distinguish the forces at the two separate hip joints, lower limb motion

must be known, which would require the simulation of a more complex system. Such a simulation is beyond the scope of the current work.

6.3 Inverse dynamic analysis

Inverse dynamic analysis of human trunk is one of the greatest challenges in locomotion analysis due to the low range of motion. In this section, an inverse dynamic analysis of human trunk during walking is presented. The results are to be compared with the simulation results to validate the developed model. The emphasis of this section is to elaborate the inverse dynamic model and the technique of the measurement.

6.3.1 Gait Measurements

The experimental protocol was based on those of Cappozzo (1981) and Stokes (1989). The gait measurement was conducted in the Biomechanics Laboratory at Physical Education, The University of Manitoba.

Videography principles

Video is an electronic medium that uses charge, voltages, and magnetic fields to pick up, transfer, and store visual images. The Peak Motion Measurement System is one of less expensive photogrammetric systems for locomotion analysis. The basic assumption of the Peak system is that the amount of the movement on the video is directly proportional to the amount of actual movement. This assumption means that the camera image plane is parallel to the plane in which the motion is to take place. In other words, the optical axis of the camera lens is perpendicular to the plane of motion. (see Figure 6.1). The standard video camera operates at a 60 Hz (hertz) frame rate, or sample frequency.

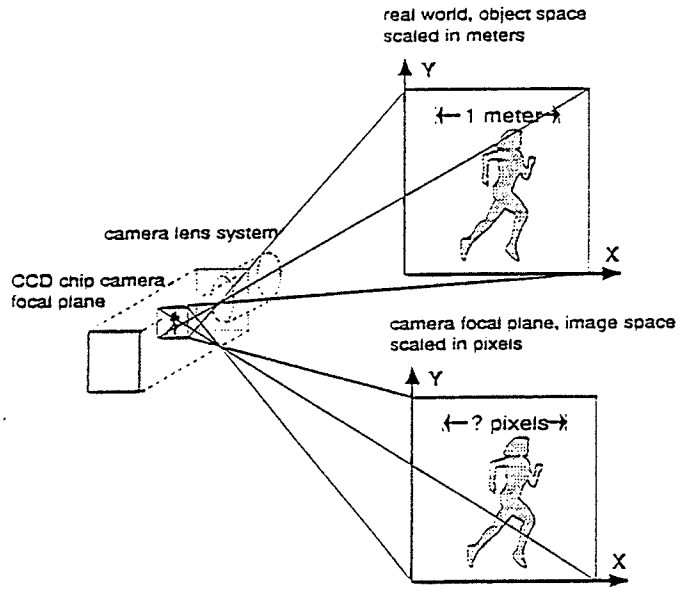

Figure 6.1 The camera image plane is parallel to the object plane (reproduced from the menu of Peak Motion Measurement System).

There are methods to obtain three-dimensional coordinate data from multiple two-dimensional views. The peak system uses the Direct Linear Transformation (DLT) method (Abdel-Aziz and Karara, 1971). By digitizing a control object of known coordinates, the image space may be calculated and any movement throughout the image space can be determined. The DLT method establishes a direct linear relationship between digitized coordinates from two or more camera views and the three-dimensional space coordinates by using the intersections of lines or vectors, from each camera view to determine the point in space. Line intersections work optimally from cameras positioned perpendicularly; line intersections work worst at positions nearly parallel. The relationships between the location of the same point in the object space and image space are shown below:

$$u + \frac{l_1X + l_2Y + l_3Z + l_4}{l_9X + l_{10}Y + l_{11}Z + 1} = 0$$

$$v + \frac{l_5X + l_6Y + l_7Z + l_8}{l_9X + l_{10}Y + l_{11}Z + 1} = 0 \qquad (6.1)$$

where **u** and **v** are the positions in the image space and **X**, **Y** and **Z** are the known positions of the control points in the object space. Supplying a set of control points with known **X**, **Y** and **Z** coordinates for the points on the calibration frame, the coefficients l_i, **(i=1,...,11)** can be determined. A minimum of six non-coplanar points are required. More control points will improve accuracy, but the point of diminishing returns is 20 points. The control points must be digitized, providing horizontal and vertical orientations of the video camera. Control points must be accurately measured and digitized to reduce error in gait data. For a two-camera, three-dimensional system, six non-coplanar points on the calibration frame are required. Once the camera parameters are known, any unknown point in the object space may be obtained. These camera parameters are constants as long as the position of the camera, the lens focus, and focal length remain unchanged (see Figure 6.2). For the measurements conducted in this thesis, the DLT parameters are calculated and listed in Table 6.1.

Experimental protocol

The movements of the trunk were recorded using The Peak5 Motion Measurement System. A passive marker system was used in which half ping-pong balls served as markers. Such markers were tracked by two video cameras. One camera faced the left sagittal plane and the other faced the dorsal plane. The markers were located at the following anatomical landmarks: the bony landmark at the sacrum, the left iliacrest, the

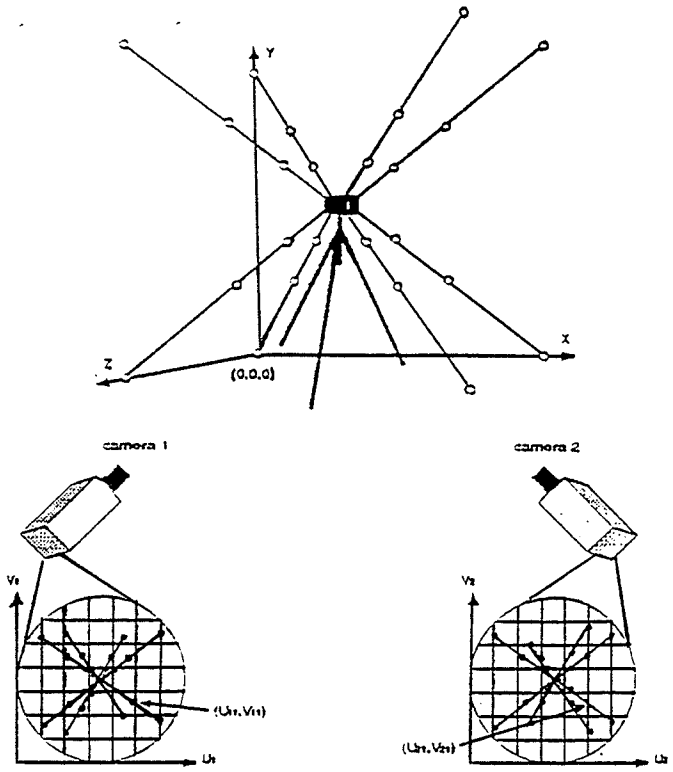

Figure 6.2 Calibration frame (reproduced from the menu of Peak Motion Measurement System).

Table 6.1 DLT parameters for the measurement setup.

	camera 1	camera 2
	DLT para.	DLT para.
1	-89.086958	46.3222136
2	2.29575	-6.068890
3	131.084055	186.116376
4	28.864432	7.775701
5	13.255251	18.958232
6	150.124488	144.380419
7	37.814534	-6.321953
8	9.793642	8.368506
9	0.032688	0.062735
10	-0.009536	-0.005992
11	0.139512	-0.039817

estimated gravity center, the left acromional process and the first thoracic vertebra. Calibration of the three-dimensional system was performed prior to each measurement trial. A wire pyramid, shown in Figure 6.2, containing 24 markers whose positions were accurately known was placed in the object space. When an a priori calibration accuracy was obtained, the camera positions were fixed and the calibration frame was removed. One normal subject performed repeated trials of normal walking and walking with the left knee fixed. Several practice trials were used to determine the subject's preferred (free) walking speed, and to check the equipment and to explain the experimental protocol. The subject was also asked to keep the upper limbs flexed so that the arm and the forearm formed an approximated 90^0 angle in order not to cover the markers on the pelvis. This arm position has little effect on the trunk movement as was proven by Cappozzo (1983). During the tests, the subjects wore their everyday shoes, care was taken to avoid extra-high heels or too-rigid soles.

6.3.2 Processing of raw kinematic data and derivative estimation

The converted coordinates of the center of the markers from the camera image space are called raw data and they contain additive noise from many sources: electronic noise in optoelectric devices, spatial precision of the TV scan or film digitizing system, and human error in film digitizing. All of these errors will result in random errors in the converted data. It is therefore essential that the raw data be filtered.

In the processing of any time-varying data, no matter what their sources are, the sampling theorem must not be violated. The theorem states that "the process signal must be sampled at a frequency at least twice as high as the highest frequency to be considered

in the data". If we sample a signal at too low or too high a frequency, we get aliasing errors. For human locomotion (normal walking), it was shown by Winter (1982) that kinetic and energy analysis can be done with negligible error using standard 24-frame per second movie camera.

Several procedures can be employed for adjusting measurements containing random errors. A number of papers have been published in recent years presenting these procedures with particular reference to their use in studies of biomechanics (Winter *et al.*, 1974; Cappozzo *et al.*, 1975; Zernicke *et al.*, 1976; and Murphy and Mann, 1990). In this work, the measurement data were filtered using a low-pass, fourth order, zero lag filter at a cut-off frequency of **4Hz**, which is the same as the approach used in Macnnon and Winter (1993). The corresponding velocity and acceleration trajectories were determined using numerical differentiation.

6.3.3 Anthropometric measurements

Anthropometric measurement was made on the test subjects with the objectives of determining the mass and the gravity center of the upper body, and estimating the inertial properties of the upper body segments. The required anthropometric measurements are body mass, height, shoulder height and trochanter height. Using these anthropometric quantities, the following inertia parameters were estimated for the upper body of the subject: mass, segment length, distance between the gravity centers of the head and the trunk, and moments of inertia about the principal axes passing through the gravity center. Some of the relevant methods provided in the literature were reviewed and estimations were made accordingly by Chaffin and Andersson (1992). Different procedures often lead

to remarkably different results and the anthropometric parameters have the nature that could not be proven. The method of determining the anthropometric data provided by Chaffin and Andersson (1992) were used for the dynamic analysis of the current study. The required anthropometric measurements are listed in Table 6.2 for one subject and the calculated inertial properties are listed in Table 6.3.

Table 6.2. Basic measurements for anthropometry calculations.

body weight **W** (kg)	height (m)	shoulder height (m)	trochanter height(m)
56.7	1.68	1.41	0.9

Table 6.3. The inertial properties of one subject.

mass of the head and neck (kg)	4.76
mass of the torso and the upper limbs (kg)	34.13
length of the head (m)	0.27
length of the trunk (m)	0.51
distance between the CG of the trunk and the trochanter (m)	0.31
distance between the CG of the head and CG of the trunk (m)	0.31
radius of gyration of the trunk (m)	k_x=0.18 k_y=0.11 k_z=0.22
radius of gyration of the head (m)	k_x=0.084 k_y=0.092 k_z=0.086
mass inertia of the trunk (kgm^2)	I_x=1.57 I_y=0.39 I_z=1.63
mass inertia of the head (kgm^2)	I_x=0.03 I_y=0.04 I_z=0.035
total mass inertia of the upper body (kgm^2)	I_x=1.69 I_y=0.425 I_z=2.235

In biomechanical computations of effect of the moment of inertia, the concept of radius of gyration **K** is used. It is a derived variable that expresses the radial distance from the axis of rotation at which the mass of the segment can be concentrated without altering the moment of inertia of the segment. The radius of gyration is computed as follows (Chaffin and Andersson, 1992):

$$\mathbf{K} = \sqrt{\frac{\mathbf{I}}{\mathbf{M}}}$$

where **I** is the moment of inertia about the principal axis and **M** is the mass of the segment.

6.3.4 Dynamic calculations

The dynamic equations that will be used to calculate the trunk forces and torques are derived in Appendix B and are shown in equations B.5.

6.3.5 Accuracy

The accuracy of the results depends upon two factors: the accuracy of the experimental data and the accuracy with which the adopted model reflect the real system. The relationship between variation in the final results and experimental errors was estimated using a sensitivity analysis: various sets of basic data were perturbed and the consequent variation in the end results were observed.

Experimental errors

The errors in the measured coordinates of the markers were, as is always the case, of two types; systematic and random. Systematic errors were due mainly to optical distortions within the cameras, to the deformation of photographic material, and to the inaccuracy with which the system constants were measured. The systematic errors are

estimated by comparing the measured locations of the control points (markers of the calibration frame) with their true locations which are known. The residuals are shown in Table 6.4. The first column shows the twenty four control points. The second and third columns display the computed coordinates and the residual values. The computed coordinates contain the coordinates that the DLT algorithm computed for the control points. The residual values contain the differences between the computed values and the actual coordinates of the control points. The last column displays the resultant distance between the measured and computed points. The average mean square error displays the net error for all points for **x**, **y**, **z** and origin position. This number provides a representative measure of the intrinsic error of the camera configuration and arrangement. Finally, the average volume percent error position gives the overall error of the calibration. When the differences between the actual control point coordinates in the DLT setup are used correctly, the three-dimensional Peak5 system will produce **x**, **y**, and **z**-coordinates within an accuracy of **0.5** percent. The calibration is acceptable if the errors are within 0.5 percent of the calibrated field of view. For example, the Peak5 calibration frame is approximately **2.2 m** in **x** and **y** direction, the error of the position should be within **17.5 mm.** It is shown from Table 6.4 that the maximum error of the position is **17mm** at control points **g** and **h**. Thus, the systematic errors are within the acceptable regions.

Essentially the random error may be attributed to the digitization process of the marker positions in the image space, i.e., quantization and inaccuracy related to the digitizer cursor alignment on the marker image. An analysis of the sensitivity of the calculated was assessed by repeating the digitization of the same frame thirty-one times. The

Table 6.4 Residual of the digitized control points. Number of control points is 24 and the degrees of freedom is 37

point	computed			residual			position
	X (m)	**Y** (m)	**Z** (m)	**X** (m)	**Y** (m)	**Z** (m)	
a	-0.002	-0.007	-0.003	-0.002	-0.007	-0.003	0.009
b	0.448	0.427	0.347	0.008	0.003	0.003	0.009
c	0.822	0.729	0.595	-0.003	0.004	0.006	0.007
d	-0.018	1.912	0.002	-0.001	-0.002	-0.008	0.008
e	0.479	1.502	0.348	0.015	-0.004	0.010	0.010
f	0.818	1.217	0.589	-0.005	0.004	0.001	0.007
g	2.230	1.911	-0.004	0.001	-0.003	-0.016	0.017
h	1.727	1.504	0.347	-0.013	-0.001	0.010	0.017
i	1.399	1.212	0.594	0.007	0.001	0.007	0.010
j	2.218	0.005	0.001	0.001	0.005	0.001	0.006
k	1.735	0.424	0.347	-0.001	-0.001	0.005	0.005
l	1.380	0.727	0.591	-0.011	0.001	0.002	0.011
m	2.228	-0.002	1.582	0.010	-0.005	-0.000	0.011
n	1.739	0.422	1.234	0.002	-0.004	-0.006	0.008
o	1.397	0.726	0.994	0.006	-0.000	0.001	0.006
p	2.232	1.914	1.596	0.001	-0.003	0.005	0.006
q	1.734	1.510	1.240	-0.007	0.003	-0.003	0.008
r	1.389	1.216	0.992	-0.003	0.003	-0.001	0.005
s	-0.011	1.916	1.597	0.004	0.002	0.003	0.005
t	0.472	1.504	1.241	-0.003	-0.002	-0.003	0.004
u	0.827	1.213	0.993	0.003	0.001	-0.001	0.003
v	-0.003	0.000	1.581	-0.004	0.000	-0.004	0.005
w	0.472	0.472	1.236	-0.008	0.003	-0.003	0.009
x	0.828	0.728	0.990	0.003	0.001	-0.004	0.005
Average mean square error				0.007	0.003	0.006	0.009
Average volume % error				0.294	0.170	0.363	0.279

standard deviation of the random error on the calculated coordinates in the object space was estimated to be **5.4mm**, **1.4mm** and **1.7mm** in the **x**, **y** and **z** directions, respectively. These values did not significantly depend on the position of the digitized point in the stereoscopic field. From the above error estimation, it can be seen that the random error in the **x** direction is much higher than those in **y** and **z** directions, and this is due to the fact that the calculation of the **x** coordinate is based on positions of the markers on the image space from the camera facing the sagittal plane. The markers are partially shown on the image plane. Therefore, more estimation was involved in location the cursor during digitization. Such errors are believed acceptable as compared to the similar studies (Cappozzo, 1983).

A further error has to be considered due to skin movement relative to the relevant bony landmarks which allows for the unavoidable movement of the markers relative to the bony landmarks. It must be emphasized that this movement correlates very well with main movement, i.e. it has the same type of periodicity. This fact inhibited the possibility of reducing its influence on the measurements by means of conventional smoothing methods. The relevant error could only be minimized by exercising a cautious choice of the anatomical landmarks.

As far as the body segment inertial parameters were concerned, the sensitivity analysis was carried out. Certain errors were imposed on the basic data of normal walking and the consequent variation in the end results were tabulated. The error in the mass of the upper body (including the head, arms and trunk) was hypothesized to be within 10%. The effect

of such an error in the final results was estimated based on the dynamic equations shown in Appendix B. The maximum differences between the final results from two sets basic data are reported in Table 6.5. It is shown that the maximum differences in the horizontal forces are within 6N which is not very sensitive to the error in the mass of the upper body, but the difference in the vertical force is significant (**50N**). This is because 10% increase in mass causes about **40N** increase in weight. The effect on the torques are within **4Nm**.

The inaccuracy in the coordinates of the center of the mass of the upper body was assumed to be within **2cm**. It can be seen that the greatest effect of such an error is on $\mathbf{M}_\theta$ (**8Nm**) and $\mathbf{F}_y$ (**8N**) (see Table 6.5). As far as the mass moments of inertia are concerned, a pessimistic error of 30% was hypothesized for the moments of inertia of the upper body about its principal axes fixed at the gravity center and the consequent variation of the final results are within **8Nm** (Table 6.5).

Other input variables which had important effects on the final result accuracy were the accelerations of the base point. An error of 30% was assumed for each base point acceleration and the differences of the final results are shown in Table 6.5. It is obvious that even a low error in the acceleration in the **x** direction can cause significant change in the force in the walking direction (approximately 35N) and in the segment torque $\mathbf{M}_\theta$ (about **11Nm**). The error in the vertical acceleration has a small effect on the segmental torques but a larger effect on the vertical hip force (about **24N**). The error in the **z** direction has little effect on the torque of $\mathbf{M}_\theta$ but a larger effect on the torque $\mathbf{M}_\psi$ (**3.5Nm**) and the force in the same direction (**17.5N**). Therefore, it is concluded that the

trunk forces and torques are sensitive to the accelerations at the base point, but less sensitive to the mass moment of inertia.

Table 6.5 The maximum differences of the final results between the basic data and the disturbed data.

	F_x (N)	F_y (N)	F_z (N)	M_θ(Nm)	M_ψ(Nm)
Mass (10%)	5.6	46.6	3.8	3.2	1.5
I_x (30%)	—	—	—	1.9	6.1
I_x (30%)	—	—	—	0	0.44
I_x (30%)	—	—	—	7.6	2.36
ρ (2cm)	3.86	7.4	2.24	7.94	3.42
$\ddot{\tilde{f}}(t)$ (30%)	35.01	—	—	10.5	0.2
$\ddot{\tilde{g}}(t)$ (30%)	—	23.34	—	0.97	0.97
$\ddot{\tilde{h}}(t)$ (30%)	—	—	17.5	0	3.5

In order to validate the measurements in this study, the experimental results were qualitatively compared with the previous studies (Stokes and Forssberg 1989). For example, the range of motion of the gravity center was measured as 4.8 cm in the vertical direction, as compared to the measured displacement of 4.7 ± 1.7 cm reported by Stokes and Forssberg (1989). In the bilateral direction, our measurement was 4.2 cm as compared to 5.1 ± 1.1 cm from Stokes and Forssberg (1989).

In summary, the dynamic analysis of the trunk movement is one of the greatest challenges in human locomotion analysis due to the fact that the range of motion of the trunk is low (approximated 8^o). The measurement conducted in this work is a preliminary study, the error analysis and sensitivity analysis show that the first order features of the

trunk movement and dynamics, namely the frequencies and the magnitudes of the movement, the forces and torques during walking are reasonable. However, to characterize the higher order features, more sensitive equipment and technique are required.

6.4 Gait Simulations

To substantiate the capacity of the proposed model in this dissertation, three case studies are presented for three gait patterns; normal walking, walking with the left knee fixed and walking of an adult with cerebral palsy. The simulation results of the first two cases were compared with the results calculated based on the gait measurements described in Section 6.3. The results for the third case are of a predictive nature since measurements and inertial parameters were not available.

A typical gait pattern from one subject was chosen for the comparison to the simulation results since inertial parameters are particular to individual subject. The values of the anthropometric parameters of the subject are listed in Table 6.3. The only kinematic input to the simulation model is the accelerations of the point related to the bony landmark at the sacrum. The control gains in the model were adjusted to produce the displacements of the gravity center similar to those obtained from the measurement. Note that the displacements of the gravity center were chosen for comparison since they are important features of upper body movement and are easily calculated from the Euler angles. The predicted torques from the control algorithm were then compared with the trunk torques calculated from the kinematics of the gait measurements.

6.4.1 Normal Gait

In this case, the subject was asked to walk at a comfortable speed. The measured displacements of the bony landmark at the sacrum for the normal gait are shown in Figure 6.3. The simulated gravity center motion is shown by solid lines in Figure 6.4, while the dotted lines are the measured displacements of the gravity center. The simulation results match the measurements reasonably well. The difference of the displacement ranges at the gravity center is within 20%. The torques at the hip joints were predicted by the model and are shown by solid lines in Figure 6.5. The dotted lines are the torques calculated based on the gait measurements. The difference of the amplitudes are within 15%. It is seen that the torques: *(a)* guarantee the stability of the inverted pendulum, *(b)* move the pendulum in a way similar to the upper body movement, and *(c)* are reasonably close to the torques originated from the hip joints as determined by inverse dynamics based on measurements.

6.4.2 Walking with the Left Knee Fixed

In this example, the subject was asked to wear a knee brace and to walk. The measured displacements of the bony landmark at the sacrum in the inertial coordinate system are shown in Figure 6.6. The simulated displacements and the measured displacements of the gravity center, in the inertial coordinate system, are shown in Figure 6.7. The difference between the simulated and the measured displacement ranges is within 20% of the measured values. The amplitudes of the predicted torques, shown in Figure 6.8, match within 15% of those obtained through the experimental data. It is seen that the simulated motion at the gravity center follows the trend of the experimental measurements and the

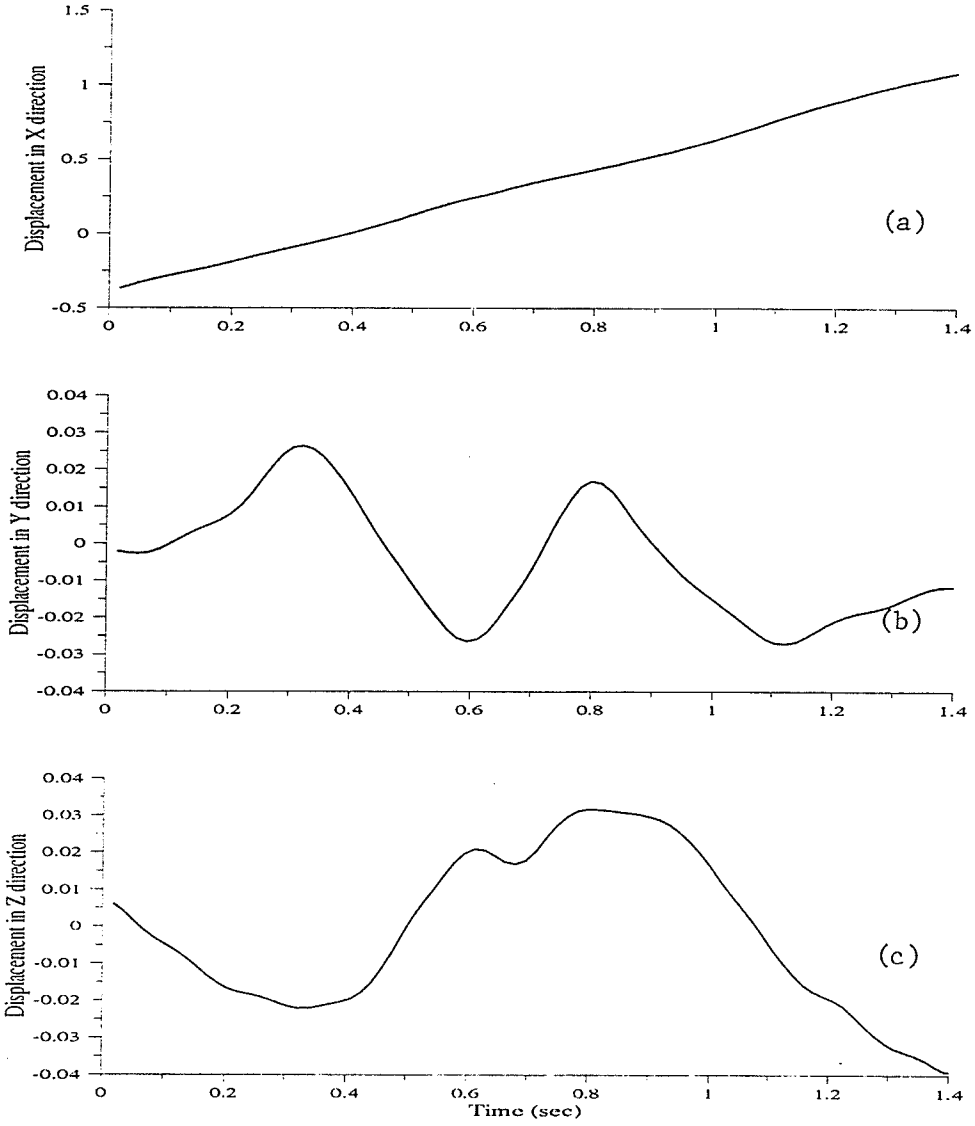

Figure 6.3 Measured Displacement of the bony landmark at the sacrum during normal walking ; stride period: **1.12s**; mean speed: **1.1m/s**; mean stance duration: **61%** of stride period.

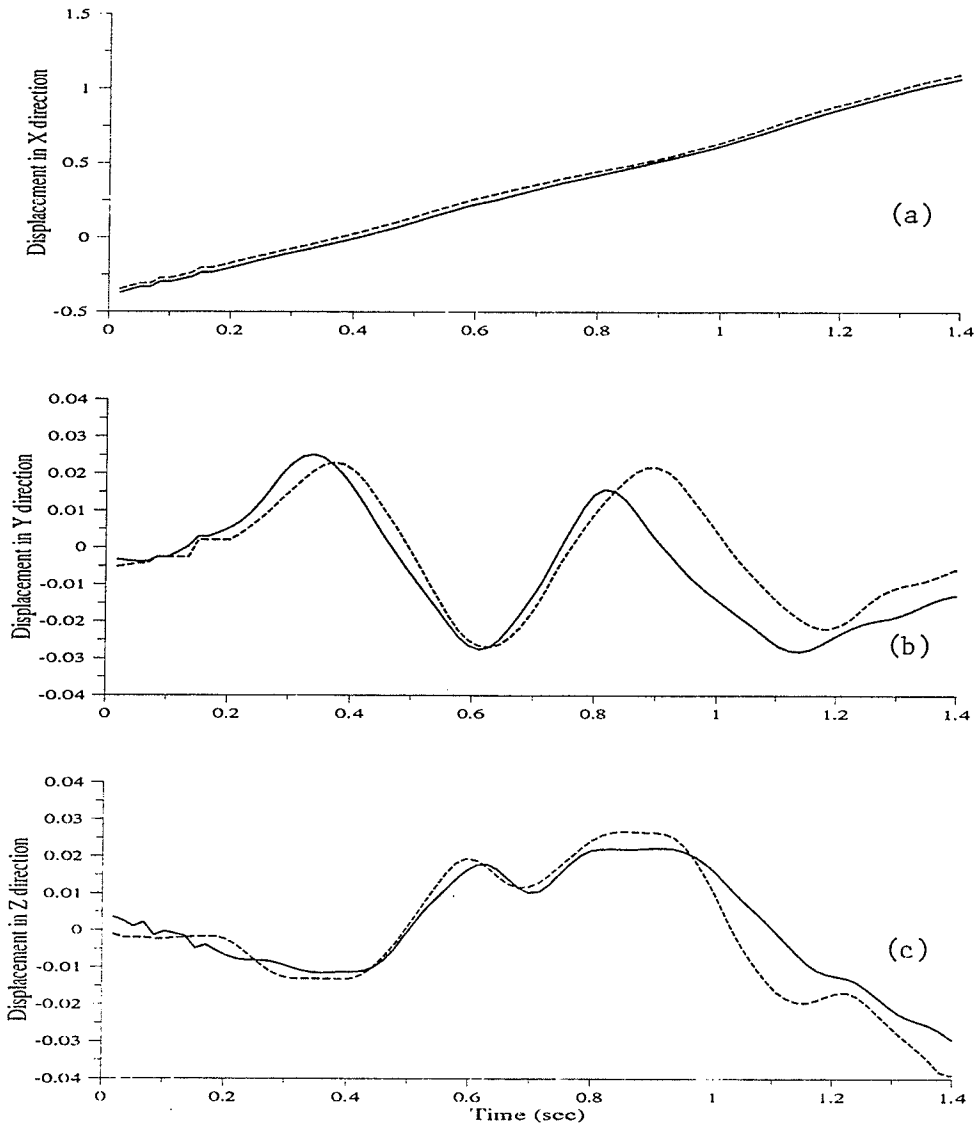

Figure 6.4 Comparison between the simulated (——) and the measured (-----) displacements of the gravity center for normal walking.

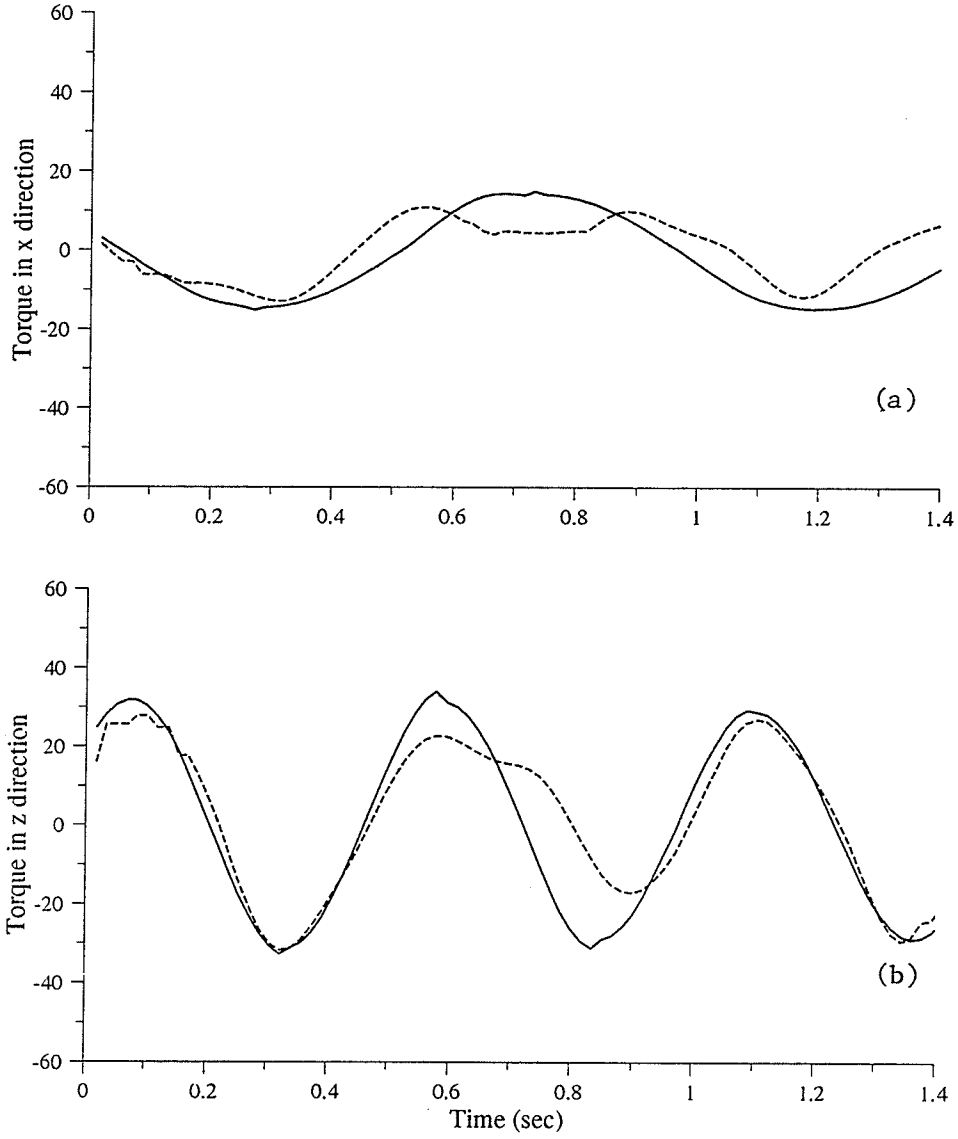

Figure 6.5 Comparison between the torques predicted from the proposed model (——) and the torques calculated based on the gait measurements (-------) for normal walking.

predicted torques, using the model developed in this dissertation, match these from measurements.

6.4.3 Walking of an Adult with Cerebral Palsy

The model developed in this study was used to predict the torques for walking of an adult male with cerebral palsy. The hip motion for such a gait pattern was reported by Vaughan *et al.* (1992) and is shown in Figure 6.9. The displacement of the bony landmark at the sacrum in the walking direction is shown in Figure 6.9(a) after the constant speed was filtered. The physical and geometrical parameters used in this case are listed in Table 6.6 and are based on the information from Vaughan *et al.* (1992). The control gains were chosen in order to allow the gravity center to move within the range of walking as shown in Figure 6.10. The required torques were then predicted by the model developed here and are shown in Figure 6.11. For this case, the abduction-adduction torque was predicted as −40Nm to 60Nm and the flexion-extension torque as −75Nm to 85Nm which are within the human physiological limits.

Table 6.6 The anthropometric parameters of the adult male with cerebral palsy.

Body mass (kg)	**69.5**
Stature (m)	**1.80**
Upper body mass (kg)	**47.32**
Inertia $\mathbf{I_x = I_z = I_0}$ **(kgm^2)**	**3.1**
Inertia $\mathbf{I_y}$ **(kgm^2)**	**0.62**
ρ (m)	**0.34**

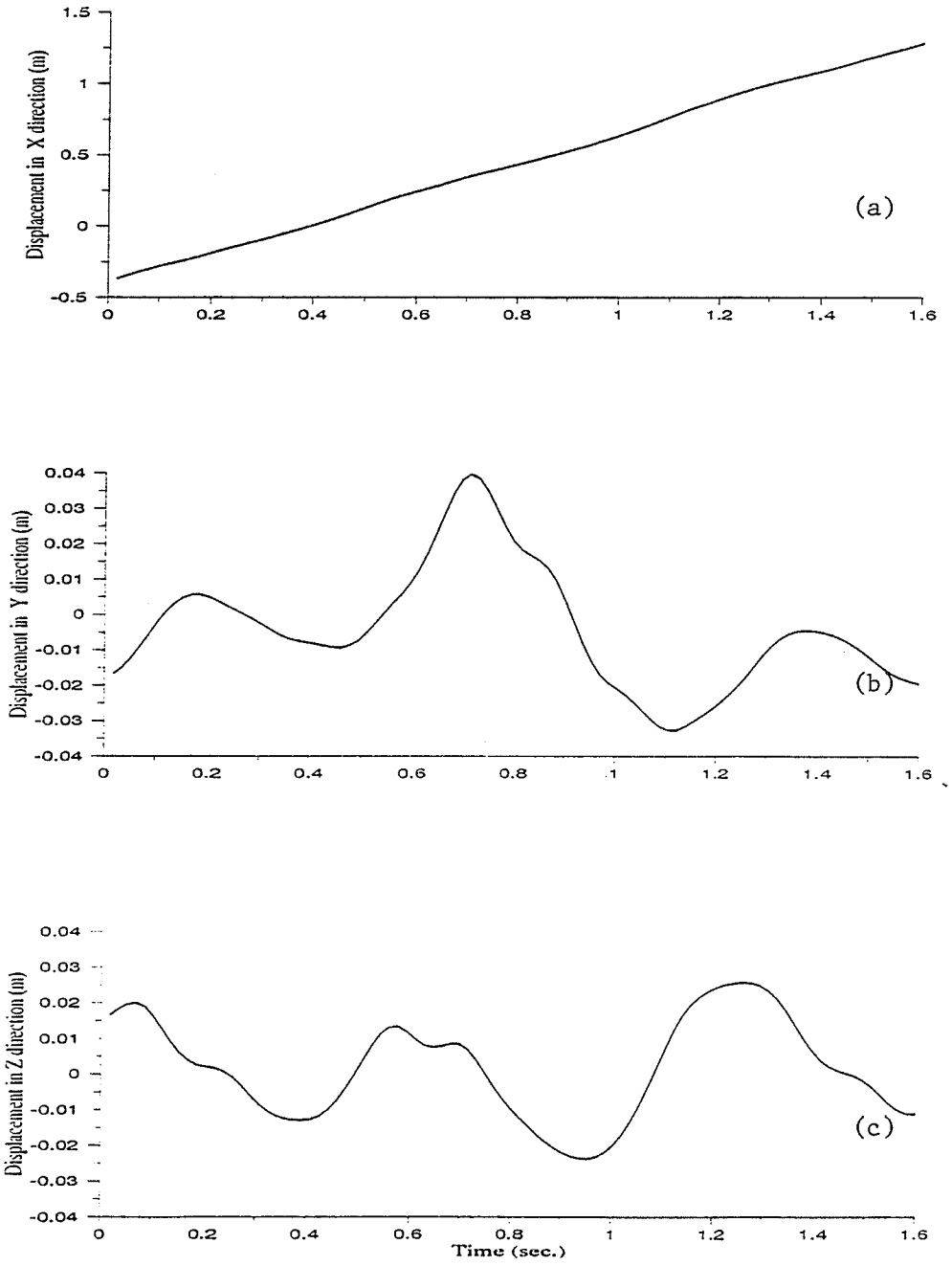

Figure 6.6 Measured displacements of the bony landmark at the sacrum during walking with the left knee fixed.

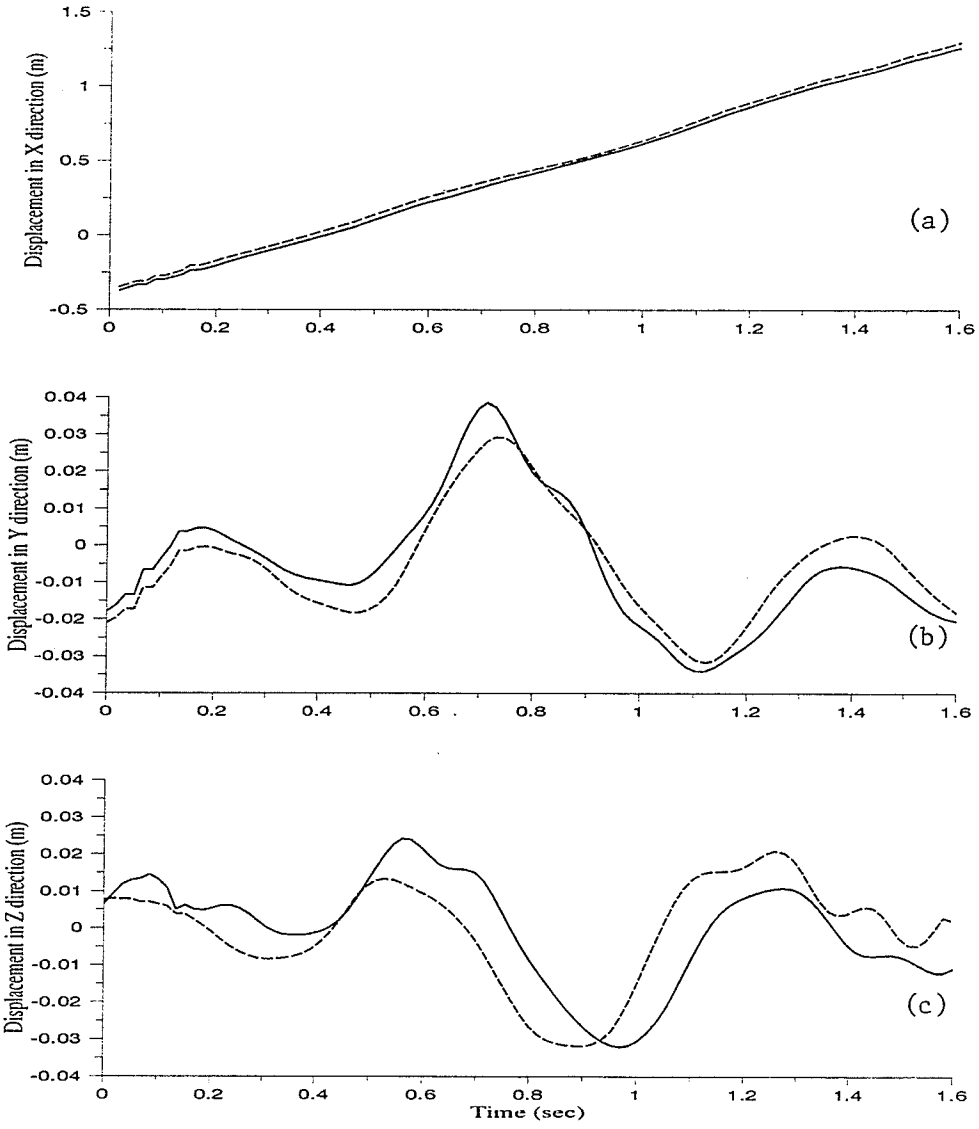

Figure 6.7 Comparison between the simulated (——) and the measured displacements of the gravity center (—·—·—) for walking with the left knee fixed.

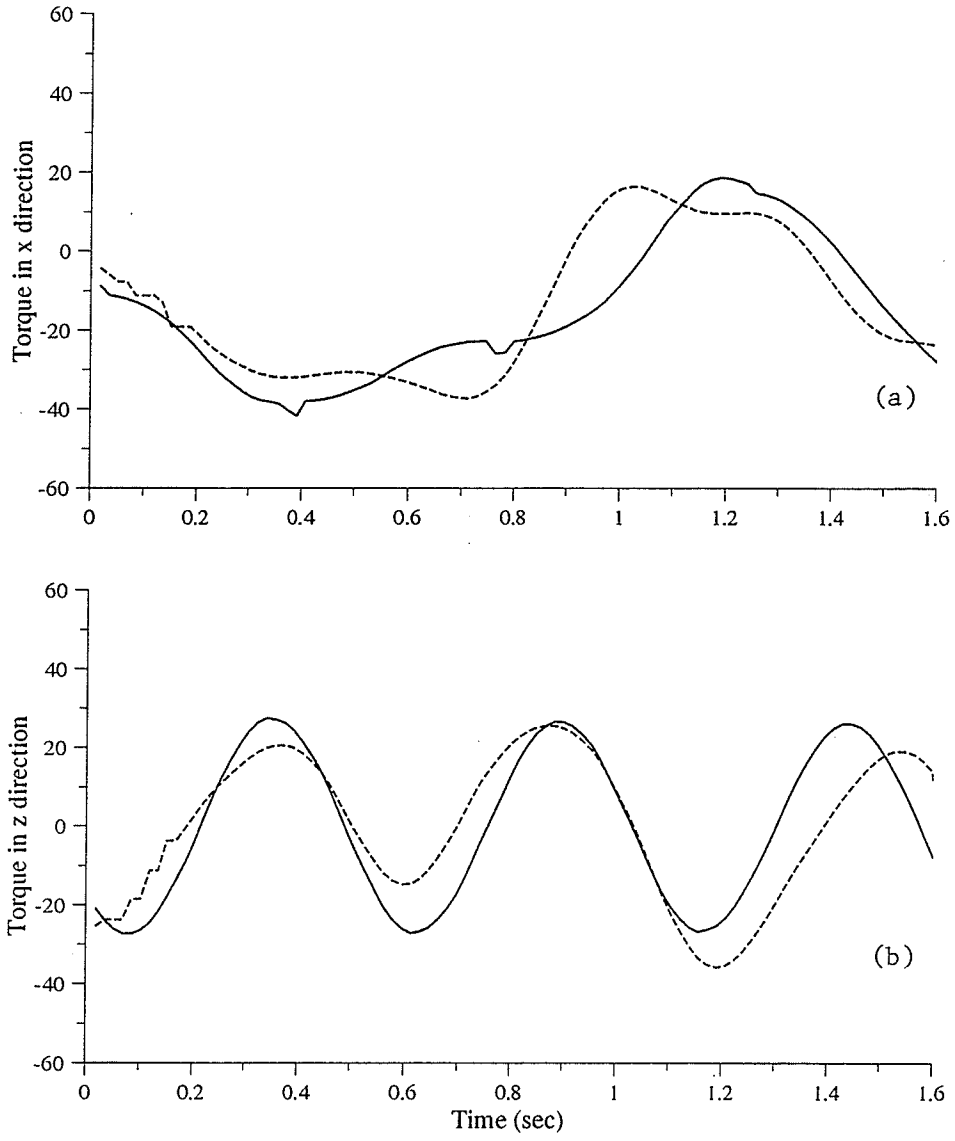

Figure 6.8 Comparison between the torques predicted from the proposed model (——) and the torques calculated based on the gait measurements (------) for walking with the left knee fixed.

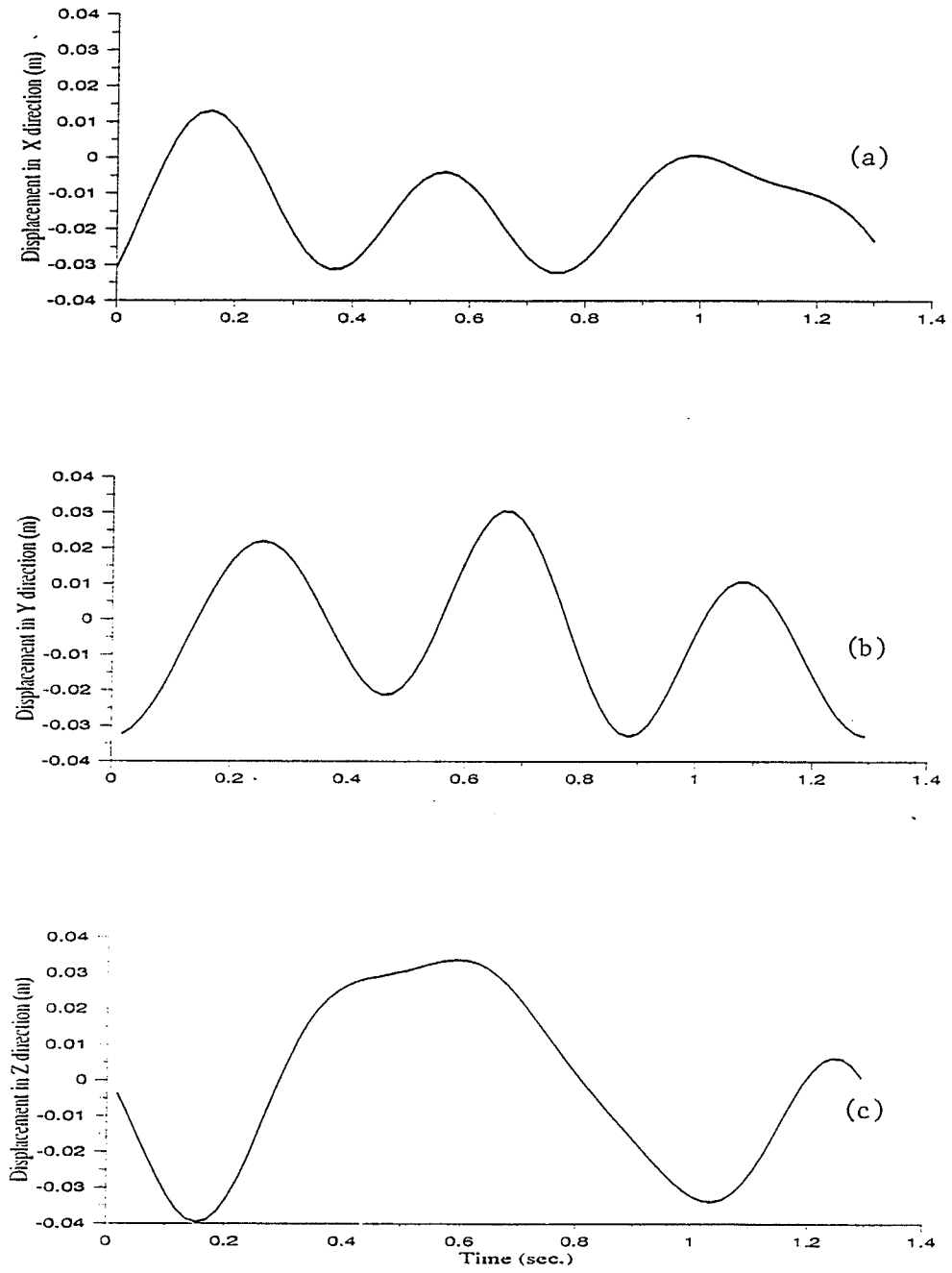

Figure 6.9 Measured displacements of the coccyx during walking of an adult with cerebral palsy. The displacement in the walking direction is the one with the constant speed filtered.

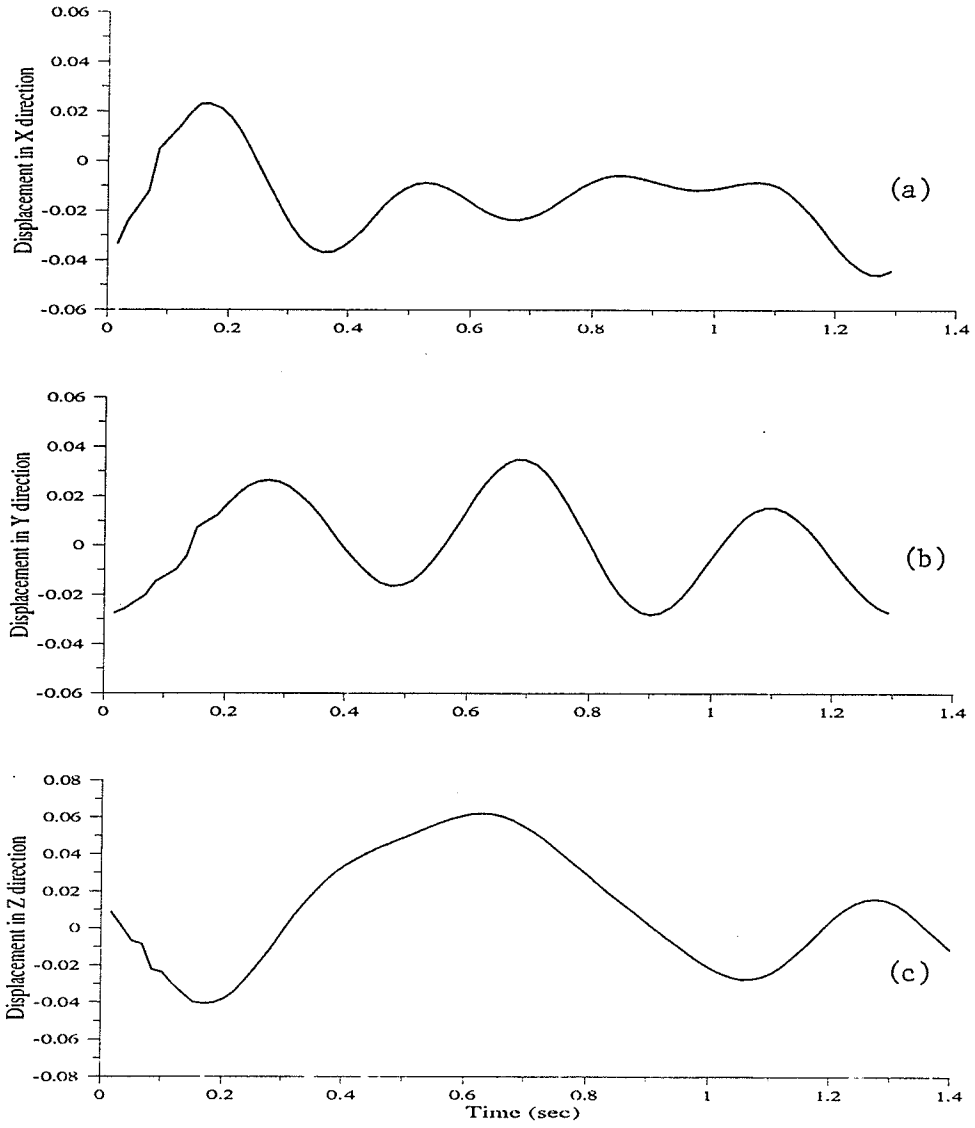

Figure 6.10 Simulated displacements of the gravity center for the walking of an adult with cerebral palsy.

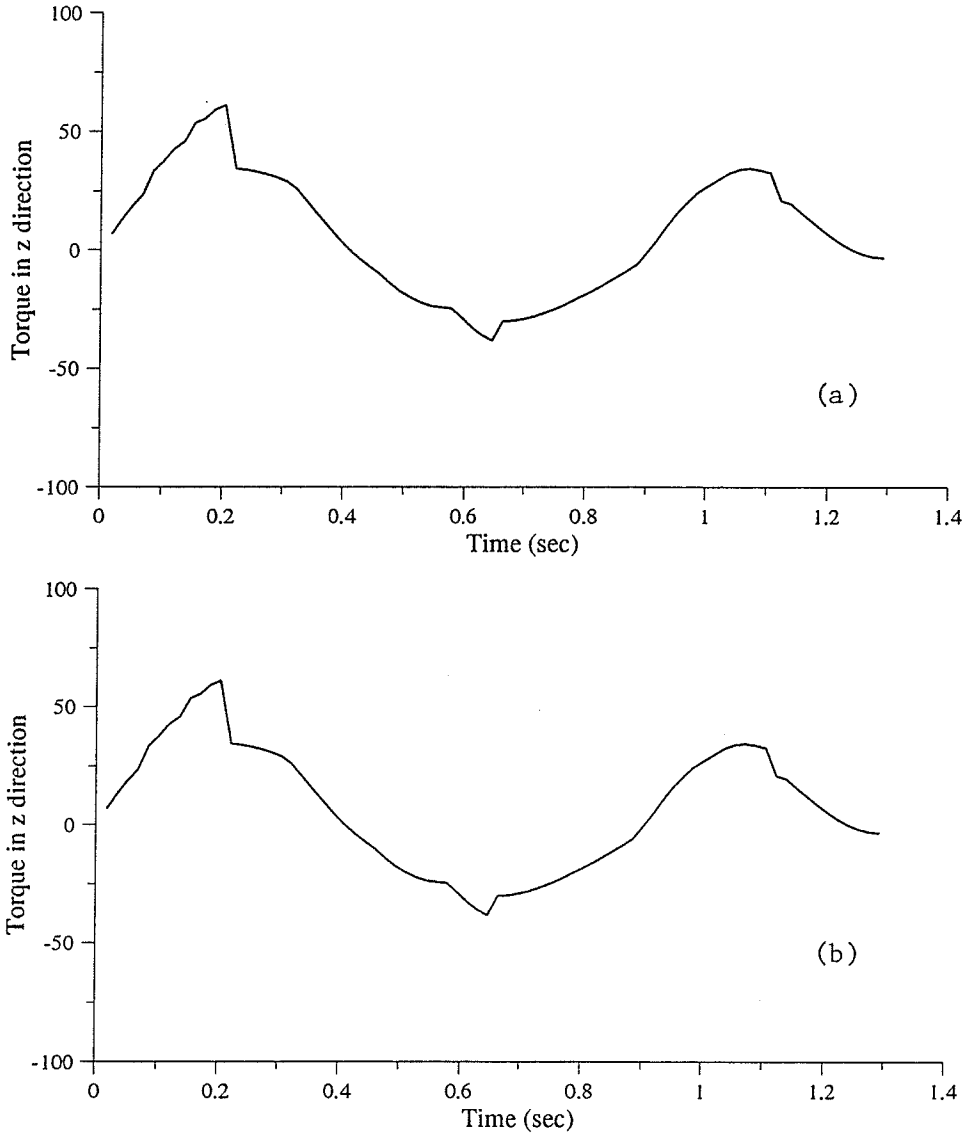

Figure 6.11 Torques predicted from the proposed model.

6.5 Summary

The dynamic model developed in the previous chapter was applied for simulating the upper body movement for various gait patterns. It is shown that such a model, though simplified, in conjunction with the proposed control algorithm can characterize the main features of the human trunk dynamics for normal and certain pathological gait patterns. As a result, acceptable state trajectory responses (i.e, close to human trunk movements) were presented suggesting that the control algorithm may be similar to that used by humans. Compared with the work by Chow and Jacobson (1972), the base point in the model was allowed to move in 3-D space in a general way to resemble both normal and abnormal walking of human subjects. From a review of the literature, this appears to be the first time that a model of the upper body has been developed which is capable of both considering the system stability and simulating the gait quantitatively.

Three case studies for three different gait patterns were presented which substantiate the method. For the first two examples, the simulation results follow the trend of experimental measurements reasonably well. The main features of the upper body motion, such as the range and the frequency of the displacements and torques, as well as the time instants where the maxima and minima occur, were characterized and compared reasonably well with those obtained based on measurement (keeping in mind that the model is at its initial stage of the development and improvements are expected). This characterization indicates that the stability model developed here has the potential to synthesize the motor control mechanisms of the upper body for normal and for some pathological gait patterns. The pathological gait patterns, however, are restricted to the

gaits in which the effect of self rotation can be ignored as compared with the effect of the other two rotations. For example, an injury at the hip joints usually causes a significant increase in self rotation, in which case, the model presented here needs to be extended. Also, the effect of swinging arms in the model is still to be investigated.

The last example demonstrated one application of this study which may predict the stability of the human upper body for pathological gaits. It is expected to function as follows: given the base point motion (presumed or measured) corresponding to some gait patterns, the stabilizing torques (analogous to the trunk torques originated from the hip joints) can be predicted by the developed model. Such torques may then be compared with those physiological limits of the subject so that the stability of walking can be assessed. In the case study of walking of an adult with cerebral palsy, the model was used to predict the torque ranges. From a review of the literature, it appears to be the first time that such predictions have been made without the measurement of all displacement data.

6.6 Limitations of the model and the measurements

The main limitation of the model is that the physical model is over-simplified. Such limitations show on two aspects — complexity of the physical model and design of the controller. Firstly, the trunk should be modeled as two separate links — the thorax and the pelvis. Through the gait measurements, it was found that the reciprocal rotation of the thorax and the pelvis is important. Such reciprocal rotation plays an important role in reducing the momentum exchange between such two segments. The swinging arms should also be separated because the swinging of the arms increases dramatically for pathological

gait patterns. Because of the complexity of the movement and the linkage system, oversimplification was often made in the simulation of human locomotion (Winter, 1991).

The design of the controller is based on Lyapunov stability theory. Stability of the upper body during walking is one of the primary requirements for the modeling. Other requirements, such as the efficiency of the energy exchange between the upper body and the lower limbs and other anatomical constraints, have not yet been considered.

The above limitations explain that, at this stage, only the first-order features of the upper body movement and the dynamics i.e., amplitudes and the frequencies, can be expected to compare with the measurements. The comparison of higher order characteristics of the upper body movements and dynamics cannot be made until the model is further extended.

Another important limitation that inhibits the comparison of the higher order features is the unsatisfactory accuracy of the gait measurements. Due to the fact that the range of motion of the trunk is much lower than that of the lower limbs, the relative error is higher. Therefore, lower cut-off frequency was used to filter the noise. A lower cut-off frequency may lose the useful data associated with higher frequencies. Based on the considerations from the above two aspects, only the amplitudes and the frequencies of the first order inter-segmental torques were compared in this work.

CHAPTER SEVEN

CONCLUSIONS

7.1 Contributions of this thesis

A methodology to study the control and the stability of a base-excited inverted pendulum about its upright position was developed. The pendulum has two degrees of rotational freedom and the base point can move in the three dimensional space without any restrictions except that the accelerations must be continuous. An immediate application of such a study is to model the dynamics of the human upper body during walking. The effects of the base point motion on the stability of the inverted pendulum model have not been investigated before and several extensions of theory, such as the method of stability analysis and non-smooth analysis, etc., were required before the inverted pendulum model could be used to study the dynamic behavior of the human upper body during walking. Using the proposed model, the first order features, namely the frequency and magnitude, of the human upper body movements and dynamics, were simulated and compared favorably with those from the gait measurements. From the work in this dissertation, several contributions have been realized.

1) *Non-smooth analysis*: Since discontinuous control strategies are inevitable in order to validate Lyapunov functions for the class of inverted pendulum system investigated in this thesis, the control system became non-smooth and non-smooth analysis was required which included the definition of the solution concept and the existence and the uniqueness of the solution. In this dissertation, Filippov's solution theory was used to define the solution concept for the proposed control system. The existence and uniqueness of

Filippov's solution were verified rigorously for the proposed non-smooth control systems. Such a solution analysis has been addressed to be important in the literature, but has not been performed for many non-smooth dynamic systems due to the fact that "much heavier mathematical machinery" is required. It is believed that, for the first time, the uniqueness of Filippov's solution was proven when the discontinuity surface is the intersection of several discontinuity surfaces and the method used here is beneficial to the solution analysis of other non-smooth dynamic systems, such as sliding mode control system, dynamic systems with friction and optimal control systems, etc.

2) *Stability analysis of non-smooth systems*: It was proven mathematically that Lyapunov's second method can be used for the stability analysis of non-smooth dynamic systems under the condition of the existence and the uniqueness of Filippov's solution. Furthermore, a method to construct smooth Lyapunov functions for non-smooth systems was developed, and it was demonstrated that for a number of engineering systems, smooth Lyapunov functions can be constructed in a easier way as compared with non-smooth Lyapunov functions discussed in the previous work. With the above extension of Lyapunov's second method and especially the method of construction of smooth Lyapunov functions, stability analysis of non-smooth systems became practical.

3) *Construction of Lyapunov functions*: Chin's integral method (Chin, 1987) was extended to remove the requirement of compatibility between the state-space model and a Lyapunov function imposed in Chin's integral method. As shown in the examples, the extended integral method developed in this work gives users more flexibility and the stability analysis for more dynamic systems, smooth or non-smooth, can be studied.

4) *Design of robust discontinuous control strategies*: Two piecewise continuous control strategies were developed to stabilize the inverted pendulum about its upright position. The first piecewise continuous controller, designed based on the total stability theory, guarantees that the solution trajectory can be arbitrarily close to the upright position under the condition of small perturbations. Such a stability was proven using the extended Lyapunov's second method, Lyapunov-like theorem based on Barbalet's lemma and total stability theory in which a Lyapunov function was constructed by the extended integral method. The above piecewise control strategy was improved by removing the restriction of small perturbations. The improved control law can keep the trajectory of the control system close to the upright position within a controlled bound. A scalar function which satisfies all the conditions of a Lyapunov function was constructed as a measure of the above bound.

The robustness of the proposed control systems with respect to those uncertainties in physical parameters and in the measurement of the base point accelerations was also examined. It was shown that the system stability is largely insensitive to these classes of uncertainties.

5) *Design of continuous control strategy*: To better reflect the implementation scenario, the discontinuous terms in the piecewise continuous control law were replaced by continuous functions. Such a replacement makes the stability analysis challenging. It was found that the continuous controller guarantees that the inverted pendulum can be stabilized in a controlled region around the upright position. The generalized Lyapunov analysis, in which a quasi-Lyapunov function was constructed, was applied to prove the

above practical stability. The analysis of the robustness of the discontinuous control system can be extended to the continuous one.

6) *Simulations of the human upper body movement and dynamics*: The proposed inverted pendulum model was further used to simulate the upper body movements for normal and pathological human gait studied as part of this work. The simulation results were compared with the results from the gait measurements. The purpose of such a comparison is to establish the promise of the model for further studies. It was found through the simulation that the inverted pendulum model can produce the first order features of the movement and dynamics of the human upper body during walking. The simulated displacements of the estimated gravity center match those from the measurements reasonably well and the control torques follow the trend of the trunk torques applied at the hip joints. Such an agreement between the simulated results and the measurements shows the potential of the developed model for further study of motor control mechanisms of human beings.

7.2 Future work

Several recommendations are made for future work.

(1) In order to use the proposed model to simulate the higher order features of the upper body movement and its dynamics during walking, the model needs to be extended to include self-rotation and to be expanded to multi-linkage system.

(2) The control strategies are designed based on Lyapunov's stability theory. For the purpose of modeling human motor control mechanisms of up-right posture during

walking, other criteria, such as optimization of energy exchange between the upper body and the lower limbs and some anatomical constraints should be considered.

(3) Several improvements in gait measurements are imperative in order to enhance the accuracy of the measurement. Firstly, at least three video cameras instead of two cameras should be used and, secondly, an automatic digitization system is essential to improve the accuracy. It was estimated that the largest random error caused by manual digitization is about **7mm**. Due to the low range of motion of the trunk, such errors can cause the results to be misleading.

With the above future developments, the model may be used to offer some insights to the motor control mechanisms of human walking and be useful for practical implementation for stabilization of the upper link in bipedal robots.

REFERENCES

Abdel-Aziz, Y. I. and Karara, H. M., 1971, Direct linear transformation from comparator coordinates into object space coordinates in close-range photogrammetry, *ASP Symposium on Close-Range Photogrammetry*, American Society of Photogrammetry, Falls Church, 1-18.

Aubin, J. P. and Cellina, A., 1984, *Differential Inclusions* (Berlin, Heidelberg: Springer-Verlag).

Anderson, C. W., 1989, Learning to control an inverted pendulum using neural networks, *IEEE Control System Magazine*, 31-37.

Anderson, M. J. and Grantham, W. J., 1989, Lyapunov optimal feedback control of a nonlinear inverted pendulum, *ASME Journal of Dynamic Systems, Measurement, and Control,* 111, 554-558.

Barbashin, E.A., 1960, The construction of Liapunov functions for non-linear systems. *Proc. 1st International Congress of IFAC,* Moscow, 943-947.

Barto, A. G., Sutton, R.S. and Anderson, C. W., 1983, Neuronlike adaptive elements that can solve difficult learning control problems, *IEEE Transactions on Systems, Man, Cybernetics*, 13, 834-846.

Cai, L. and Song, G., 1993, A smooth robust nonlinear controller for robot manipulators with joint stick-slip friction, *Proceedings of IEEE International Conference on Robotics and Automation,* Atlanta, Georgia, 449-454.

Cappozzo, A., Leo, T. and Pedotti, A., 1975, A general computing method for the analysis of human locomotion, *Journal of Biomechanics*, 8, 307.

Cappozzo, A., Figura, F., Leo, T. and Marchetti, M., 1978, Movements and mechanical energy changes in the upper part of the human body during walking, *Biomechanics* VI-A (Edited by E. Asmussen and K. Jorgenson), University Park Press, Baltimore, 272-279.

Cappozzo, A., 1981, Analysis of the linear displacement of the head and trunk during walking at different speeds, *J. Biomechanics* 41, 411-425.

Cappozzo, A., 1983, The forces and couples in the human trunk during level walking, *J. Biomechanics* 16: 265-277.

Chaffin, D. B. and Andersson, G.B., 1992, *Occupational Biomechanics*, (New York, NY: John Wiley & Sons), 63.

Chen. B., Hines, M. J. and Hemami, H., 1986, Dynamic modeling for implementation of a right turn in bipedal walking, *Journal of Biomechanics*, 19, 195-206.

Chin, P.S. M., 1986, A general method to derive Lyapunov function for non-linear systems. *Int. J. Control*, 44, 381-393.

Chin, P.S.M., 1987a, Scalar-Lyapunov-function method for single- and multimachine problems in power system. *Int. J. Control*, 45, 1737-1749.

Chin, P. S. M., 1987b, Generalized integral method to derive Lyapunov functions for non-linear systems. *Int. J. Control.* 46, 933-943.

Chin, P. S. M., 1988, Stability of non-linear systems via the intrinsic method. *Int. J. Control*, 48, 1561-1567.

Chin, P. S. M., 1989, Stability results for the solutions of certain fourth-order autonomous differential equations. *Int. J. Control*, 49, 1163-1173.

Chow, C.K. and D.H. Jacobson, 1971, Studies of human locomotion via optimal programming, 10, *Mathematical Biosciences*, 239-306.

Chow, C. K. and Jacobson, D. H., 1972, Further studies of human locomotion: postural stability and control, *Mathematical Biosciences*, 15, 93-108.

Clarke, F. H., 1983, *Optimization and Nonsmooth Analysis*, (New York, NY: John Wiley & Sons).

Corless, M., 1993, Control of uncertain nonlinear systems, *ASME Journal of Dynamic Systems, Measurement, and Control*, 115, 362-272.

Dubosin, G. N., 1940, On the problem of stability of a motion under constantly acting perturbations, *Trudy gos. astron. Inst. Sternberg*, 14.

Filippov, A. F., 1960, Differential equations with discontinuous right-hand side, *Math. Sbornik*, 51, 99-128 (English Translation: *American Mathematical Society Translations*, 42, 191-231, 1964).

Filippov, A. F., 1979, Differential equations with second members discontinuous on intersecting surfaces, *Differentsial'nye Uravneniya*, 15, 1814-1832 (English Translation: *Differential Equations*, 15, 1292-1299, 1980).

Filippov, A. F., 1988, *Differential Equations with Discontinuous Right Hand Sides* (Boston, MA: Kluwer).

Gagnon, M., Robertson, G. and Norman, R., 1987, *Kinetics, Standardizing Biomechanical Testing in Sport* (Edited by D.A. Dainty and R.W. Norman), Human Kinetics Publishers, Champaign, IL, 1987.

Guez, A. and Selinsky, J, 1988, A trainable neuromorphic controller, *Journal of Robotic Systems,* 5, 363-388.

Geromel, J. C. and DA Cruz, J. J., 1987, On the robustness of optimal regulators for nonlinear discrete-time systems, *IEEE Transactions on Automatic Control,* 32, 703-710.

Hahn, W., 1963, *Theory and Application of Lyapunov's Direct Method* (Englewood Cliffs, NJ: Prentice Hall).

Hemami, H. and Golliday, G. L., 1977, The invertde pendulum and biped stability, *Mathematical Biosciences*, 34, 95-110.

Hemami, H. and Farnsworth, R. L., 1977, Postural and gait stability of a planar five link biped by simulation, *IEEE Transactions on Automatic Control*, 22, 452-458.

Hemami, H. and Wyman, B. F., 1979, Modeling and control of constrained dynamic systems with application to biped locomotion in the frontal plane, *IEEE Transactions on Automatic Control,* 24, 526-535.

Hemami, H., 1980, A feedback on-off model of biped dynamics, *IEEE Transactions on Systems, Man, and Cybernetics,* 10, 376-383.

Hemami, H. and Chen, B., 1984, Stability analysis and input design of a two-link planar biped, *International Journal of Robotics Research*, 3, 93-100.

Hemami, H. and Katbab, A., 1982, Constrained inverted pendulum model for evaluating upright postural stability, *ASME Journal of Dynamic Systems, Measurement, and Control*, 111, 343-349.

Henders, M. G. and Soudack, A. C., 1992, 'In-the-large' behavior of an inverted pendulum with linear stabilization, *International Journal of Nonlinear Mechanics,* 27, 129-138.

Huaux, A., 1967, On the construction of Lyapunov functions. *I.E.E.E. Trans. Automation and Control*, 12, 465.

Khalil, H. K., 1992, *Nonlinear Systems*, (New York, NK: Macmillan Publishing Company).

Koenigsberg, W. D. and Frederick, D. K., 1970, Output feedback control with application to unstable linear systems, *Joint Automatic Control Conference*, Atlanta, Georgia, 674-682.

Krasovskii, N. N, 1954, On stability of motion in the large for constantly acting disturbances, *PMM*, 18, 95-102.

LaSalle, J. P., 1960, Some extensions of Liapunov's second method, *IRE. Trans. Circ. Thy.*, CT-7, 520-527.

Levi, M., 1988, Stability of the inverted pendulum—a topological explanation, *SIAM Review*, 30, 639-644.

Lyapunov, A. M., 1892, The general problem of the stability of motion (Translated by Fuller, A.T.) *International Journal of Control*, 52, 531-773; also (London: Taylor & Francis, 1992).

Mackinnon, C. D. and Winter, D. A., 1993, Control of whole body balance in the frontal plane during human walking, *J. Biomechanics* 26, 633-644.

Mansour, J. M., Lesh, M. D, Nowak, M. D. and Simon, S. R., 1982, A three-dimensional multi-segmental analysis of the energetics of normal and pathological human gait, *J. Biomechanics* 15: 51-59 (1982).

Marino, R. and Nicosia, S., 1983, Hamiltonian-Type Lyapunov functions. *I.E.E.E. Trans. automatic Control*, 28, 1055-1057.

Medina, D. F. and Zadoks, R. I., 1992, Nonlinear behavior of a parametrically excited, inverted pendulum, *Proceedings of 38th Annual Meeting of the Institutes of Environmental Sciences*, Nashrille, TN, 89-94.

Miyagi, H. and Taniguchi, T., 1980, Application of the Lagrange-Charpit method to analyze the power system's stability. *Int. J. Control* 32, 371-379.

Mori, S., Nishihara, H. and Furuta, K., 1976, Control of unstable mechanical system Control of pendulum, *International Journal of Control*, 23, 673-692.

Mukherjee, T. K. and Bhattacharyya, B., 1972, Transient stability of a power system by the second method of Lyapunov, *Int. J. Systems Sci.*, 3, 439-448.

Murphy, M. C. and Mann, R. W., 1990, A comparison of smoothing and digital filtering/differentiation of kinematic data, ...

Murray, R. M., Li, Z. and Sastry, S.S., 1994, *A Mathematical Introduction to Robotic Manipulation* (Boca Raton, FL: CRC Press).

Onyshko, S. and Winter, D.A., 1980, A mathematical model for the dynamics of human locomotion, *J. Biomechanics* 13, 361-368.

Paden, B. E. and Sastry, S. S., 1987, A calculus for computing Filippov's differential inclusion with application to the variable structure control of robot manipulators, *IEEE Transactions on Circuits and Systems*, 34, 73-82.

Pandy, M. G., 1987, *Models for Understanding the Dynamics of Human Walking*, Ph.D dissertation, Department of Mechanical Engineering, Ohio State University, Columbus, Ohio, U.S.A.

Pandy M. G., Berme N., 1988, Synthesis of human walking: a planar model for single support. *J. Biomechanics* 12, 1053-1060.

Pandy M. G., Berme N., 1989a, Quantitative assessment of gait determinants during single stance via a three-dimensional model—Part I. normal walking. *J. Biomechanics* 22, 717-724.

Pandy, M. G. and Berme, N., 1989b, Quantitative assessment of gait determinants during single stance via a three-dimensional model-part 2. pathological gait, *J. Biomechanics* 22, 725-733.

Phelps III, F. M. and Hunter, JR., J. H., 1965, An analytic solution of the inverted pendulum, *American Journal of Physics*, 35, 285-295.

Ponzo, P. J., 1965, On the stability of certain non-linear differential equations, *I.E.E.E. Trans. Automatic Control*, 10, 470.

Qu, Z. and Dorsey, J., 1992, Robust control by two Lyapunov functions, *International Journal of Control*, 55, 1335-1350.

Rahmani, S., 1979, *An Experimental Study of Planar Models for Human Gait Utilizing On-Line Computer Analysis of Television and Force Plate Data*, Ph.D dissertation, Department of Electrical Engineering, Ohio State University, Columbus, Ohio, U.S.A.

Reissig, R., 1959, Uber die total stabilitat erzwungener Reibungsschwingungen, *Abh. Deutsche Akad. Wiss. Kl. Math. Phys. Techn.*, 6-28.

Reissig, R., 1960, Stabilitatskriterien fur ein lineares System mit veranderlichen Parametern, *Z. angew. Math. Mech.*, 40, T112-T113.

Saunders, J. B., De, C. M., Inman, V.T. and Eberhart, H.D., 1953, The major determinants in normal and pathological gait, *J. Bone Jt Surg.* 35A: 543-558.

Schaefer, J. F. and Cannon, R. H., 1966, On the control of unstable mechanical systems, *Proceedings of 3rd Congress of the IFAC*, London, England, 6C.1-6C.13.

Scheiner, A., Ferentcz, D.C. and Chizek, H. J., 1994, Simulation of the complete gait cycle using a 23 degree-of-freedom model, *Proc. 13th Biomedical Engineering Conf.*, Washington, DC, 59-62.

Shevitz, D. and Paden B., 1994, Lyapunov stability theory of nonsmooth systems, *IEEE Transactions on Automatic Control*, 39, 1910-1914.

Siegler, S., Seiktar, R. and Hyman, W., 1982, Simulation of human gait with the aid of a simple mechanical model, *J. Biomechanics* 15: 415-425.

Slotine, J. J. and Sastry, S. S., 1983, Tracking control of nonlinear systems using sliding surfaces, with application to robot manipulators, *International Journal of Control*, 38, 465-492.

Slotine, J. J. and Li W., 1991, *Applied Nonlinear Control*, (Englewood Cliffs, NJ: Prentice-Hall, Inc.).

Southward, S. C., Radcliffe, C. J. and MacCluer, C. R., 1991, Robust nonlinear stick-slip friction compensation, *ASME Journal of Dynamic Systems, Measurement, and Control*, 113, 639-644.

Spong, M. W. and Vidyasagar, 1989, *Robot Dynamics and Control*, (John Wiley & Sons).

Stokes, V.P. and Forssberg, H., 1989, Rotational and translational movement features of the pelvis and thorax during adult human locomotion, *J. Biomechanics* 22, 43-50.

Thornton-Trump, A.B. and Brodland, G.W., 1987, Gait reaction reconstruction and a heel strike algorithm, *J. Biomechanics* 20: 767-772.

Thorstensson, A., Nilsson, J., Carlson, H. and Zomlepher, M.R., 1984, Trunk movements in human locomotion, Acta Physical Scand, 121: 9-22.

Utkin, V. I., 1977, Variable structure systems with sliding modes, *IEEE Transactions on Automatic Control*, 22, 212.

Utkin, V. I., 1992, *Sliding Modes in Control and Optimization*, (Berlin, Heidelberg: Springer-Verlag).

van der Zweep, J., Remillard, N., Wu, Q., Thornton-Trump, A.B. and Alexander, M., 1995, Motion analysis of the human trunk for pathological gait, Submitted for presentation at 15th Canadian Congress of Applied Mechanics.

Vaughan, C. L., Davis, B. L. and O'Connor, J. C., 1992, *Dynamics of Human Gait*, (Champaign, Illinois: Human Kinetics Publishers).

Vaughan, C.L., and Sussman, M.D., 1993, Human Gait: From Clinical Interpretation to Computer Simulation, *Current Issues in Biomechanics* (M.D. Grabiner, Editor): 53-68, (Champaign, IL: Human Kinetics Pub.).

Vidyasagar, M. 1993, *Nonlinear Systems Analysis* (Englewood Cliffs, NJ: Prentice Hall).

Vorovich, I. I., 1956, On the stability of motion with random disturbances, *Izv. Akad. Nauk SSSR, Ser. Mat.*, 20, 17-32.

Vrkoc, Ivo, 1959, Integral stability, *Czechoslov. Math. Zurn.*, 9 (84) 71-129.

Vukobratovic, M., Frank, A. A. and Juricic, D., 1970, On the stability of biped locomotion, *IEEE Transactions on Bio-medical Engineering*, 17, 25-36.

Vukobratovic, M. and Stepanenko, J., 1972, On the stability of Anthropomorphic systems, *Mathematical Biosciences,* 15, 1-37.

Vukobratovic, M. and Stepanenko, J., 1973, Mathematical models of general anthropomorphic systems, Mathematical Biosciences, 17, 191-242.

Vukobratovic, M. and Stokic, D., 1975, Postural stability of anthropomorphic systems, *Mathematical Biosciences,* 25, 217-236.

Wagner, D. M., 1977, Survey of measurable selection theorems, *SIAM Journal of Control and optimization*, 15, 859-903.

Whalen, M.T., *Three-Dimensional Biomechanical Analysis of the Stationary and Penalty Corner Drives in Field Hocky,* M.Sc. Thesis , Faculty of physical Education and Recreation Studies, The University of Manitoba, 1992.

Widrow, B., 1987, The original adaptive neural net broom-balancer, *Proceedings of IEEE International Symposium on Circuits and Systems,* Philadelphia, PA, 351-357.

Winter, D. A., Sidwall, H. G. and Hobson, D. A., 1974, Measurements and reduction of noise in kinematics of locomotion, *Journal of Biomechanics*, 7, 157.

Winter, D. A., 1991, *Biomechanics and motor control of human movement*, (John Wiley & Sons, Inc.).

Wu, Q., Sepehri, N., Thornton-Trump, A. B. and Onyshko, S., 1995, An extended integral method to derive Lyapunov functions for nonlinear systems, *International Journal of Control,* 62, 717-736.

Yang, J. 1994, A control study of a kneeless biped locomotion system, *Journal of Franklin Institute*, 331B, 125.

Zernicke, R. F., Caldwell, G. and Roberts, E. M. 1976, Fitting biomechanical data with cubic spline functions, Res. Q. 47, 9.

APPENDIX A

Definition of Euler Angles

OX, OY and OZ form the inertial frame of reference and oxyz represents the body coordinate system. When the torso is in the upright position, the two coordinate systems coincide. The Euler angles are generated by three-step rotations as follows:

Step 1: Rotate the torso about OZ or oz', as shown in Fig. A.1(a), to form θ in Figure A.1(b). θ describes the pitch motion of the body in the sagittal plane OXY.

Step 2: Rotate the torso about ox', as shown in Figure A.1(b), to generate ψ in Figure A.1(c). ψ corresponds to rollover action of the body.

Step 3: Rotate the torso about oy" as shown in Figure A.1(c), to form angle φ in Figure A.1(d). φ describes the self rotation of the body.

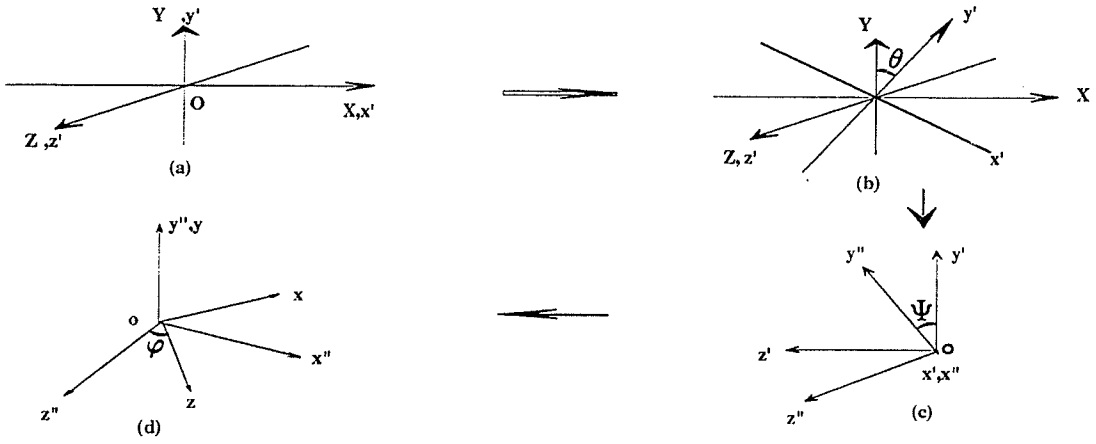

Fig. A.1 Definition of Euler angles

Appendix B

Derivation of the dynamic equations to calculate trunk torques

In this appendix, the dynamic equations are derived using Lagrangean method to calculate the trunk torques. Euler angles are described in Appendix A. The base point motion is described by $\tilde{f}(t)$, $\tilde{g}(t)$ and $\tilde{h}(t)$. The relationship between the displacements at the gravity center and the Euler angles is shown as follows

$$\begin{aligned} x_c &= \tilde{f}(t) + \rho \sin\theta \cos\psi \\ y_c &= \tilde{g}(t) + \rho \cos\theta \sin\psi \\ z_c &= \tilde{h}(t) + \rho \sin\psi \end{aligned} \qquad \textbf{(B.1)}$$

where x_c, y_c and z_c are the displacements at the gravity center. The tanslational kinetic energy is

$$T_{tran} = \frac{1}{2} m(x_c^2 + y_c^2 + z_c^2)$$

which can be written below

$$\begin{aligned} T_{tran} = \frac{1}{2} m[&\dot{\tilde{f}}(t)^2 + \dot{\tilde{g}}(t)^2 + \dot{\tilde{h}}(t)^2 + \rho^2\dot{\theta}^2\cos^2\psi + \rho^2\dot{\psi}^2 + 2\dot{\tilde{f}}(t)\rho(\dot{\theta}\cos\theta\cos\psi \\ &- \dot{\psi}\sin\theta\sin\psi) - 2\rho\dot{\tilde{g}}(t)(\dot{\theta}\sin\theta\cos\psi + \dot{\psi}\cos\theta\sin\psi) + 2\rho\dot{\tilde{h}}(t)\dot{\psi}\cos\psi] \end{aligned} \qquad \textbf{(B.2)}$$

The rotational kinetic energy is

$$T_{rot} = \frac{1}{2}(I_1 w_1^2 + I_2 w_2^2 + I_3 w_3^2$$

where w_1, w_2 and w_3 are the angular velocities which has the following form

$$\begin{aligned} w_1 &= \dot{\psi}\cos\phi + \dot{\theta}\sin\phi\cos\psi \\ w_2 &= \dot{\phi} - \dot{\theta}\sin\psi \\ w_3 &= \dot{\psi}\sin\phi - \dot{\theta}\cos\phi\cos\psi \end{aligned} \qquad \textbf{(B.3)}$$

Substituting (B.3) into the form of rotational kinetic energy, we have

$$T_{rot} = \frac{1}{2}[I_1(\dot{\psi}^2\cos^2\phi + \dot{\theta}^2\sin^2\phi\cos^2\psi + \dot{\theta}\dot{\psi}\sin 2\phi\cos\psi)$$
$$+ I_2(\dot{\phi}^2 + \dot{\theta}^2\sin^2\psi - 2\dot{\phi}\dot{\psi}\sin\psi)$$
$$+ I_3(\dot{\psi}^2\sin^2\phi + \dot{\theta}^2\cos^2\phi\cos^2\psi - 2\dot{\theta}\dot{\psi}\sin\phi\cos\phi\cos\psi)] \qquad \textbf{(B.4)}$$

According to Lagrangean equation shown below

$$\frac{d}{dt}(\frac{\partial T}{\partial \dot{q}}) - \frac{\partial T}{\partial q} + \frac{\partial V}{\partial q} = M_q$$

Variable q is the state variable, representing θ, ψ and ϕ, respectively. Carrying out the calculations, the dynamic equations are derived as follows

$$I_1(\ddot{\theta}\sin^2\phi\cos^2\psi + \dot{\theta}\dot{\phi}\sin 2\phi\cos^2\psi - \dot{\theta}\dot{\psi}\sin^2\phi\sin 2\psi + \frac{1}{2}\ddot{\psi}\sin 2\phi\cos\psi$$
$$+\dot{\psi}\dot{\phi}\cos 2\phi\cos\psi - \frac{1}{2}\dot{\psi}^2\sin 2\phi\sin\psi) + I_2(\ddot{\theta}\sin^2\psi + \dot{\theta}\dot{\psi}\sin 2\psi - \ddot{\phi}\sin\psi - \dot{\psi}\dot{\phi}\cos\psi)$$
$$+I_3(\ddot{\theta}\cos^2\psi\cos^2\phi - \dot{\theta}\dot{\phi}\sin 2\phi\cos^2\psi - \dot{\theta}\dot{\psi}\cos^2\phi\sin 2\psi - \frac{1}{2}\ddot{\psi}\sin 2\phi\cos\psi$$
$$-\dot{\psi}\dot{\phi}\cos 2\phi\cos\psi + \frac{1}{2}\dot{\psi}^2\sin 2\phi\sin\psi) + m\rho^2\ddot{\theta}\cos^2\psi - m\rho^2\dot{\theta}\dot{\psi}\sin 2\psi$$
$$+m\ddot{\tilde{f}}(t)\rho\cos\theta\cos\psi - m\ddot{\tilde{g}}(t)\rho\sin\theta\cos\psi - mg\rho\sin\theta\cos\psi = M_\theta$$

$$(I_1\cos^2\phi + I_3\sin^2\phi)\ddot{\psi} - (I_1 - I_3)\dot{\psi}\dot{\phi}\sin 2\phi + \frac{1}{2}(I_1 - I_3)\ddot{\theta}\sin 2\phi\cos\psi$$
$$+(I_1 - I_3)\dot{\theta}\dot{\phi}\cos 2\phi\cos\psi + m\rho\ddot{\psi} - M\rho\ddot{\tilde{g}}(t)\cos\theta\sin\psi - m\ddot{\tilde{f}}(t)\rho\sin\theta\sin\psi$$
$$+m\rho\ddot{\tilde{h}}(t)\cos\psi + \frac{1}{2}I_1\dot{\theta}^2\sin 2\psi\sin^2\phi - I_2(\frac{1}{2}\dot{\theta}^2\sin 2\psi - \dot{\theta}\dot{\phi}\cos\psi)$$
$$+\frac{1}{2}I_3\dot{\theta}^2\sin 2\psi\cos^2\phi + \frac{1}{2}m\rho^2\dot{\theta}^2\sin 2\psi - m\rho\sin\psi\cos\theta = M_\psi$$

$$I_2(\ddot{\phi} - \ddot{\theta}\sin\psi - \dot{\theta}\dot{\psi}\cos\psi) - (I_1 - I_3)\dot{\psi}^2\sin\phi\cos\psi + \frac{1}{2}(I_1 - I_3)\dot{\theta}^2\sin 2\phi\cos\psi$$
$$+(I_1 - I_3)\dot{\theta}\dot{\psi}\cos\psi\cos 2\phi = M_\phi \qquad \textbf{(B.5)}$$